Part 2

Tunneling Magnetorezistance (TMR) in Magnetic Tunnel Junctions (MTJ)

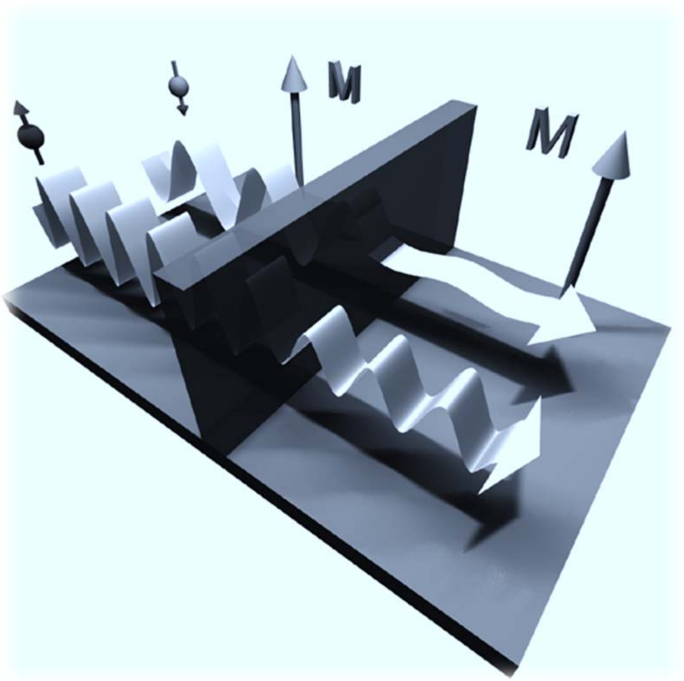

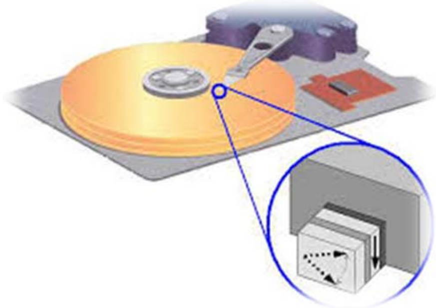

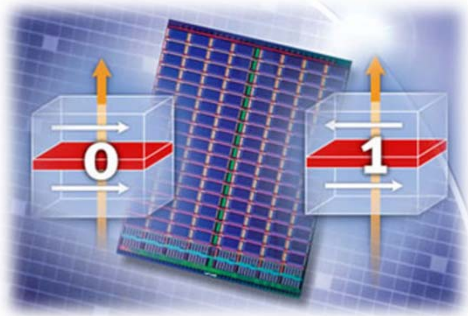

Prof. Dr. Coriolan TIUSAN UTCN - CNRS

Tunneling Magnetorezistance (TMR) ➡ consequence of spin-dependent tunneling

Tunnel effect (1928 George Gamow):
NONZERO transmission of particle-associated wave across a thin potential barrier

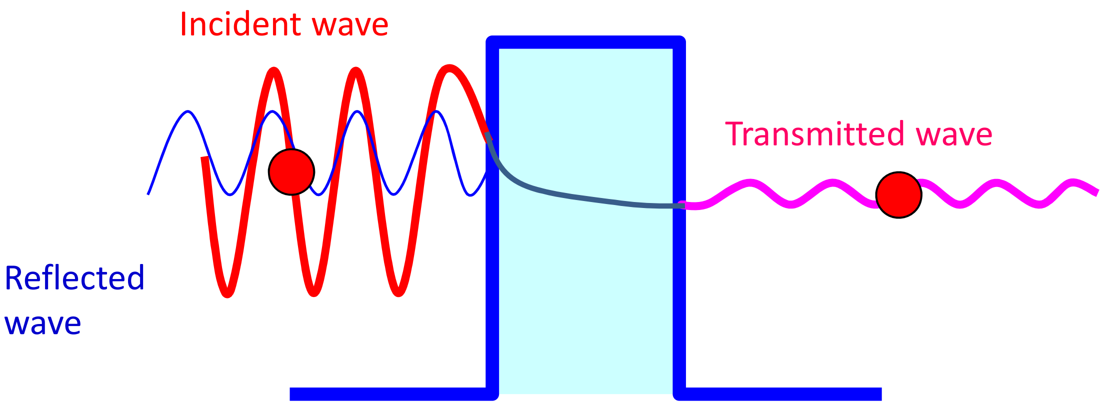

The *nature of particles as waves* (de Broglie) determines the tunnel effect

➔Pure **QM approach**

➔No Classical approach

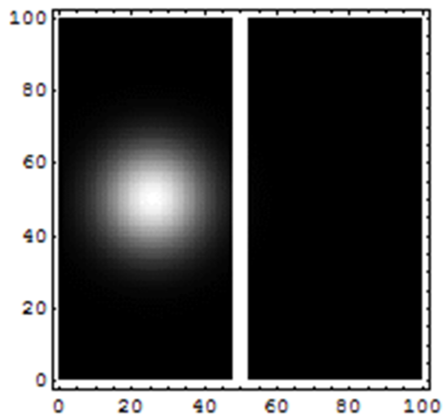

Tunnel junction:
= two metallic layers separated by a thin insulator:
=> electron propagation by tunneling

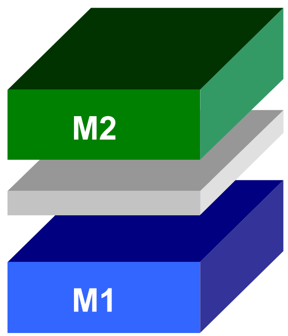

Some quantum mechanics

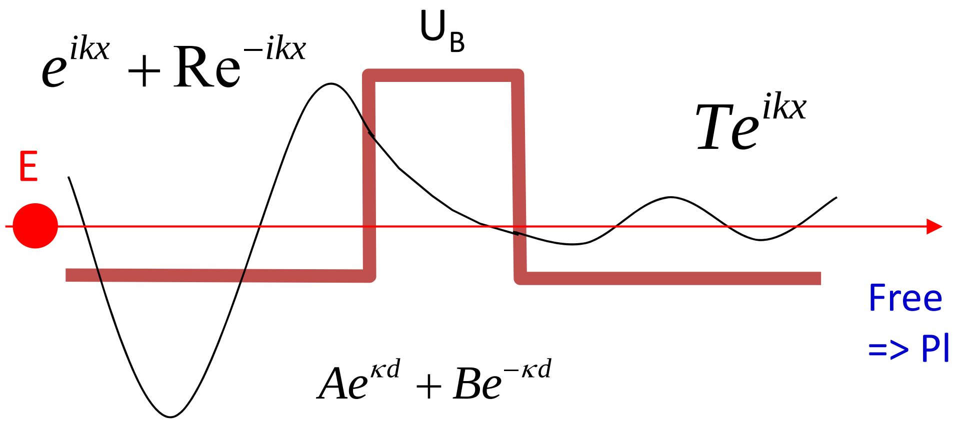

Free electrons
=> Plane wave

Schrödinger

$$\left(-\frac{\hbar^2}{2m}\Delta + U\right)\Psi = E\Psi \qquad U = \begin{cases} 0 & metal \\ U_B & barrier \end{cases}$$

$$\begin{cases} k = \sqrt{\dfrac{2m}{\hbar^2}E} & \text{metal} \\ \kappa = \sqrt{\dfrac{2m}{\hbar^2}(U_B - E)} & \text{barrier} \end{cases}$$

➡ Transmission probability: $T \sim \exp(-2\kappa d)$

➡ Tunnel current (conductivity):

$$I_{LR} = \int n_L(E) f_L^{FD}(E) \boxed{T(E)} n_R(E)\left(1 - f_R^{FD}(E)\right) dE$$

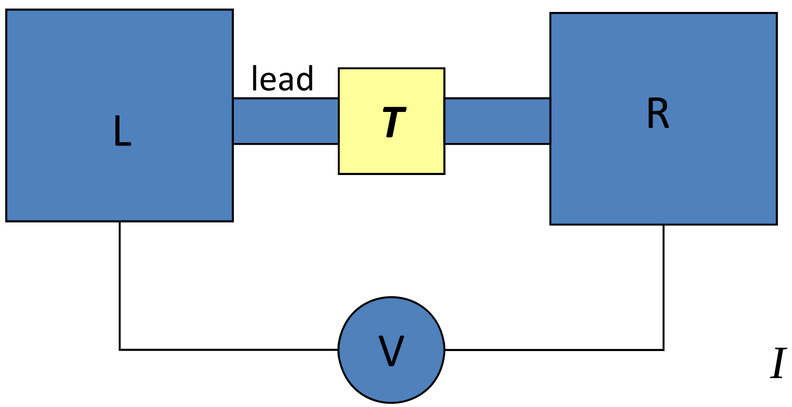

Total (net) current when biasing the junction

$$I = I_{LR} - I_{RL} =$$
$$= \int n_L(E) T(E) n_R(E + eV)\left(f_L^{FD}(E) - f_R^{FD}(E + eV)\right) dE$$

MAGNETIC TUNNEL JUNCTION – elementary brick of spintronics

Metallic layers = ferromagnetic → **Spin dependent**
- density of states $n^{\sigma}(E)$
- potential profile in the ferromagnet

FM$_1$ / I / FM$_2$ trilayer

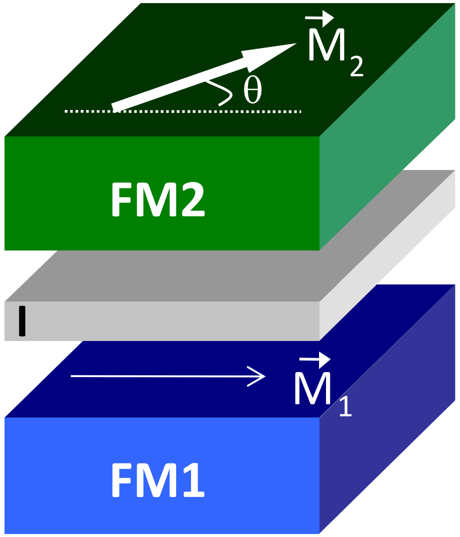

$$\boxed{\left(-\frac{\hbar^2}{2m}\Delta + U\right)\Psi = E\Psi}$$

$$U = \begin{cases} \pm h\sigma & FM,\ \sigma = \uparrow,\downarrow \\ U_B & barrier \end{cases}$$

QM → $T^{\sigma}(E)$ Spin dependent **transmission probability**

Spin dependent **current**

$$\boxed{J_{\sigma} = \int n_1^{\sigma}(E) T^{\sigma}(E) n_2^{\sigma}(E)\left[f_1(E) - f_2(E)\right] dE}$$

Mechanisms of TMR

Spin transport by quantum tunneling

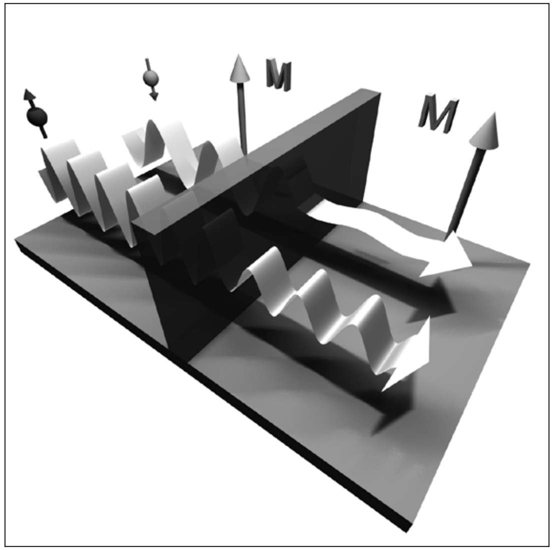

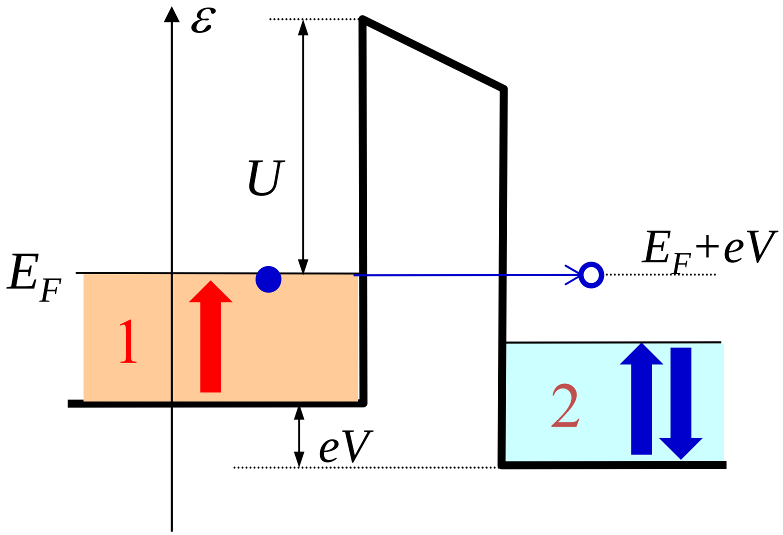

Two current model (2 independent channels)

Spin conservation during tunneling

spin up: $J^{\uparrow}$

spin down: $J^{\downarrow}$

$$\boxed{J_{tot} = J^{\uparrow} + J^{\downarrow}}$$

Quantum Mechanics

$$J_{\sigma}(V) = \int n_1^{\sigma}(E)\, \boxed{T^{\sigma}(E)}\, n_2^{\sigma}(E+eV)\left[f_1(E) - f_2(E+eV)\right] dE$$

$$T = OK \Rightarrow$$

$$\boxed{J_{\sigma}(V) \propto n_1^{\sigma}(E_F)\, n_2^{\sigma}(E_F+eV)}$$

MAGNETIC TUNNEL JUNCTION – Tunnel Magnetoresistive (TMR) effect

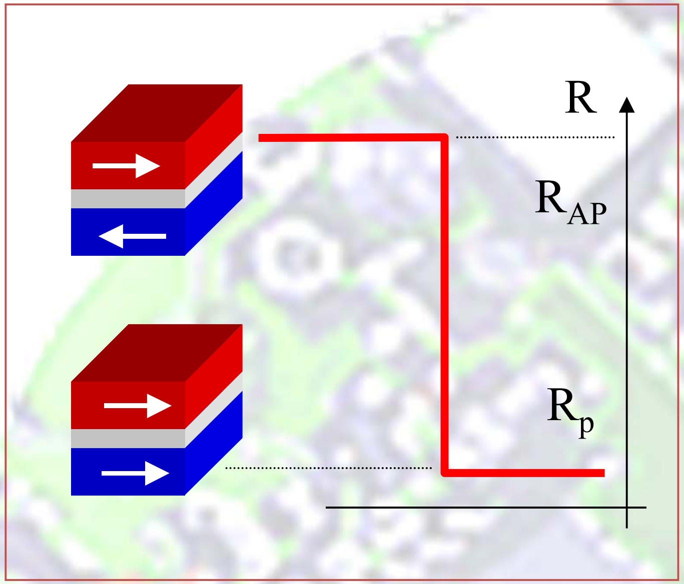

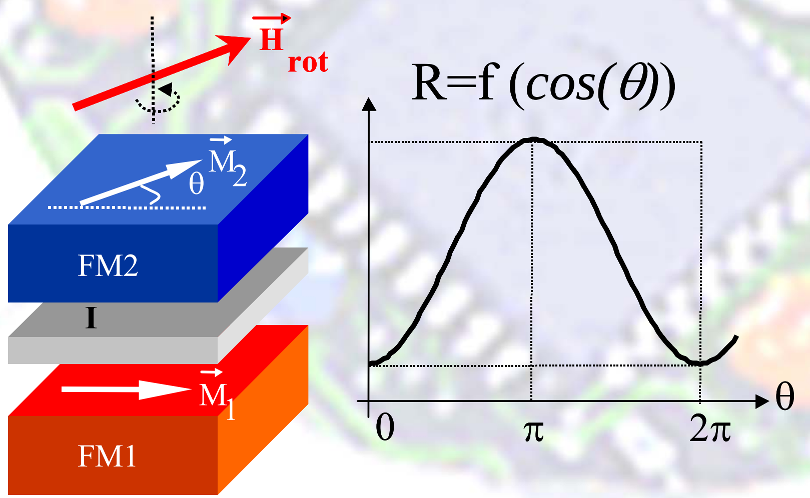

Slonczewski: *Phys. Rev.* **B39**, 6995, (1989)

Tunnel magnetoresistance:

$$TMR = \frac{\Delta R}{R} = \frac{R_{AP} - R_P}{R_P}$$

$$\boxed{\frac{\Delta R}{R} = \frac{(R_{AP} - R_P)}{R_P} = \frac{2P_1P_2}{1 - P_1P_2}}$$

with $$P_{1(2)} = \frac{n^{\uparrow}_{1(2)} - n^{\downarrow}_{1(2)}}{n^{\uparrow}_{1(2)} + n^{\downarrow}_{1(2)}}$$

Spin-valve effect

$$R = \frac{R_p + R_{ap}}{2} + \frac{R_p - R_{ap}}{2}\cos(\theta),$$

$$\theta = (\vec{M}_1, \vec{M}_2)$$

MAGNETIC TUNNEL JUNCTION – Large spin valve effect

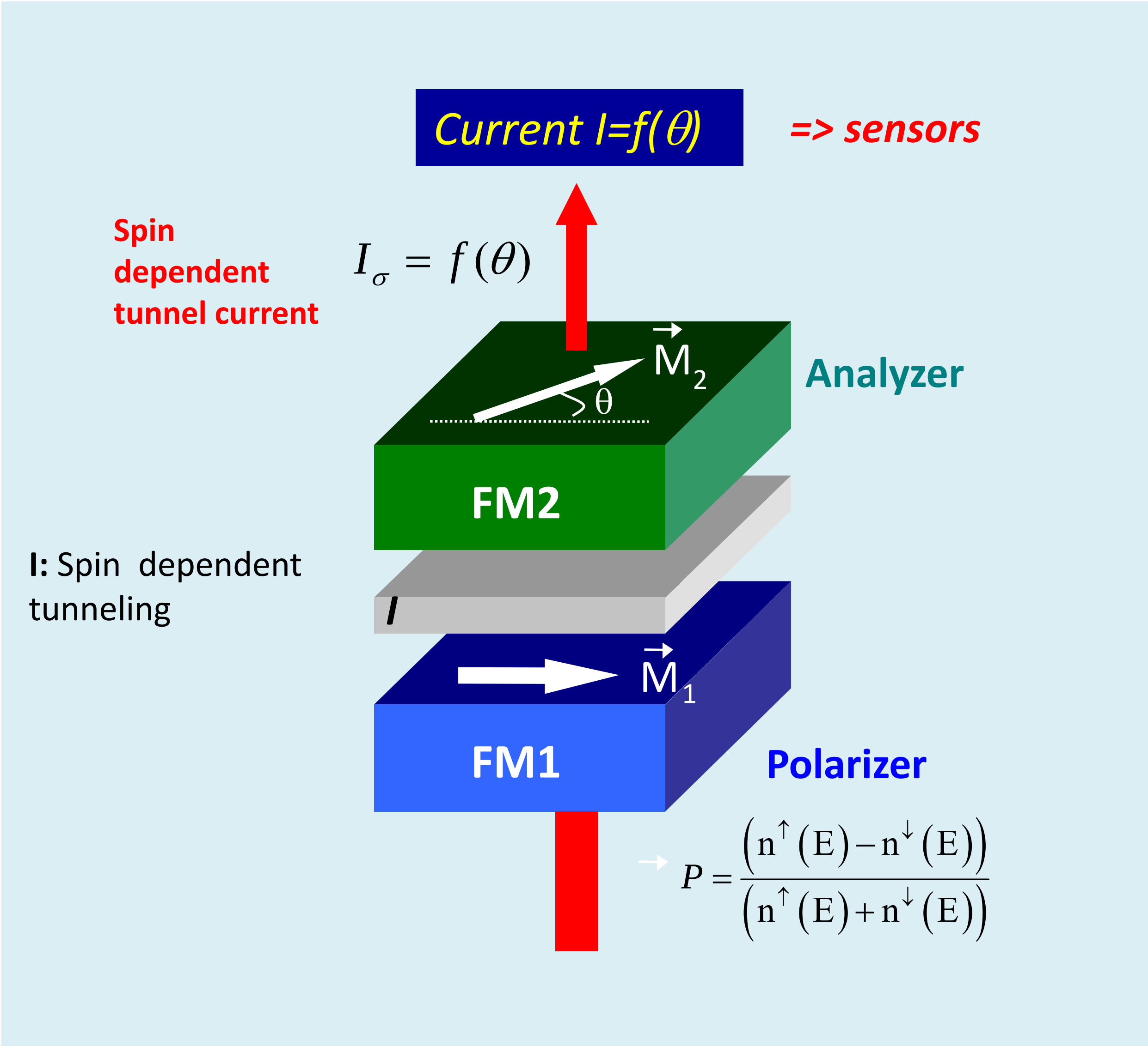

Field, rotation

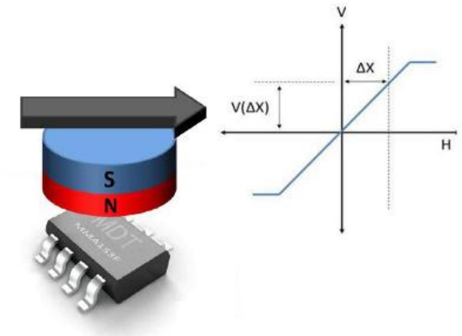

HD-Read HDD

Key parameters for MTJ

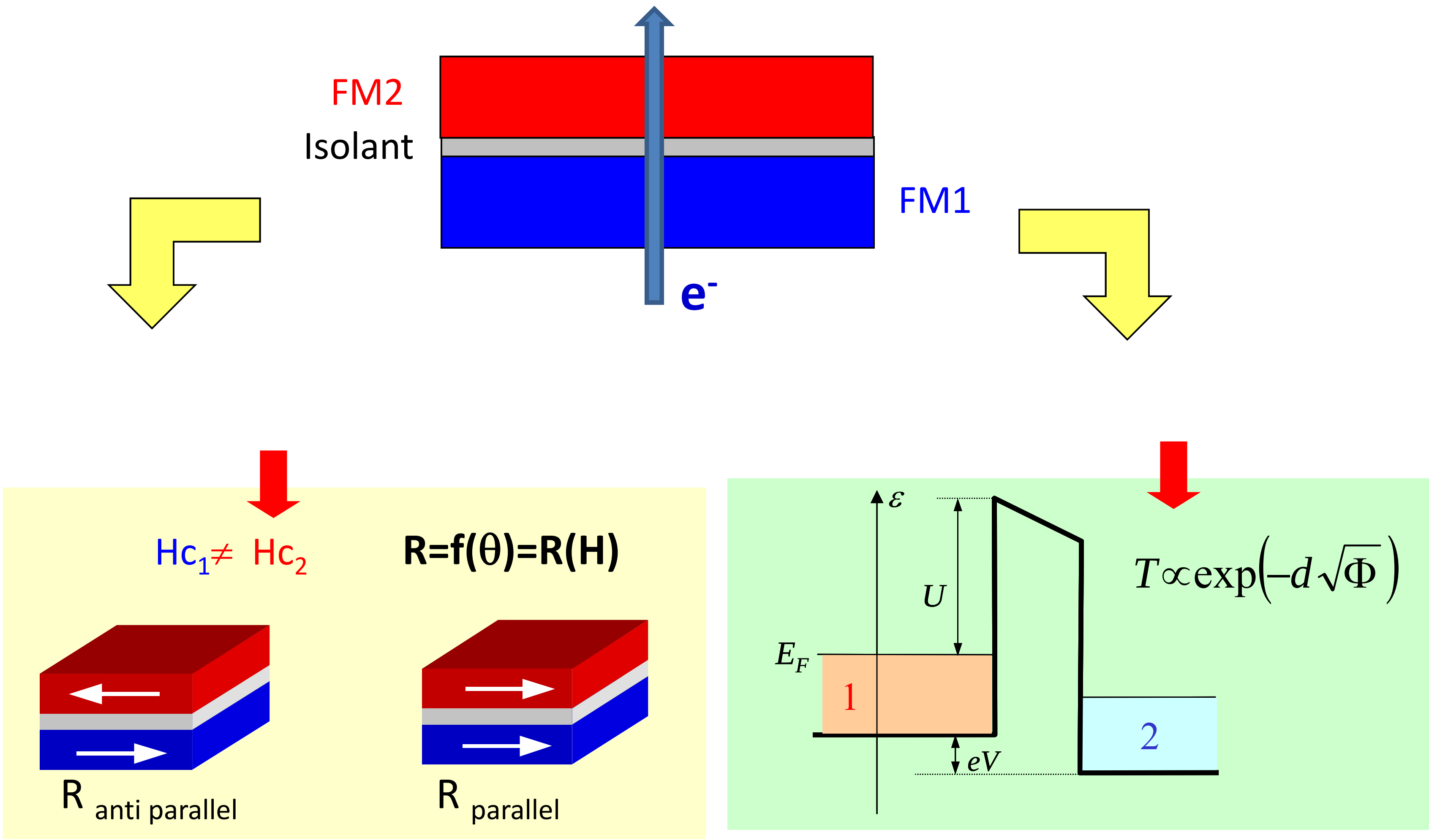

Control of magnetic properties of electrodes

Control of barrier structure at nanometer scale

(I) Control of magnetic properties

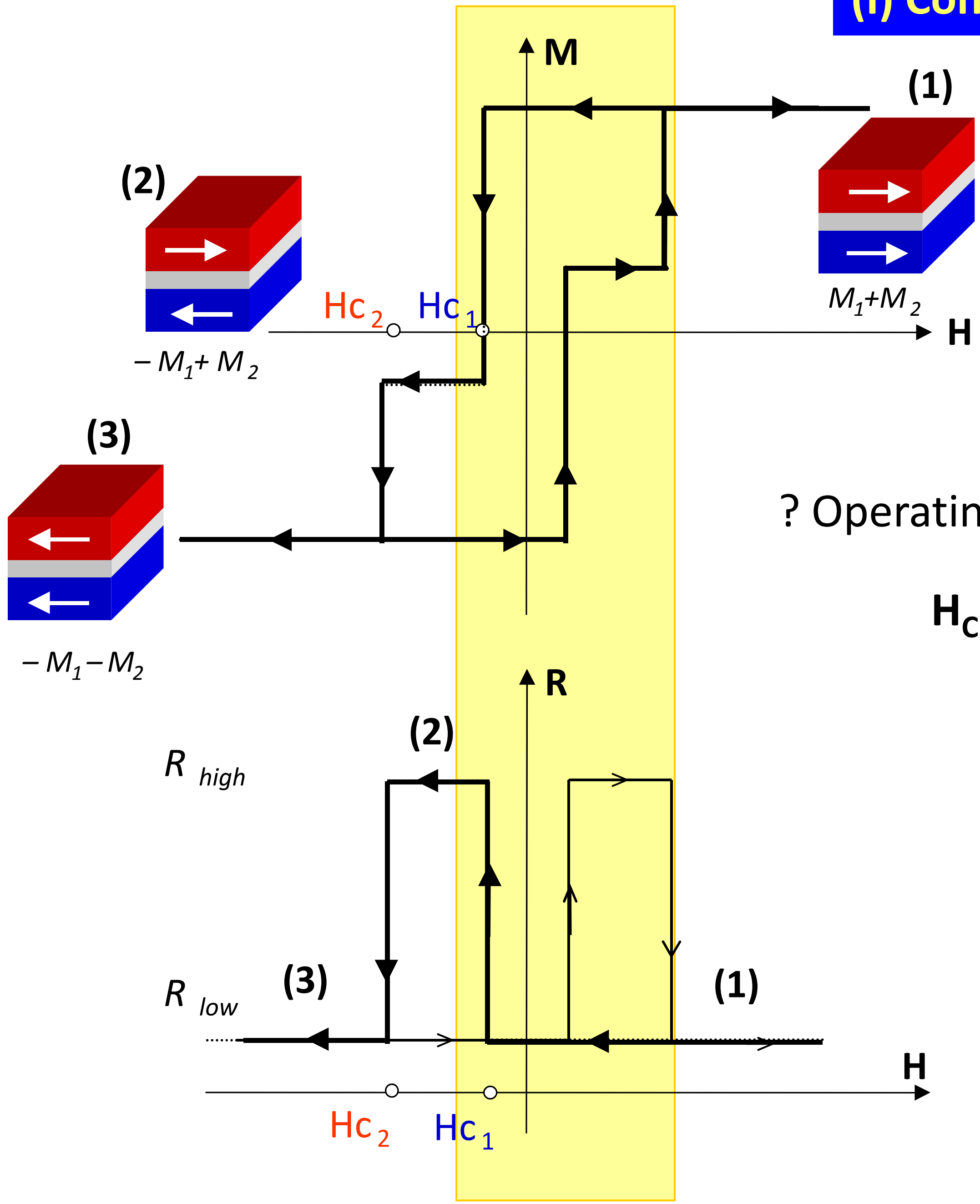

? Operating at low fields:

$H_{C1}<H<H_{C2}$

Hard-soft architecture

Operating an MTJ:
M(H) <=> R(H)

(I) Control of magnetic properties

$|H|<H_{C2}$

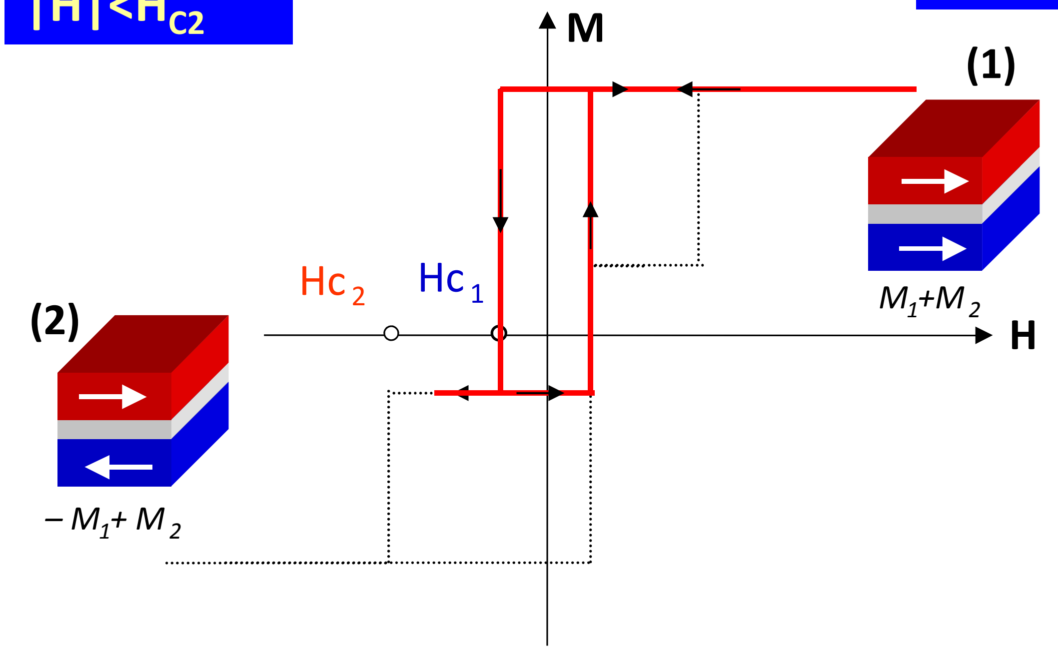

Minor loop:

- Layer M_2 blocked
- Layer M_1 mobile

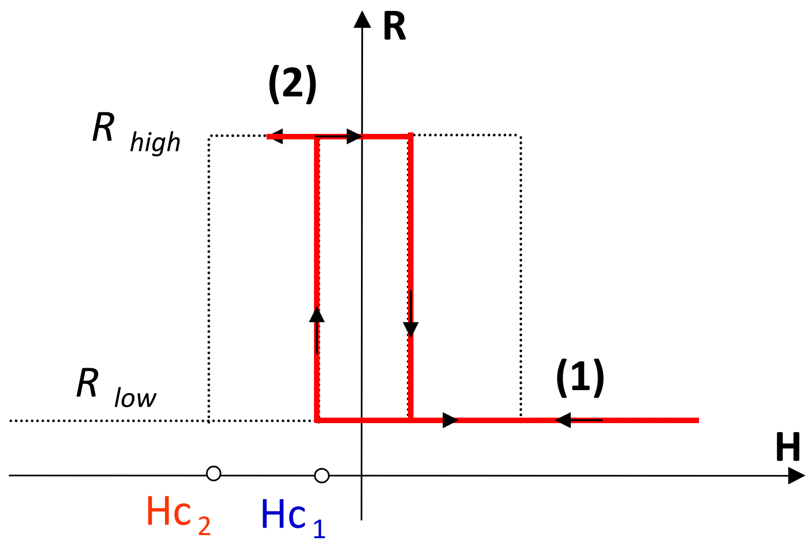

Hard-soft architecture

JTM: M(H)<=> R(H)

Hardening: difficult task in 3d FM thin films

Exchange biased SyAF *reduces stray-fields and Hard/soft dipolar coupling*

(1) Clasically

- 2 materials ≠K
  cristalline phase
  Fe(bcc) vs Co(hcp)

- ≠ aspect ratios of FM electrodes
  Complex micromagnetic problems

(2) Exchange biasing

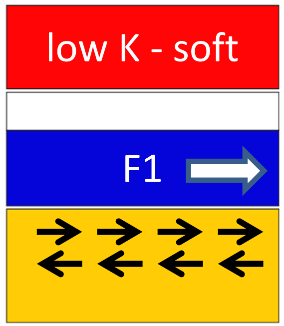

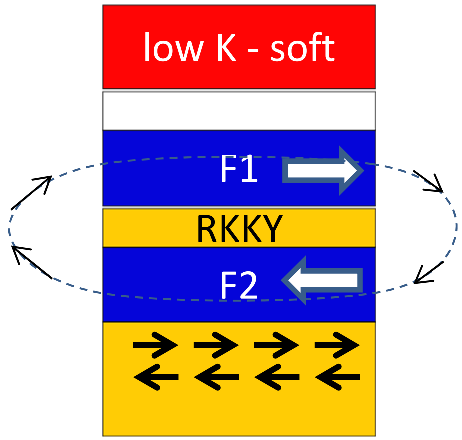

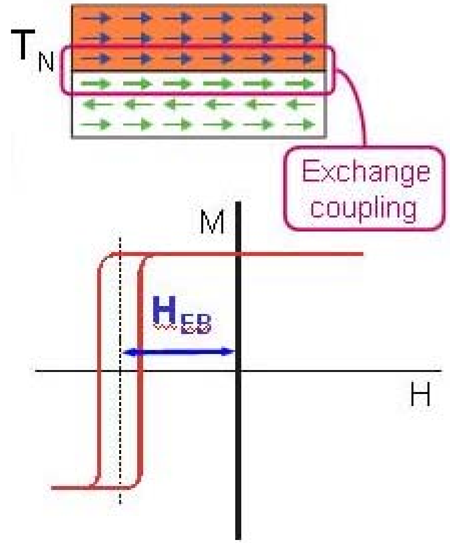

Typical Magnetoresistance versus magnetic field

hard–soft MTJ

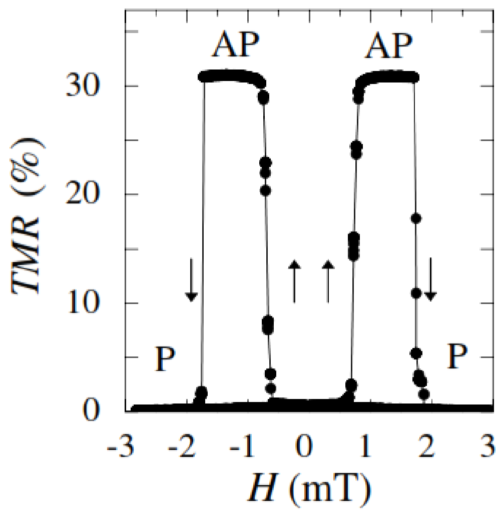

exchange-biased MTJ

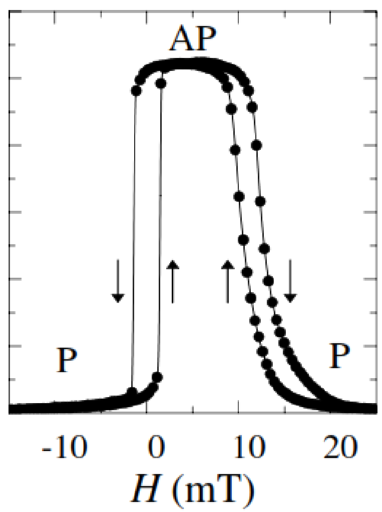

E. Tsymbal et al, J. Phys.: Condens. Matter 15 (2003) R109–R142

For applications

Beyond static =>
Complex micromagnetic problems

Dynamic magnetic properties related to fast and homogeneous magnetization switching have to be optimized:

Pillar shape, aspect ratio, FM material, switching mechanisms (field, spin-current/torques, thermal assisted…).

(II) Control of barrier structure

$$T \propto \exp\left(-d\sqrt{U}\right)$$

Control of d

Image AFM

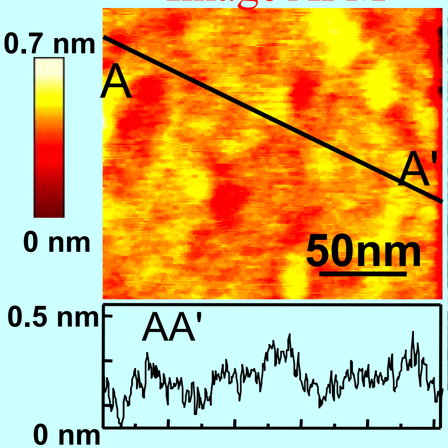

Image TEM

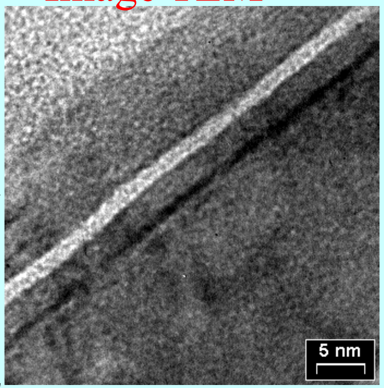

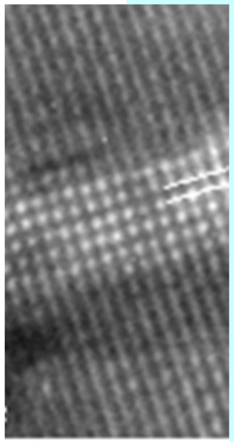

Optimisation of buffer layer
==> small roughness

*C. Tiusan et al, JAP **85**, 5276 (1999)*

Control of epitaxial growth in epitaxial (single crystal or textured) MTJs

Control of U

Tunnel cartography

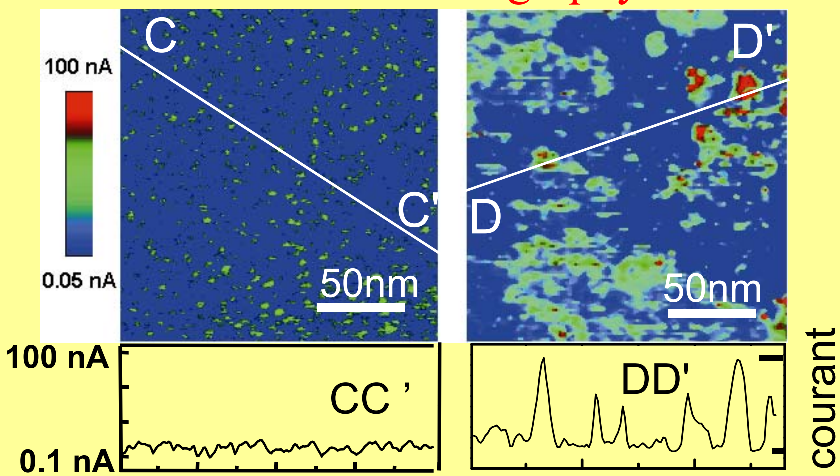

homogenuous inhomogène

Homogeneity of tunnel current

*V.DaCosta, C. Tiusan, T. Dimopoulos, K. Ounadjela, PRL **85**, 876 (2000)*

Magnetic tunnel junction – underlying Physics

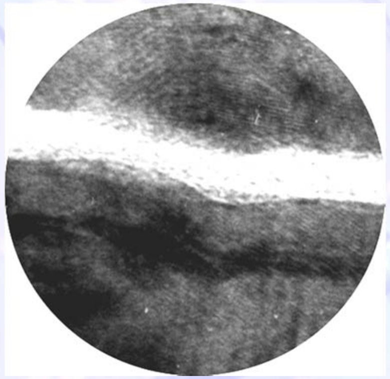

C. Tiusan et al, Phys. Rev. Lett. 85, 876 (2000);
Phys. Rev B 61, 580, (2000)

Polycrystalline MTJs : random distribution of crystallographic axes (amorphous barrier)

$\Rightarrow$ free electron model (constant potential + plane waves) $\Psi(r) = e^{ikr}$

$\Rightarrow$ Tunnel transport ***independent of*** propagation direction

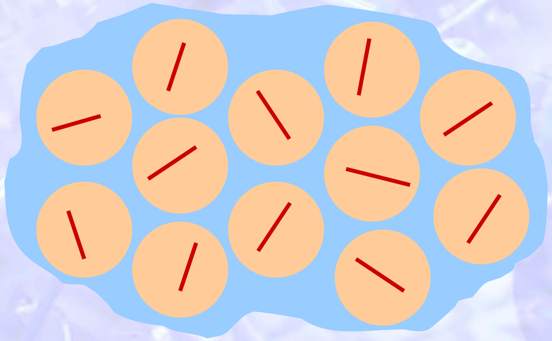

Single crystal MTJs

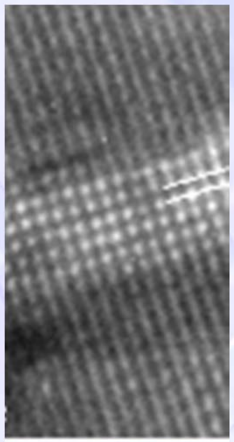

Single crystal electrodes : anisotropy of space

$\rightarrow$ properties dependent of propagation direction

$\rightarrow$ potential : crystal periodicity

$\Rightarrow$beyond the free-electrons model: Bloch waves

$$\Psi_{nk}(r) = e^{ikr} u_{nk}(r)$$

Fully epitaxial systems

Conservation of symmetry across the stack

! Model systems where theory and experiment confront

C. Tiusan et al, Appl. Phys. Lett. 82, 4507, (2003)
J. Phys. Cond. Mat. 19, 165201, (2007).

(I) Polycrystalline MTJs (Al2O3 based)

Hystorically, first MTJ systems

1995 discovery of the TMR effect at RT

The first observation of reproducible, large room temperature magnetoresistance in a CoFe/Al2O3/Co MTJ

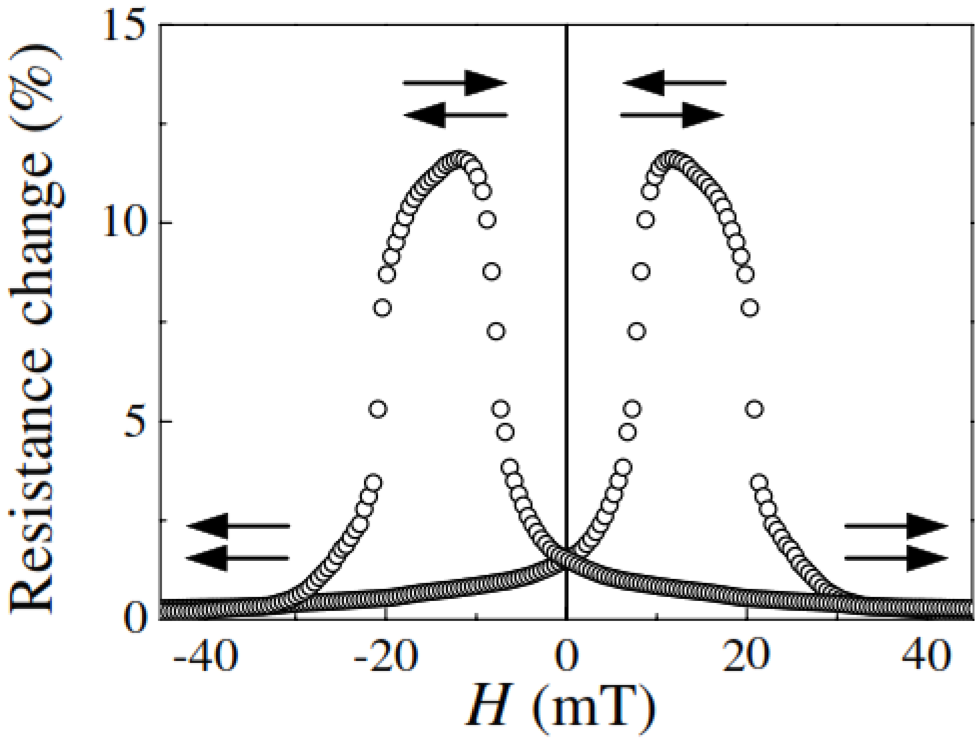

Moodera J S, Kinder L R, Wong T M and Meservey R Phys. Rev.Lett. ***74,*** *3273,* ***(****1995)*

Early experiments and models

1. Experiments on spin-dependent tunnelling

Measure the spin polarization of the tunnelling current originating from various ferromagnetic metals across an alumina insulating barrier in ferromagnet/insulator/superconductor (FM/I/S) tunnel junctions

Tedrow and Meservey

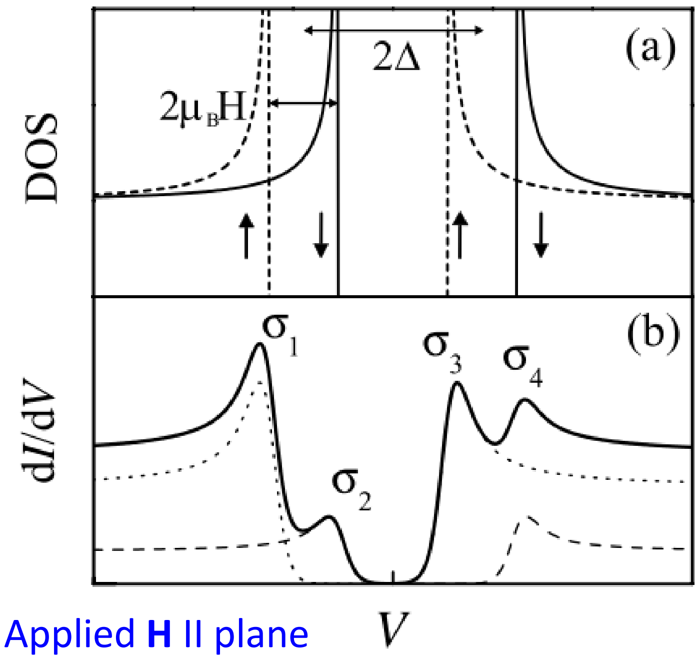

Applied **H** II plane

superconducting Al film which acts as a spin detector

$$P = \frac{G^{\uparrow} - G^{\downarrow}}{G^{\uparrow} + G^{\downarrow}} = \frac{(\sigma_4 - \sigma_2) - (\sigma_1 - \sigma_3)}{(\sigma_4 - \sigma_2) + (\sigma_1 - \sigma_3)}$$

The results of these early experiments on SDT were interpreted in terms of the DOS of the ferromagnetic electrodes at E_F

$$P_{FM} = \frac{n_{\uparrow} - n_{\downarrow}}{n_{\uparrow} + n_{\downarrow}}$$

Spin polarization

FM	$P_{exp} = \frac{G^{\uparrow} - G^{\downarrow}}{G^{\uparrow} + G^{\downarrow}}$	$P_{calc} = \frac{n^{\uparrow} - n^{\downarrow}}{n^{\uparrow} + n^{\downarrow}}$
Fe	+45%	+61%
Co	+42%	-77%
Ni	+32%	-81%

inconsistency between measured P and P_{FM}

*The inconsistency between the experimental and theoretical SP = consequence of the fact that the **tunneling conductance** depends not only on the **number of electrons** at the Fermi energy but also on the **tunneling probability**, which is different for various electronic states in the ferromagnet*

2. Stearns' model

Takes into account features of band structure in tunneling

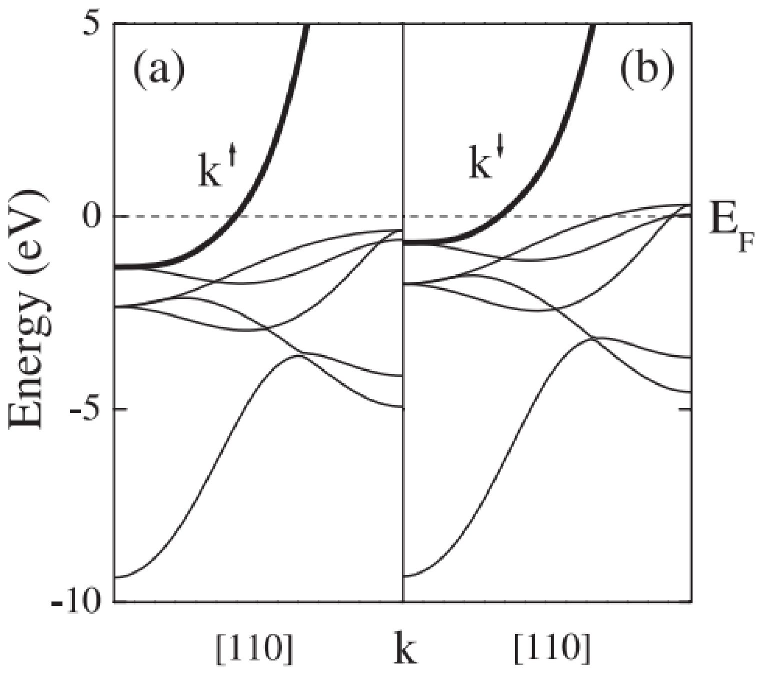

Electronic bands in bulk fcc Ni in the [110] direction for the majority-spin (a) and minority-spin (b) electrons.

- **transmission probability** depends on the effective mass which is different for different bands
- **localized d electrons** => large effective mass and therefore decay very rapidly into the barrier region
- **the dispersive s-like electrons** decay slowly

the nearly free-electron (most dispersive bands) dominate the tunnelling current

The heavy curves show the free-electron-like bands which dominate tunnelling. $k\uparrow$ and $k\downarrow$ are the Fermi wavevectors which determine **the spin polarization of the tunnelling current:**

$$P_{FM} = \frac{k^{\uparrow} - k^{\downarrow}}{k^{\uparrow} + k^{\downarrow}}$$

Using an accurate analysis of the electronic band structure, Stearns found that P_{FM} = 45% for Fe and 10% for Ni, which are consistent with the experimental data

- **Stearns: introduces the notion of TDOS (tunneling density of states)**

  early indication that the understanding of SDT requires detailed knowledge of the electronic structure of MTJs

3. Julliere's experiments and model

M. Jullière, Phys. Lett. A54, 225, (1975).

1975, first observation of TMR effect in Fe/Ge/Co MTJ (4.2K)

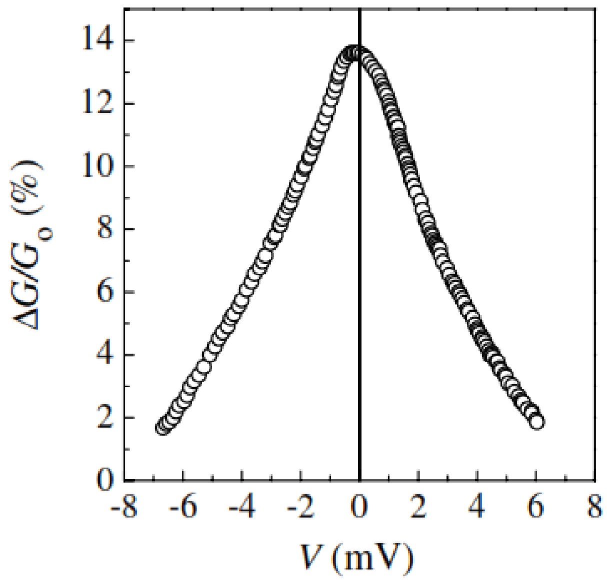

- **Correlates TMR and polarization P**

Assumptions:

- ❑ two independent current model (up, dn spin)
- ❑ tunneling from DOS up1-up2, dn1-dn2 in **P** and up1-dn2, dn1-up2 in **AP**

$$\boxed{\begin{aligned} G_P &\propto n_1^\uparrow n_2^\uparrow + n_1^\downarrow n_2^\downarrow \\ G_{AP} &\propto n_1^\uparrow n_2^\downarrow + n_1^\downarrow n_2^\uparrow \end{aligned}}$$

$$\Rightarrow \quad \boxed{TMR = \frac{G_P - G_{AP}}{G_{AP}} = \frac{R_{AP} - R_P}{R_P} = \frac{2P_1P_2}{1 - P_1P_2}}$$

with

$$P_{1(2)} = \frac{n_{1(2)}^\uparrow - n_{1(2)}^\downarrow}{n_{1(2)}^\uparrow + n_{1(2)}^\downarrow}$$

Tunneling Magnetoresistance

MTJ	Julliere	Experiment
$Ni/Al_2O_3/Ni$	25%	23%
$Co/Al_2O_3/Co$	42%	37%
$Co_{75}Fe_{25}/Al_2O_3/Co_{75}Fe_{25}$	70%	69%
$Co_{70}Fe_{30}/MgO/Co_{70}Fe_{30}$	520%	~600%

Consistency between measured SP (Tedrow-Meservey) and TMR values

4. Slonczewski's model

SP depends on both electrode and barrier

First accurate theoretical consideration of TMR

Slonczewski J C Phys. Rev. B ***39*** *6995 (1989)*

- Tunnelling between two identical ferromagnetic electrodes separated by a rectangular potential
- The ferromagnets described by two parabolic bands exchange splitted

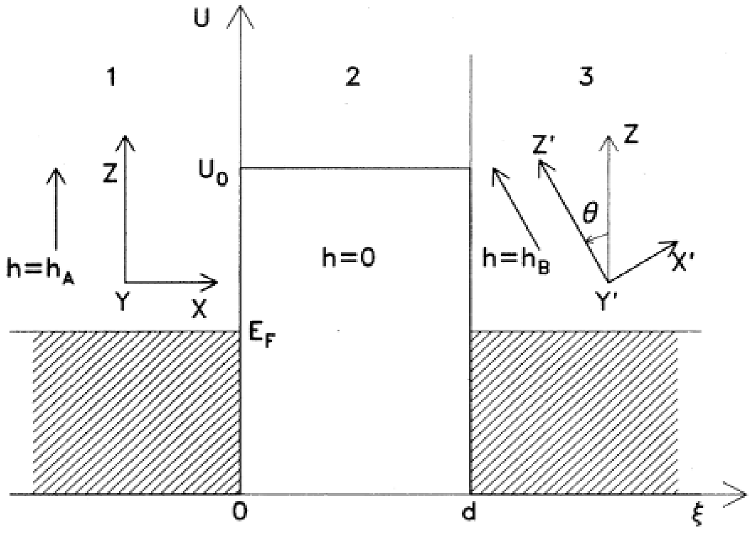

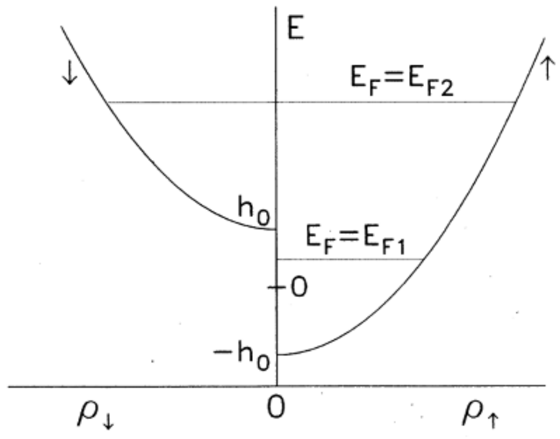

Explains the spin-valve effect

$$G(\Theta) = G_0(1 + P^2 \cos\Theta)$$

$$P = \frac{k^\uparrow - k^\downarrow}{k^\uparrow + k^\downarrow} \frac{\kappa^2 - k^\uparrow k^\downarrow}{\kappa^2 + k^\uparrow k^\downarrow}$$

Additional term depending on barrier attenuation rate

$$\kappa = \sqrt{(2m/\hbar^2)(U - E_F)}.$$

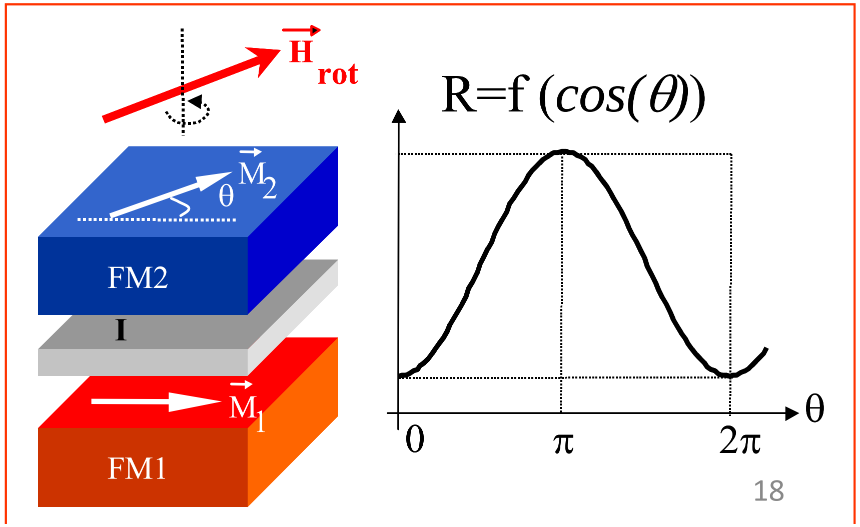

Recent experiments

Angular dependence of TMR

Moodera J S and Kinder L R 1996 J. Appl. Phys. ***79 4724***

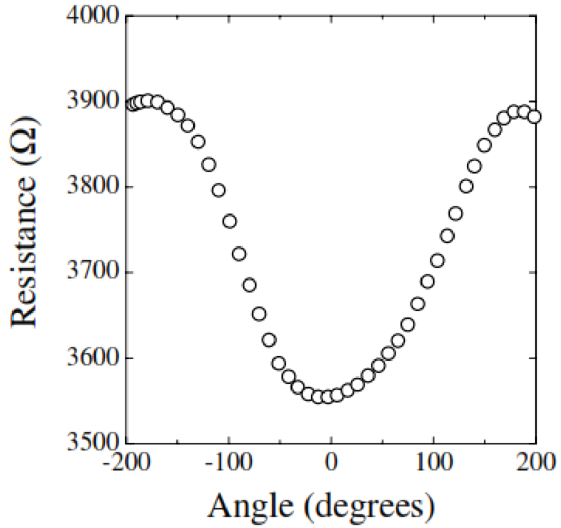

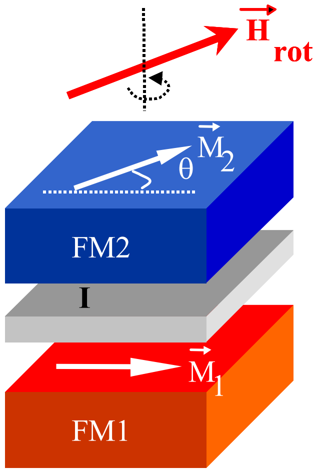

Confirms Slonczewski and open area of angular sensors

Voltage dependence

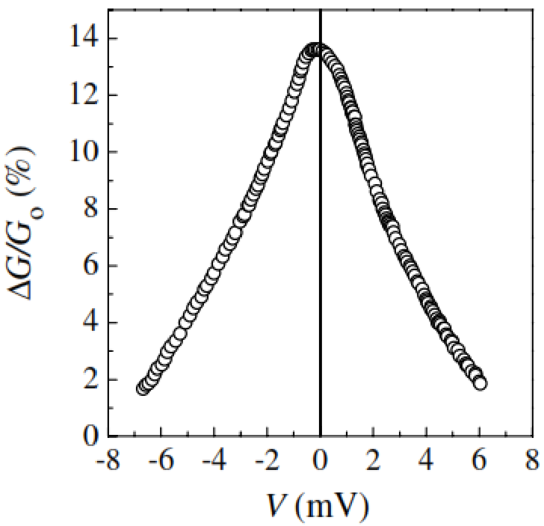

! Important for applications

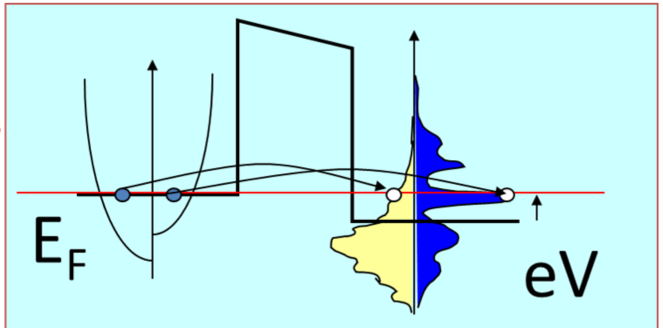

$I^{\sigma}(V) \sim n^{\sigma}_{L}(E_F)\ \ n^{\sigma}_{R}(E_F+eV)$

Intrinsic mecanisms

- ❑ barrier decreased by V reduces P (see Slonczewki factor)
- ❑ electrode DOS dependence on energy

extrinsic mecanisms:

scattering by magnons at FM/I interface

Zhang S et al, 1997 *Phys. Rev.Lett.* ***79 3744***

+ other complex mechanisms related to tunneling

Temperature dependence Important for applications **TMR decreases with increasing T**

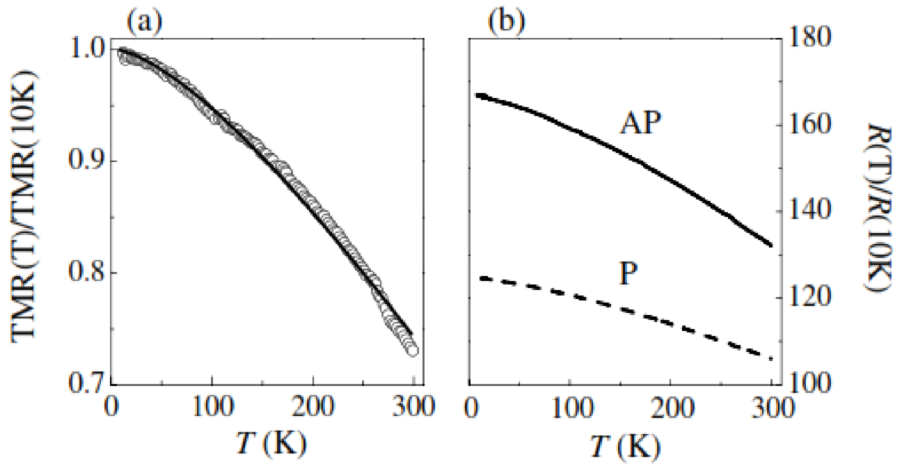

Co/Al2O3/Co MTJ

P. LeClair, PhD thesis, Univ. Eindhoven

- **the tunnelling spin polarization *P decreases with increasing* temperature**

due to **spin-wave excitations**, as does the surface magnetization (P and M follow Bloch 3/2 law)

$$\boxed{M(T) = M(0)(1 - \alpha T^{3/2})}$$

Shang C H, et al, 1998 Phys. Rev. B ***58 R2917***

- **Spin-flip scattering by magnetic impurities in the barrier** (Veydiaev)
- **Inelastic electron-phonon scattering** without spin-flip in the presence of localized states in the barrier (Tsymbal)

+ other complex mechanism (e.g. electronic structure, deffect assisted tunneling in realistic barriers, multiple hopping, etc…)

Vedyayev A et al, 2001 Phys. Rev. B ***63 064429***
Tsymbal E et al , 2002 Phys. Rev. B ***66 073201***
Glazman L I, and Matveev K A 1988 Sov. Phys. JETP 67 1267

Ferromagnet dependence

❑ TMR tuned via the FM material nature

	TMR (%)	
Junction	Julliere	Experiment
$Ni/Al_2O_3/Ni$	25	23
$Co/Al_2O_3/Co$	42	37
$Co_{75}Fe_{25}/Al_2O_3/Co_{75}Fe_{25}$	67–74	69
$LSMO/SrTiO_3/LSMO$	310	1800

Directly via the tunneling polarization

Various FM materials tested as electrodes:

Half- and full-Heusler: NiMnSb, Co2MnSi, oxides Cr2O, Fe3O4 perovskites LSMO…

combined with various other barriers SrTiO3, CeO2, ZnO,…

LSMO/STO/LSMO MTJ TMR>100%

Sun J Z 2001 Physica C 350 215

❑ TMR tuned via FM layer cristaline orientation

Given the TMR dependence of the DOS of the ferromagnetic electrodes

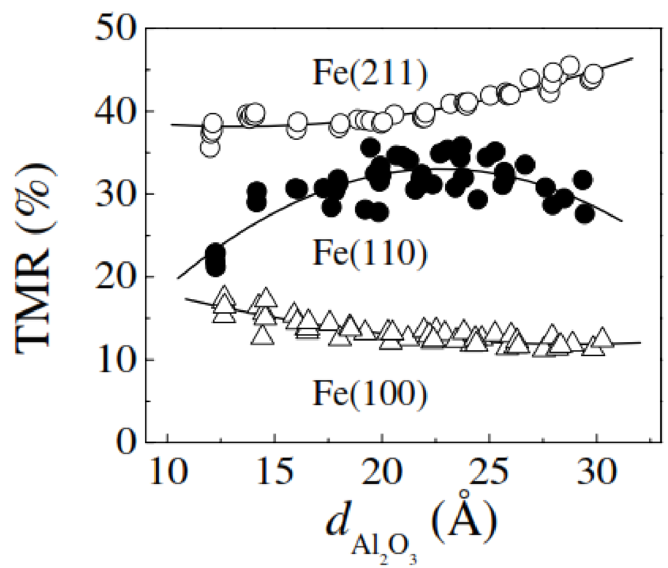

➡ **MTJs with epiaxial electrodes and amorphous barrier**

TMR at 2 K as a function of Al2O3 thickness for Fe(211), Fe(110), and Fe(100) epitaxial electrodes in Fe/Al2O3/CoFe

S: Yuasa et al, *Europhys. Lett.* ***52*** *344 (2000)*

Barrier and interface dependence

de Teresa *et al:* **the tunnelling spin polarization depends explicitly on the insulating barrier**

De Teresa et al., Science 286, 507 (1999)

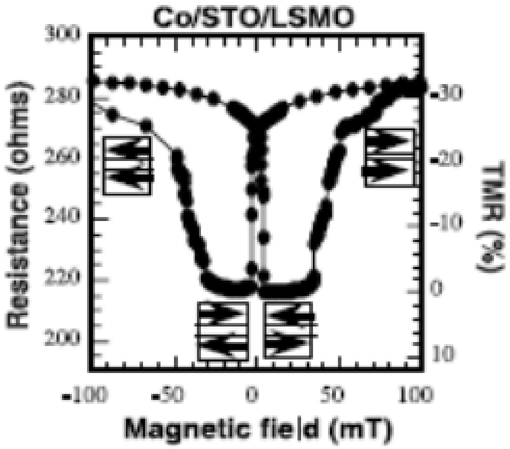

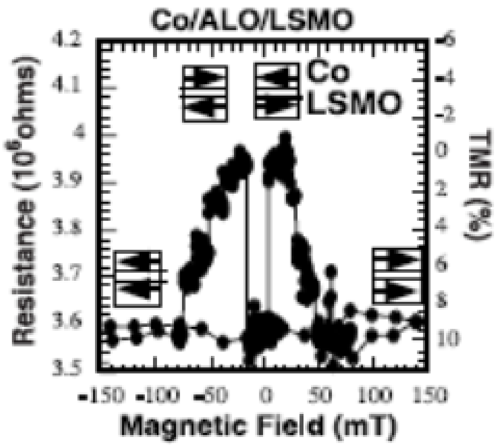

LSMO as spin analyzer (100% positive SP)

- large inverse TMR (-50%)
  for Co/SrTiO3/LSMO
- Negative spin polarization for Co/SrTiO3
- Pozitive spin polarization for Co/Al

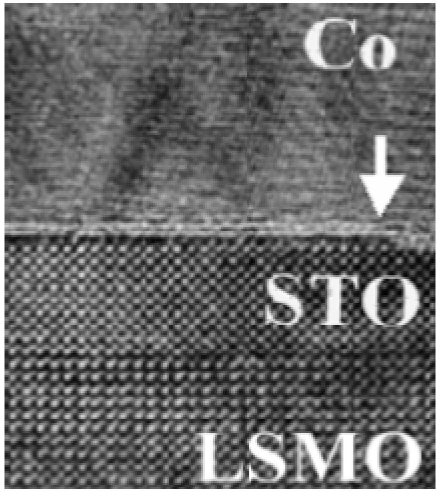

Polarization (amplitude, sign)
depends on hybridization at FM/I interface

Selection at interface of tunneling electrons
(Al2O3 selects s-like electrons, STO selects d-like electrons…)

Magnetic tunnel junction - Historically

1st generation

Tunnel magnetoresistance at RT in amorphous Alumina based MTJ:

Al2O3 age

Moodera et al, PRL (1995);
Myazaki et al, JMMM(1995).

TMR~40-70%

Best (counterintuitive result) TMR =70-80%) CoFeB/Al2O3

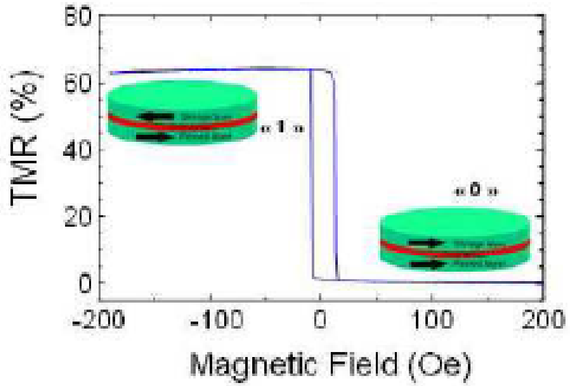

2nd generation

« Giant » tunnel magnetoresistance at RT in crystalline MgO based MTJ:

MgO age

Parkin et al, Nature Mat. (2004);
Yuasa et al, Nature Mat. (2004).

TMR~200-500%

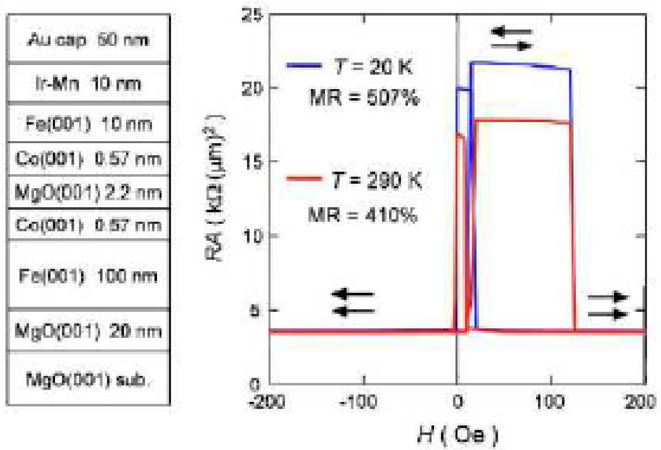

Other (oxides) barriers have been checked but less sucessfull

Magnetic tunnel junction - Historically

- **Amorphous / polycrystalline MTJs**

1995 Moodera, Miyazaki (TMR ~ 20% with amorphous Al_2O_3
Bests results : CoFeB/Al_2O_3 (TMR ~ 80%)

- **Single crystal** MgO based MTJs

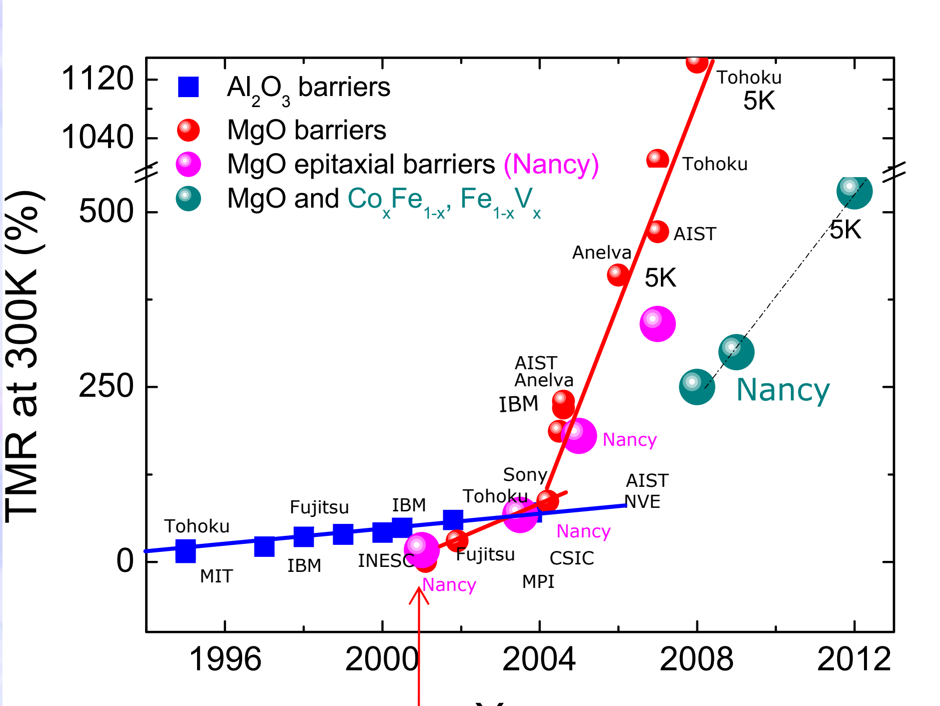

NANCY

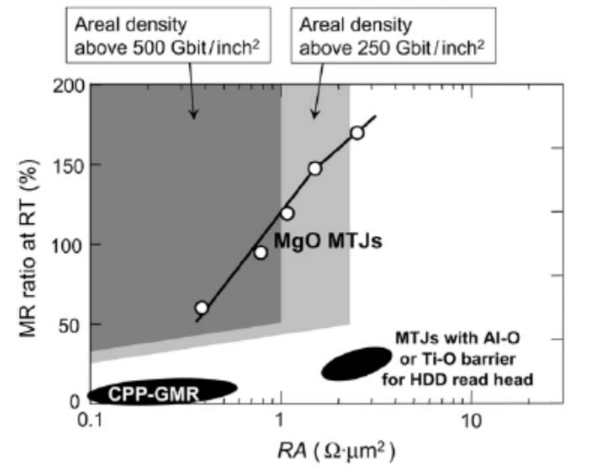

Figure 29. MR ratio at RT versus resistance-area (RA) product. Open circles are values for CoFeB/MgO/CoFeB MTJs. (Adapted from [46].) Light grey and dark grey areas are the zones required for HDDs with recording densities above 250 and 500 Gbit/inch^2.

Best result (2008):

Tohoku (H. Ohno) :
604% RT (1144% 5K)
textured CoFeB/MgO/CoFeB
(sputtering)

Single crystal MTJ– underlying physics

Why Fe(001)/MgO(001)/Fe(001) epitaxial MTJs

MODEL SYSTEM
Confront QM theory and experiment

Ideal crystallographic structure

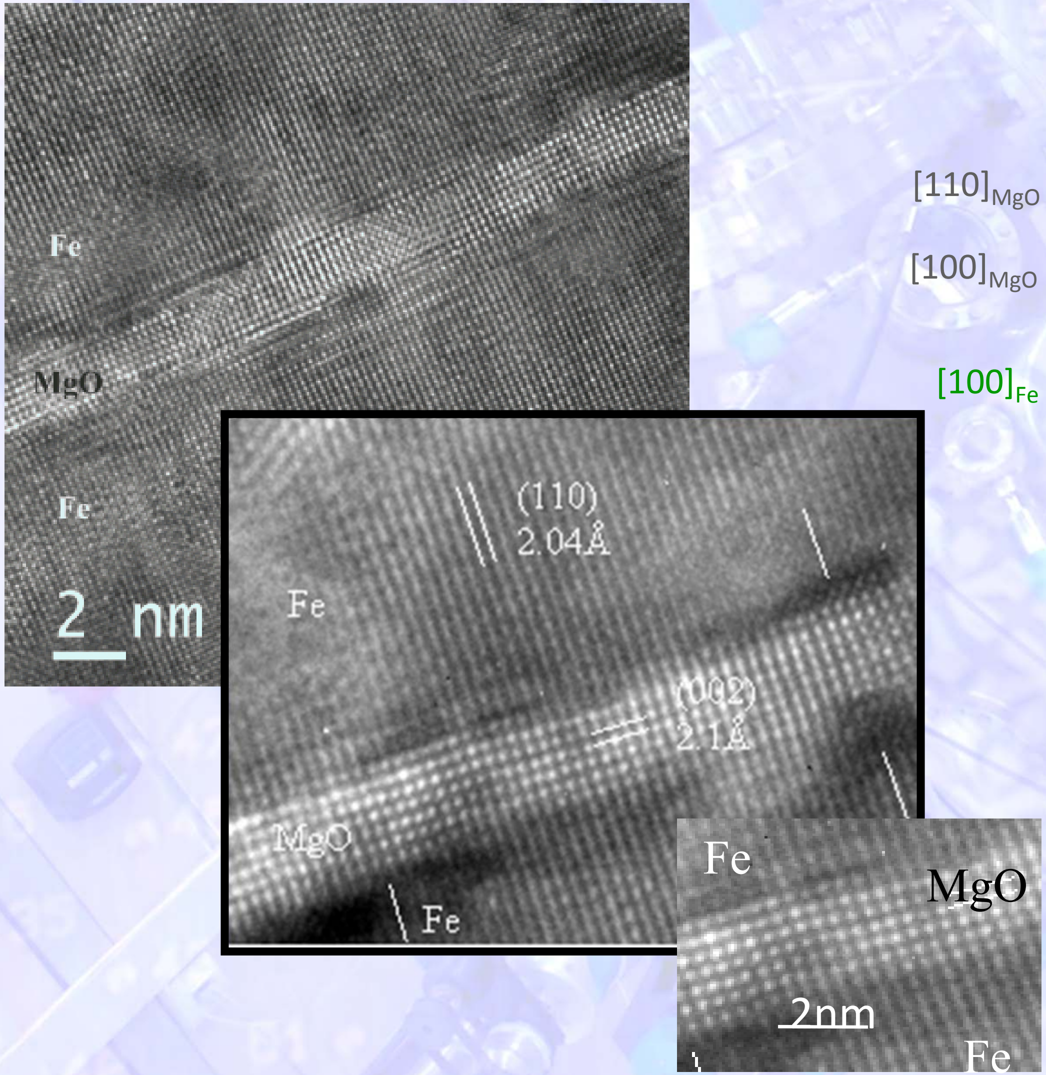

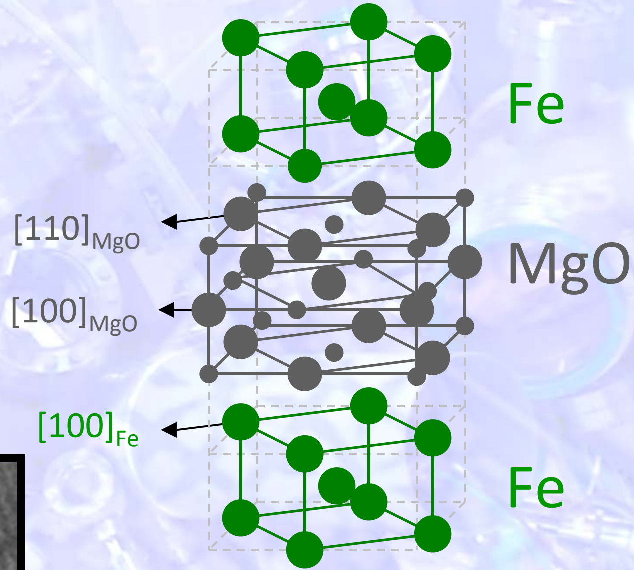

MgO
NaCl type
a= 4.21Å

Fe bcc
a = 2.87Å

Epitaxial growth
-45° rotation

Symmetry conservation

Conservation of kII

Single crystal MTJ– underlying physics

Modeling of tunnel transport in single crystal MTJs Fe(001)/MgO(001)/Fe(001)

Conservation of kII

Fe(001)/MgO(001)/Fe(001)

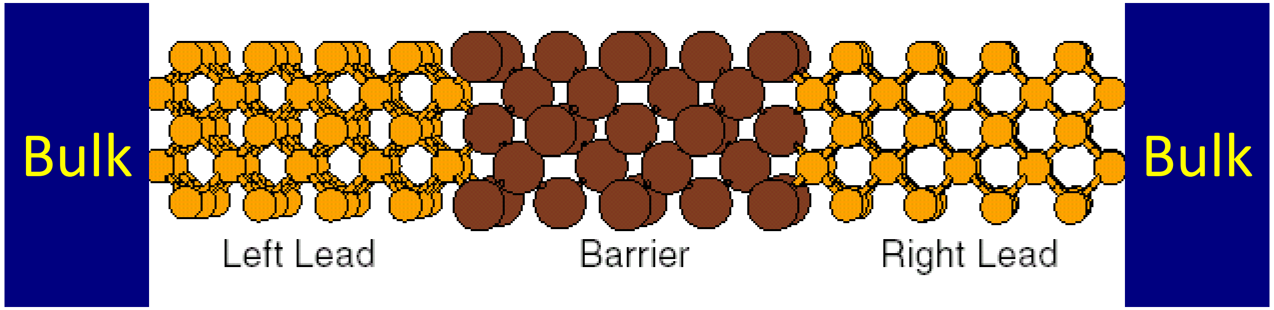

Landauer formalism

$$G = \frac{e^2}{h} \sum_{\mathbf{k}_\parallel, j, i} T(\mathbf{k}_\parallel, j, i)$$

MULTICHANNEL TRANSPORT

- The tunnel conductivity sums the transmission probability for each ($k_{||}$) channel from the state ($k_{||}$; j) to the state ($k_{||}$; i)
- Each **channel defined by a Bloch wave function in (Fe) for a given value of $k_{||}$**

Bloch wave preserve the symmetry invariance properties of the crystal

- Coherent transport with spin conservation

- **spin independent channels**
(two current model Fert-Campbell)

Tunnel transport in single crystal MTJs Fe(001)/MgO(001)/Fe(001)

Tunnel Transmission T(kII,I,j), for a k_{II} channel
matching of the real Fermi Surface of the FM metal with the complex FS of insulator

The **partial conductance G(kII)** is a direct result of the overlapping of the majority spin surface spectral densities in the two electrodes, exponentially filtered through the MgO barrier.

Majority
Surface spectral density Fe(001)

Complex FS MgO
$\mathcal{Im}\ k_{\perp}(k_x,k_y)$

G(kII)

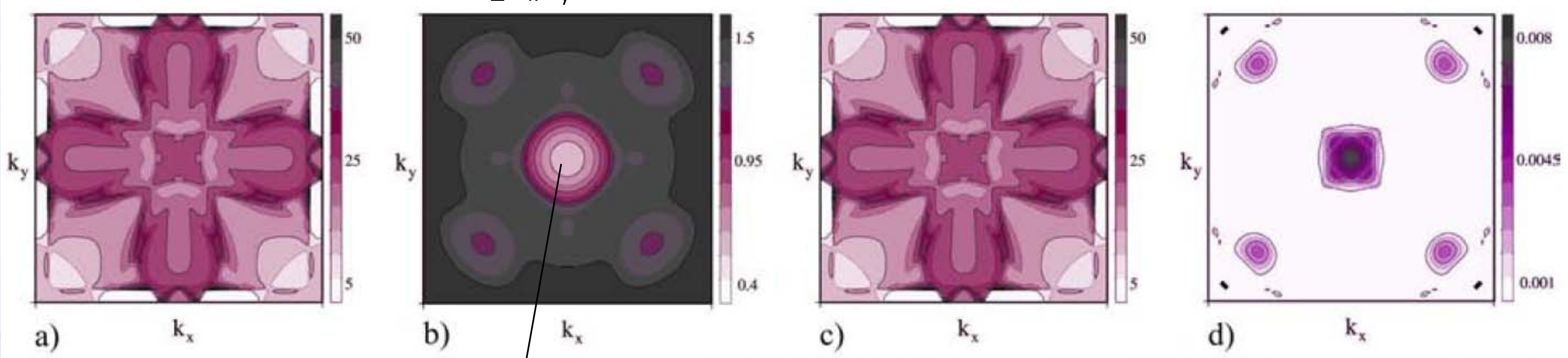

PHYSICAL REVIEW B, VOLUME 63, 220403(R)

Theory of tunneling magnetoresistance of an epitaxial Fe/MgO/Fe(001) junction

J. Mathon and A. Umerski

Large MgO thickness
transport « **dominated»** by k_{II}=0 (asympthotic regime)

Asympthotic regime : transport along $k_{||}=0$

1. Symmetry filtering within the electrodes

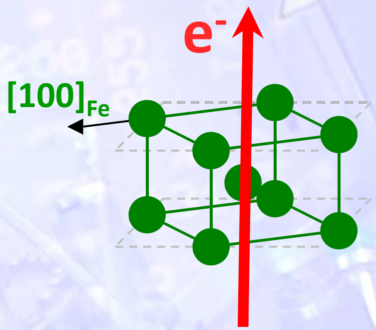

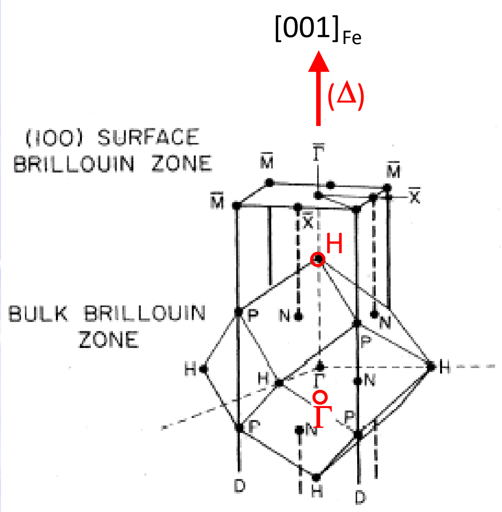

TUNNELING CHANNELS:
Selection of Bloch wave functions in Fe

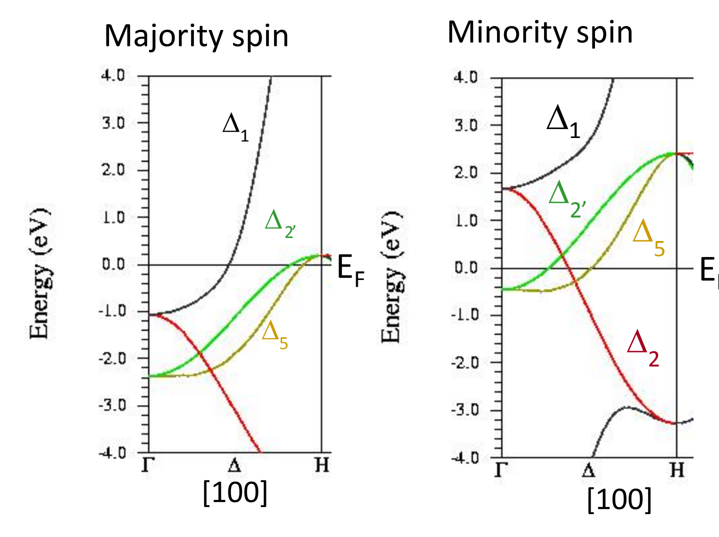

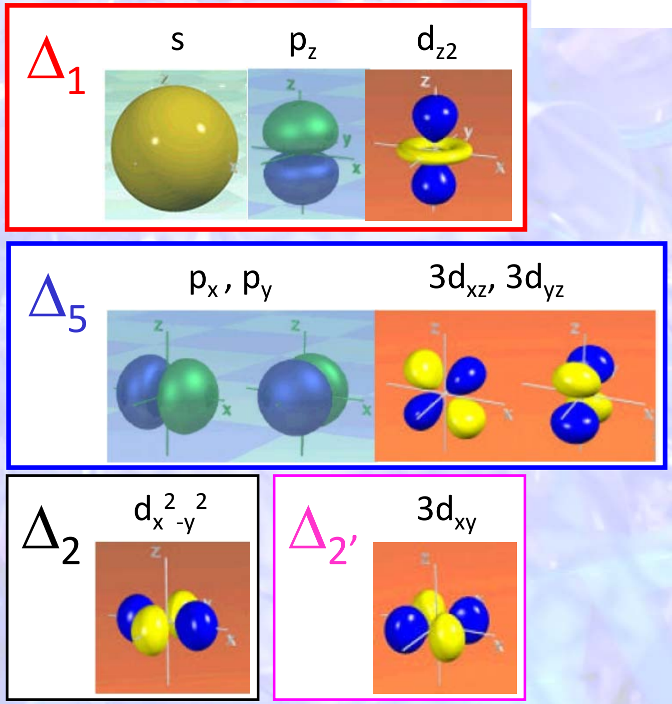

Wave Functions regrouped by symmetry

Fe(001) : half-metal* % Δ_1
=> $P^{\Delta 1}$ =100%

But other channels exist:
Δ_1, Δ_5, $\Delta_{2,\,2'}$
and $T(k_{||}\neq 0) \neq 0$

*Symmetry depenedent half metallicity SDHM

2. Symmetry dependent attenuation rates within the MgO

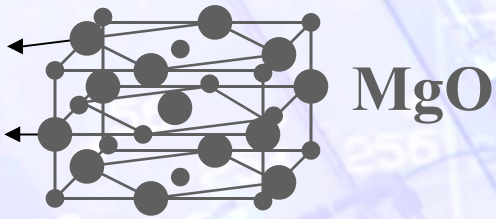

$E=E(k_{\|}, k_z)$, where $k_z=q+i\kappa$, so that $\psi \propto e^{-\kappa z}$

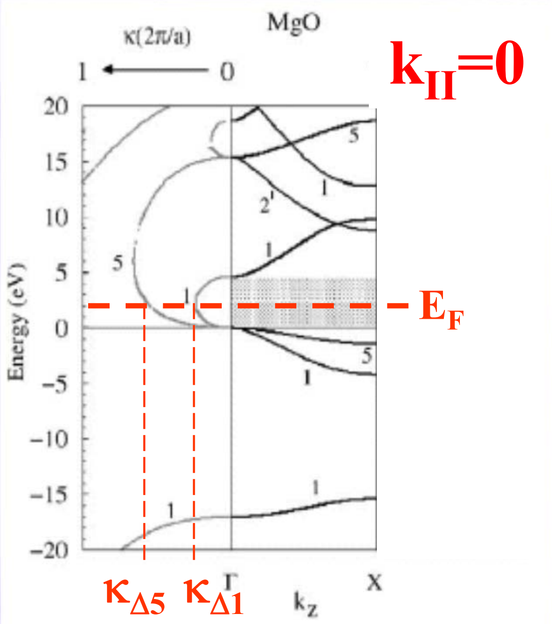

$k_z=i\kappa$ (q=0, point $\bar{\Gamma}$)

$T \sim e^{-2\kappa d}$

$\kappa_{\Delta 1} < \kappa_{\Delta 5} << \kappa_{\Delta 2, \Delta 2'}$

$k_{II}=0$

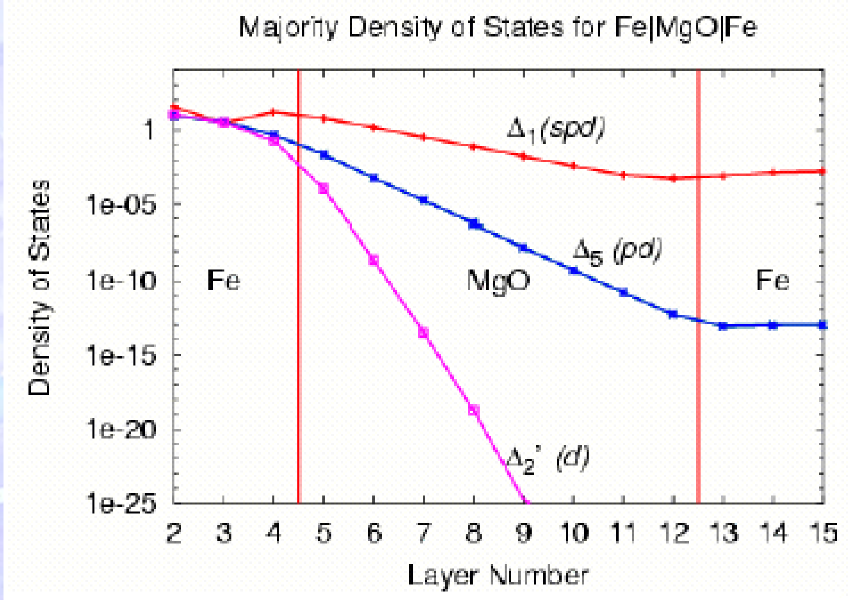

LKKR:
Butler, Zhang, Schulthess, MacLaren, Phys. Rev. B, 63 054416 (2001)
Mathon, Umerski, Phys. Rev. B, 63 220403(R) (2001)

Importance of the asympthotic regime

Large MgO thickness: Δ_1 propagation dominates
large polarisation, large TMR (> 1000%)

Experimentally

(1) Complex MBE or UHV sputtering growth

UHV 10^{-11} Torr

- High chemical purity of films
- Conservation of spin coherence in CPP transport

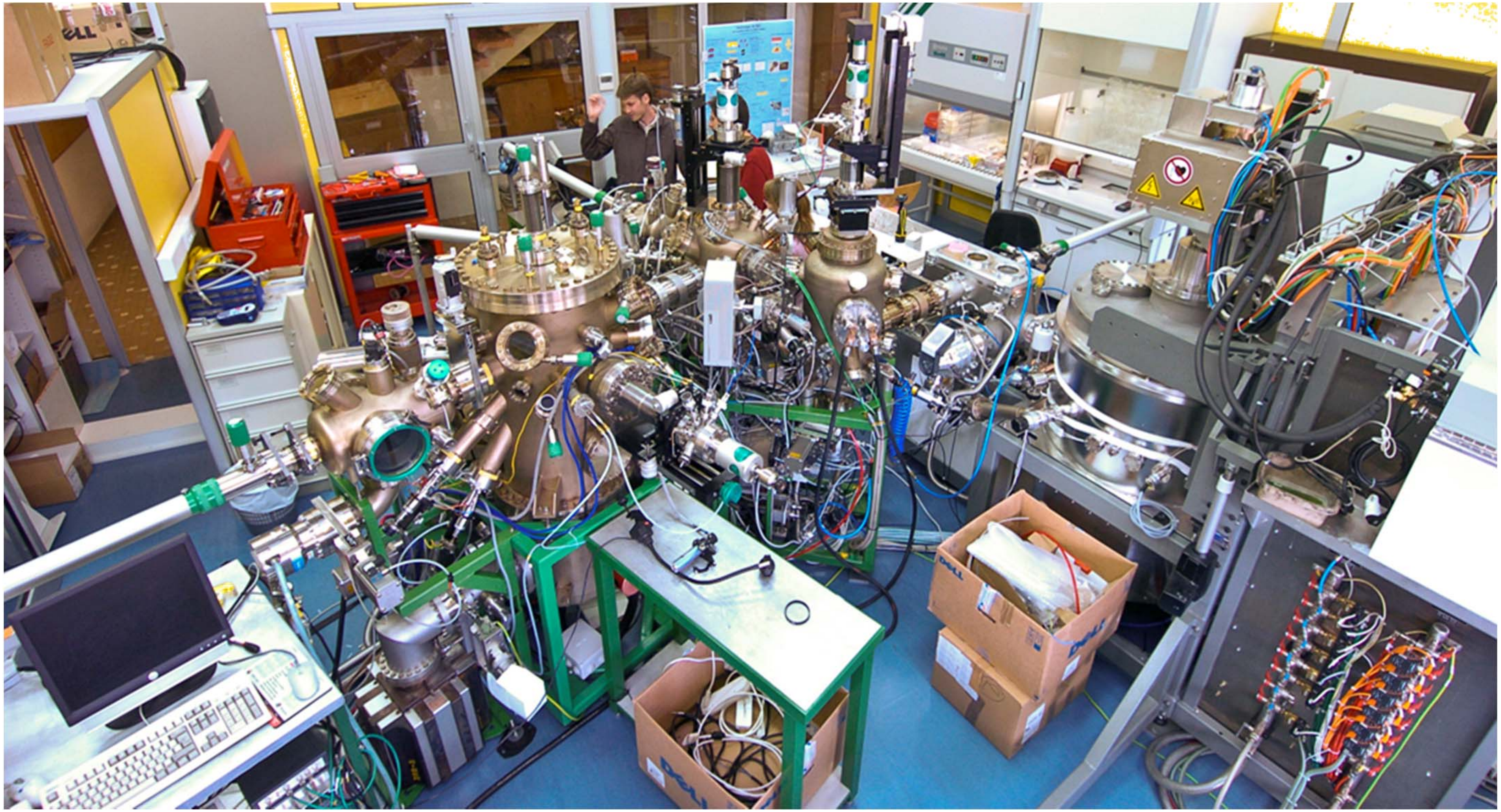

- Various growth sources (e-gun, Knudsen cell, magnetrons)
- Variable growth/in-situ annealing temperature (70-1273K)
- in-situ analysis RHEED, Auger, XPS, photoemission,…

Atomic level control of insulator thickness

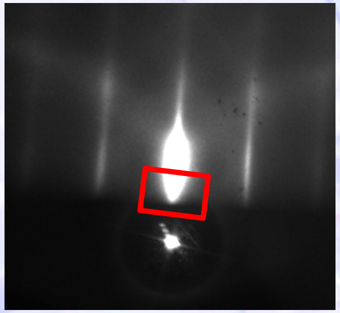

RHEED feature

Surface –diffraction technique

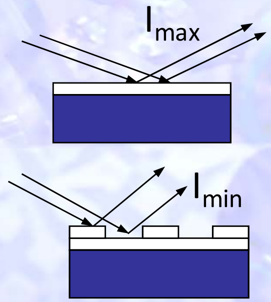

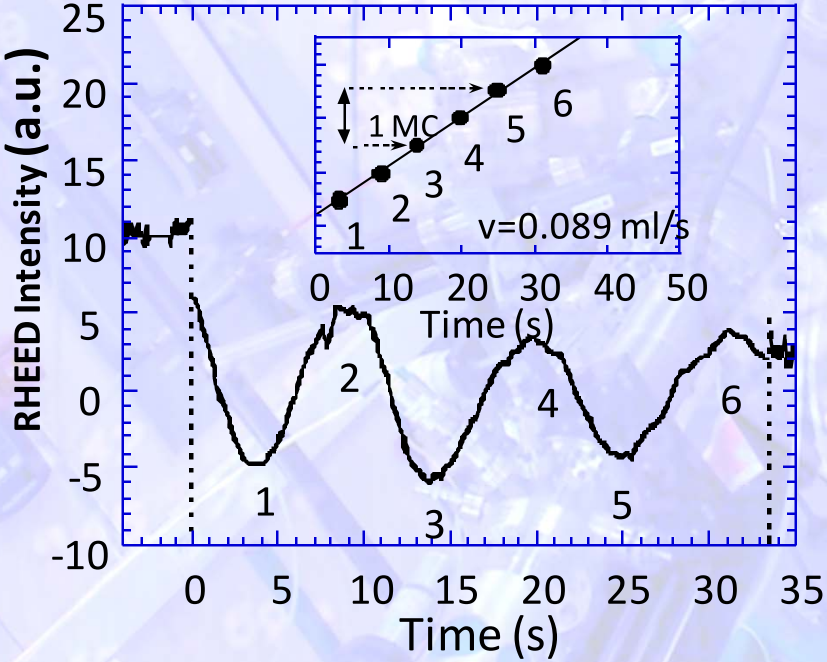

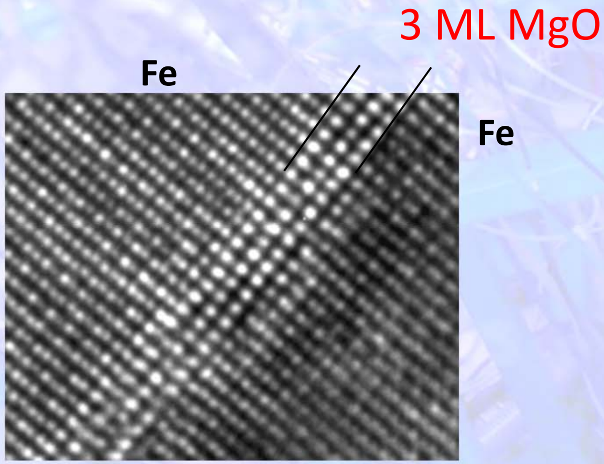

Courtesy E. Snoek CEMES, Toulouse

(2) UV, EBEAM lithography patterning of MTJ pillars

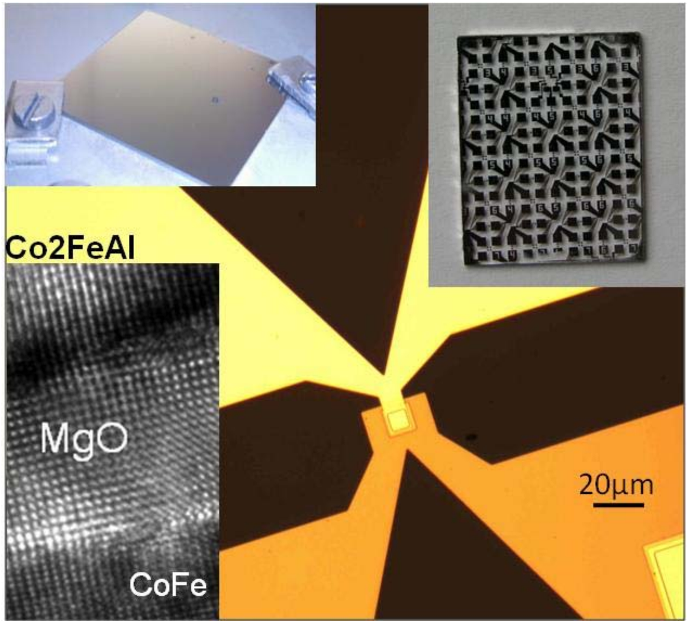

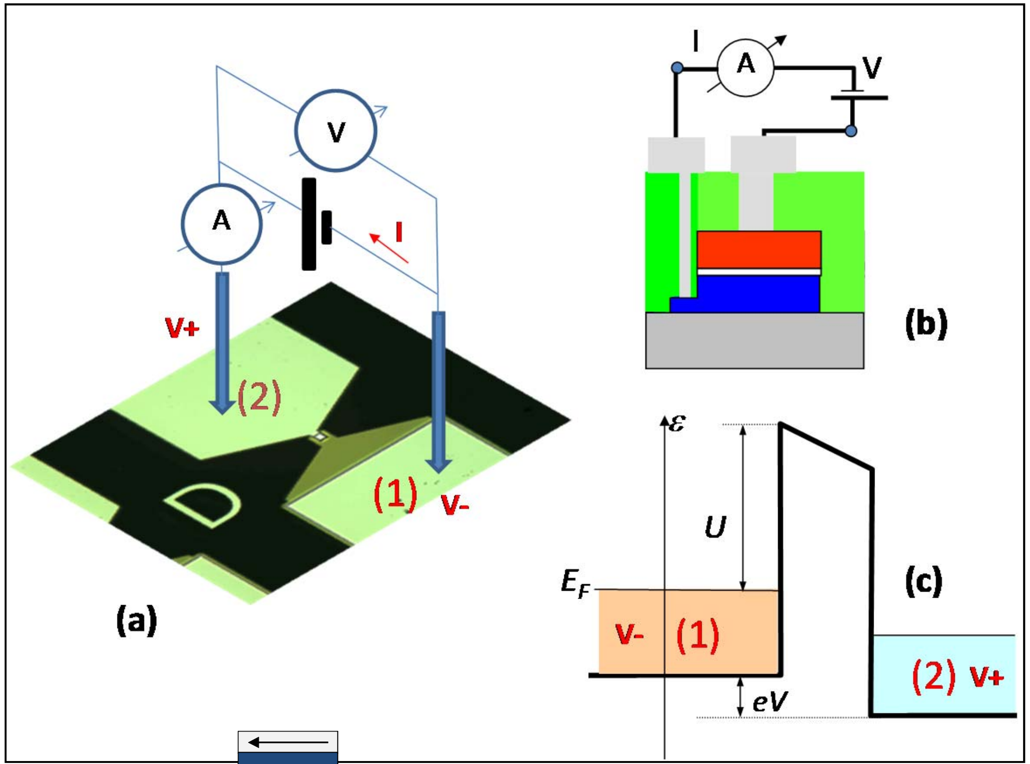

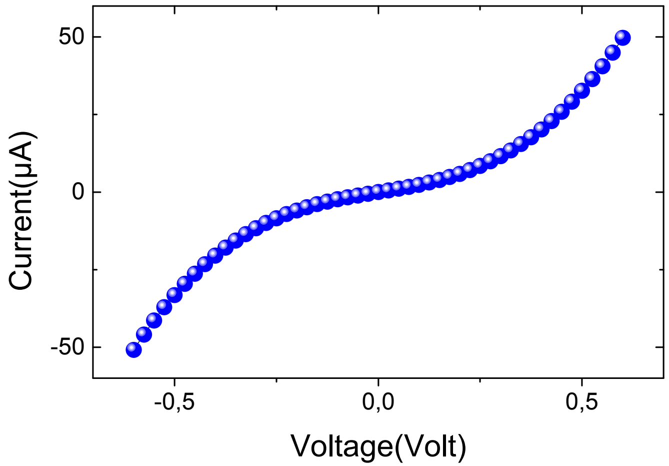

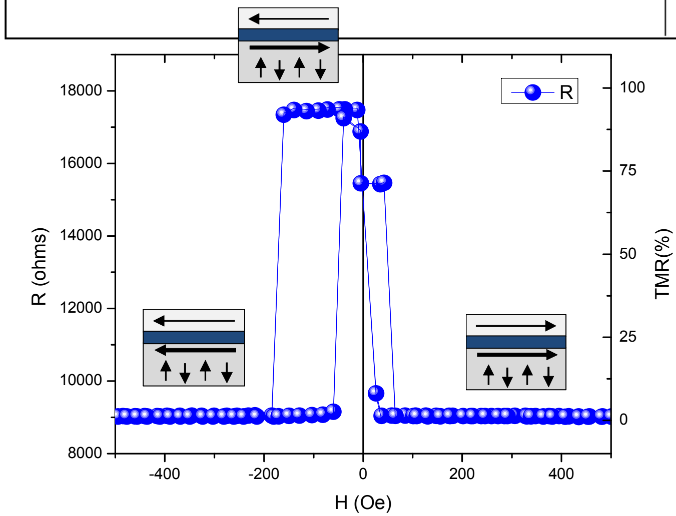

Giant TMR in Fe/MgO/Fe epitaxial MTJs

J. Faure Vincent, C. Tiusan et al, **Appl. Phys. Lett. 82**, 4507, (2003).
C. Tiusan, et al, **J. Phys.: Condens. Matter 19**, 165201, (2007).
C Tiusan et al, **Appl. Phy. Lett. 88**, 62512, (2006).

Giant TMR ~ 200% (RT), 340% (10K)

JTM Fe/MgO/Fe MTJ

UV, EBEAM lithography

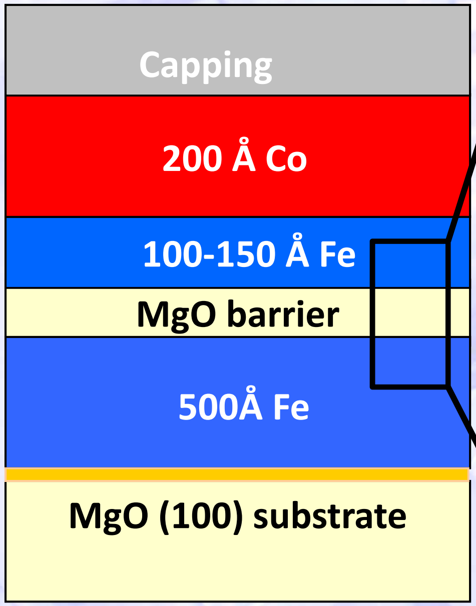

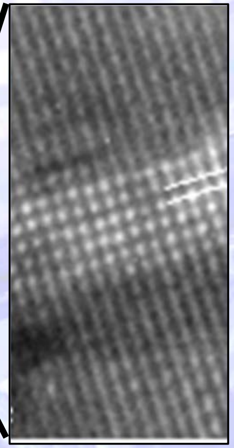

E. Snoek CEMES, Toulouse

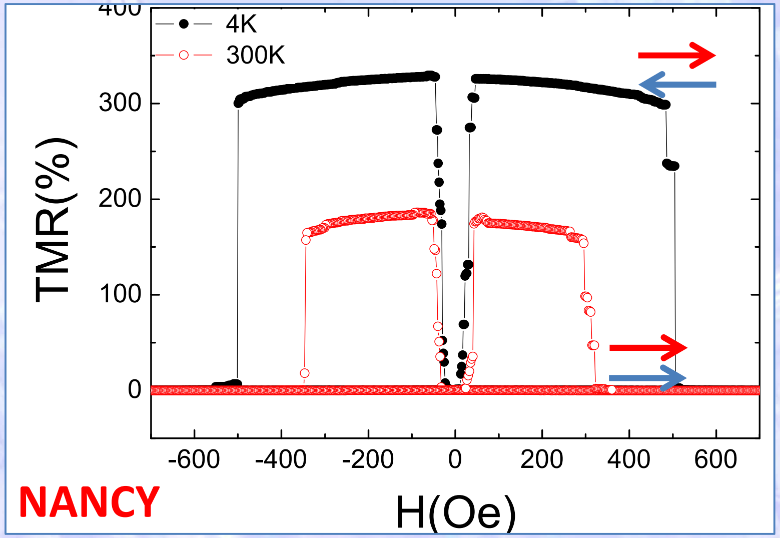

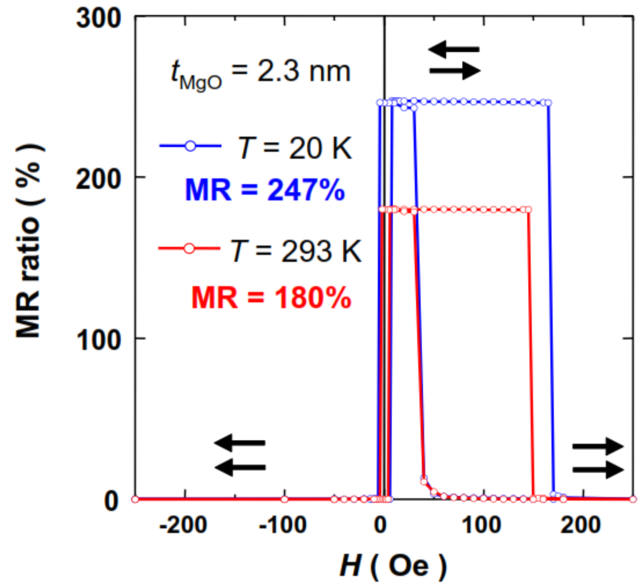

AIST MTJs with a single-crystal MgO(001) barrier

S. Yuasa *et al., Nature Materials **3, 868 (2004).***

- Electron transport physics: beyond the free electron model
- TMR amplitude: explained by spin and symmetry dependent transport

Symmetry dependent tunneling- demonstrated by tunneling spectroscopy

$$dI / dV \propto n(E_F + eV)$$

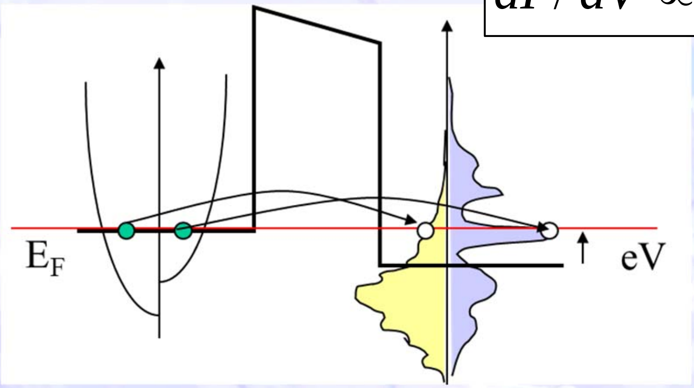

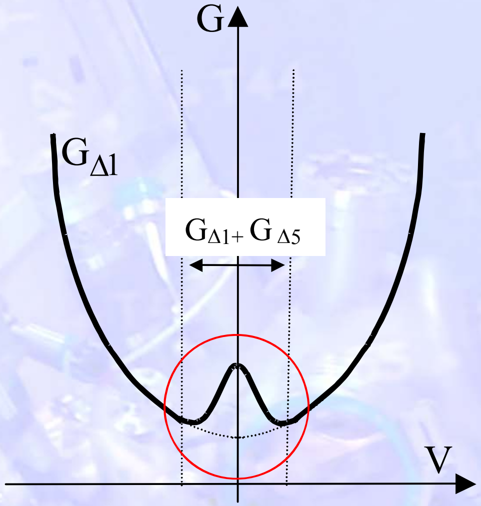

Spins UP

Configurație P

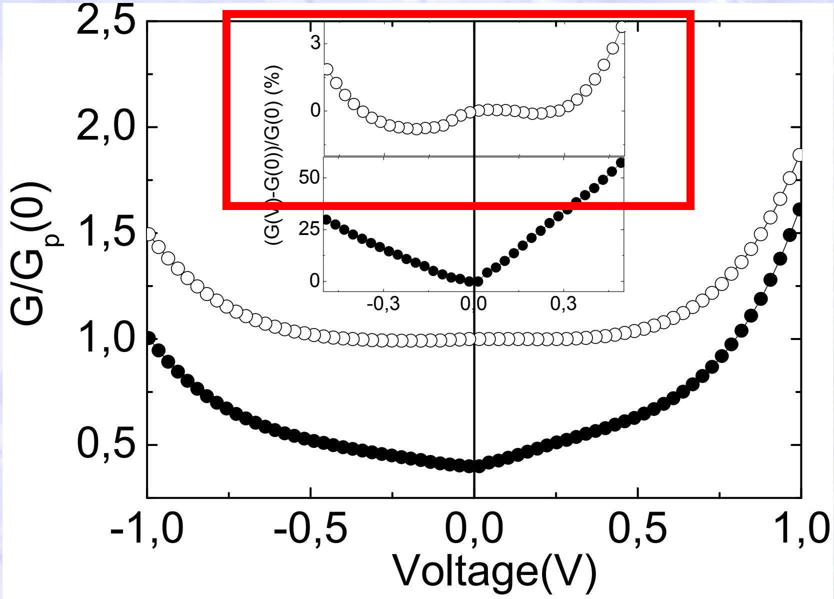

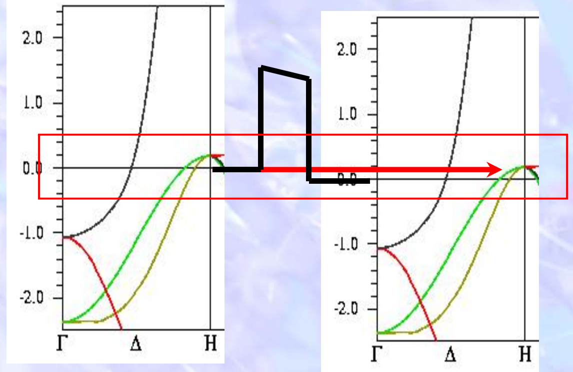

Both $\Delta 1$ cand $\Delta 5$ contribute to tunneling

Δ_5 channel activated at low voltages

R. Guerrero, C. Tiusan *et al*, **Appl. Phys. Lett. 91**, 132504 (2007)
C. Tiusan *et al*, **J. Phys.: Condens. Matter 19**, 165201 (2007)

However, record TMR in sputtered MTJs

TMR limited to 250% (Fe/MgO, 410% Co/MgO)

Epitaxial MTJ

Defects: dislocations

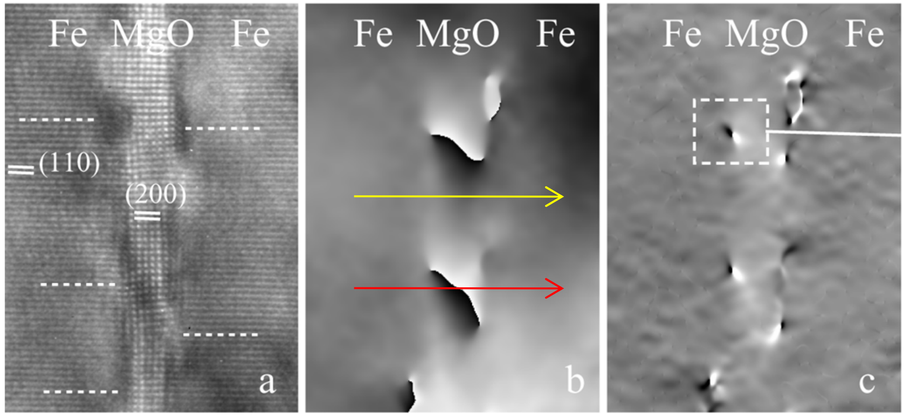

Imperfect filtering:

multichannel transport

coherent+diffusive, incoherent

E. Snoek CEMES, Toulouse

C. Tiusan, et al, J. Phys.: Condens. Matter 19, 165201, (2007)
C Tiusan et al, Appl. Phy. Lett. 88, 62512, (2006)

M. Gabor, C.Tiusan et al, J. Magn. Magn. Matter. 347,79–85, (2013).

WR 604% RT (1144% 5K)

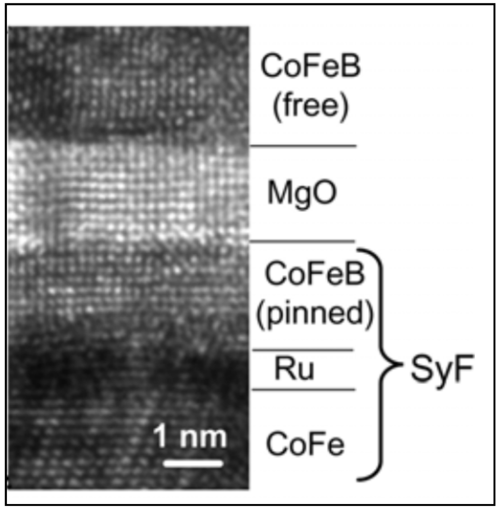

UHV Sputtered structures Annealed at HT
No disclocations, grain to grain epitaxy

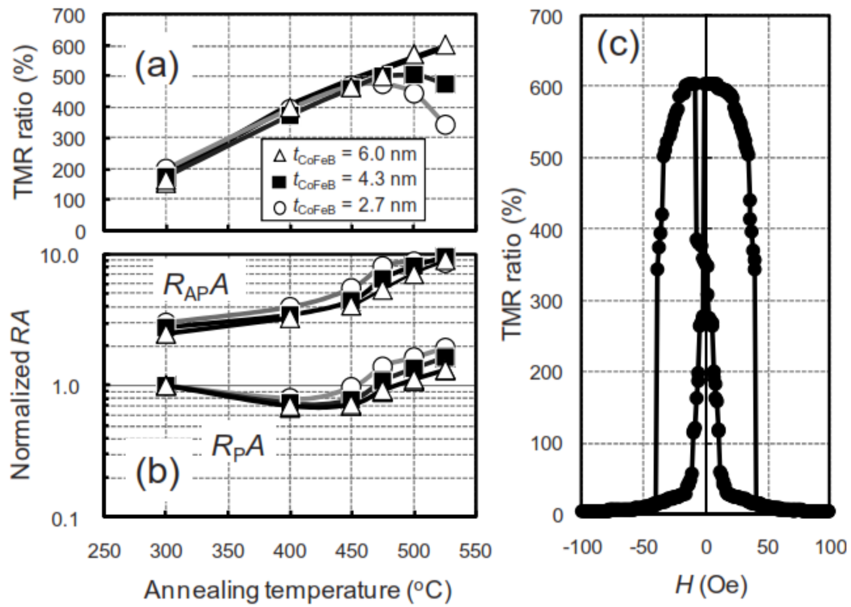

*S. Ikeda et al, Appl. Phys. Lett. **93**, 082508 (2008)*

Modulation of tunnel transport in single crystal Fe/MgO/Fe MTJs

Single crystal epitaxial MTJ: model system where theory and experiment meet
=> QM experiments

MTJ: multi channel transport; channel=[spin, symmetry]

FM Emitter:

selects the different Δ_i injected symmetries

Insulator

filter
Symmetry dependent attenuation rate

FM Collector:

selects / impose the reception states Δ_i

3 sub-systems coupled by the wave function matching at the interfaces
interface quality/ chemistry, interfacial electronic structure

Strong impact on the tunnel characteristics

By controlling the interfacial structure

Engineering of spin filtering

100% Surface polarization copeting with 100% $\Delta 1$ bulk polarization

AP

Bulk electronic structure
k_{II}=0 (asymptotic regime)

No up Δ_1 in left electrode at E_F

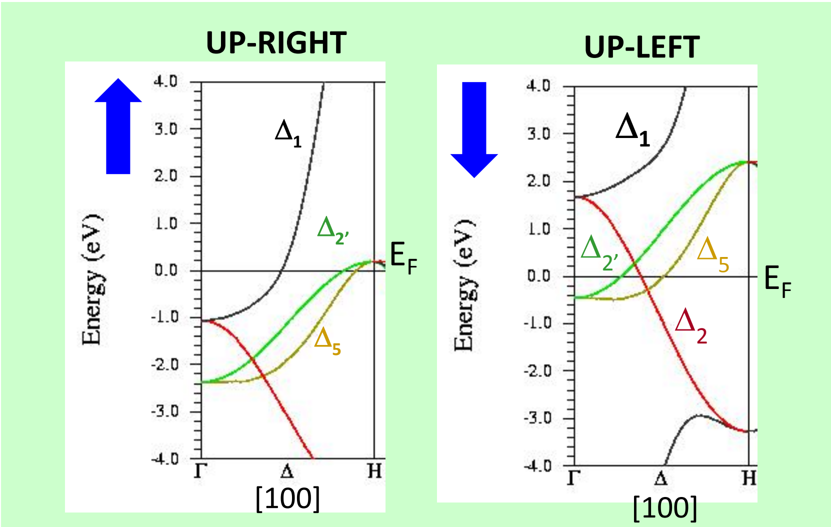

➡ Small conductivity

related to **Δ_5 electrons (k_{II}=0)**

! IRS in (k_{II}≠0)

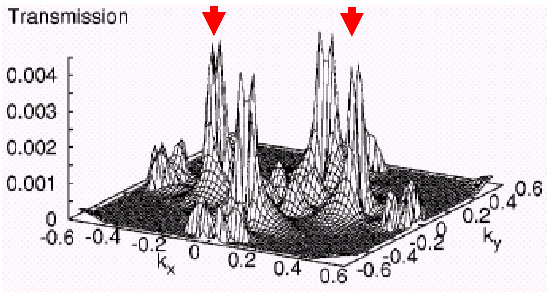

Surface electronic structure (minority spin)

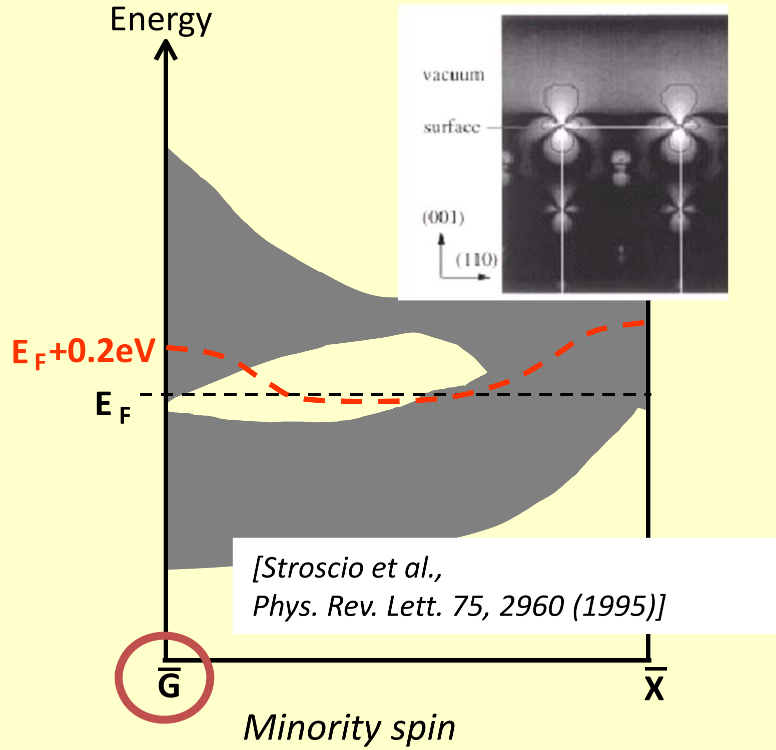

Fe(001) minority spin surf. State:

d_{z2} like orbital $\in \Delta_1$ symmetry (s, p_z, d_{z2})

Strong contribution of IRS to the Minority spin tunneling

C. Tiusan, et al, Phys. Rev. Lett. 93, 106602 (2004).

Enhanced magnetoresistance by monoatomic roughness in epitaxial Fe/MgO/Fe tunnel junctions

A. Duluard, C. Tiusan et al,

PHYSICAL REVIEW B **91**, 174403 (2015)

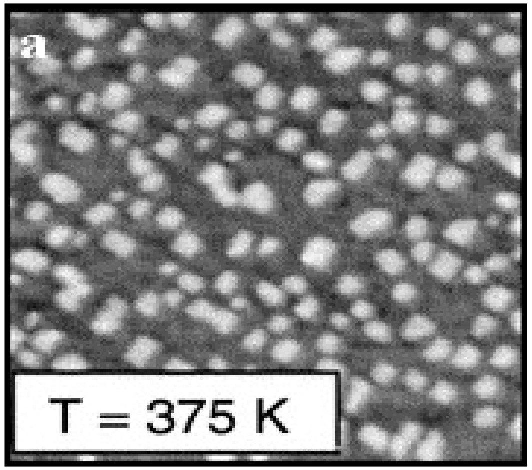

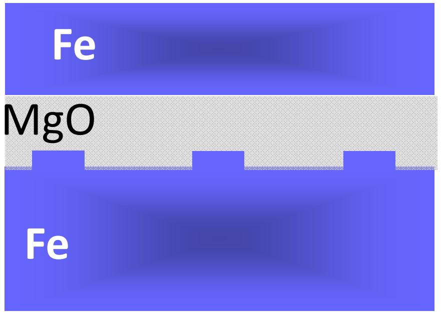

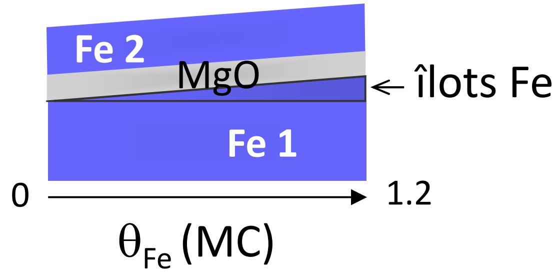

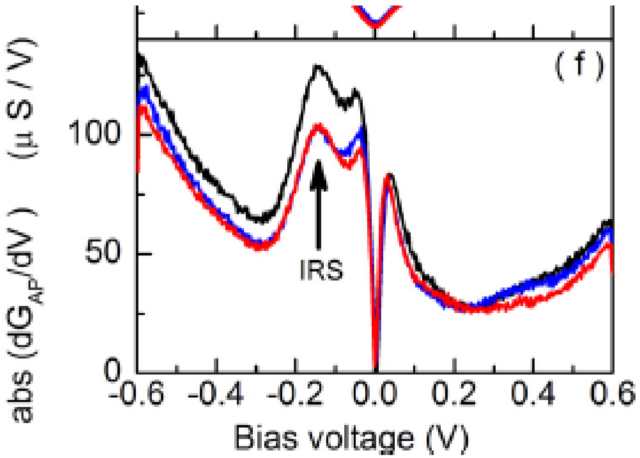

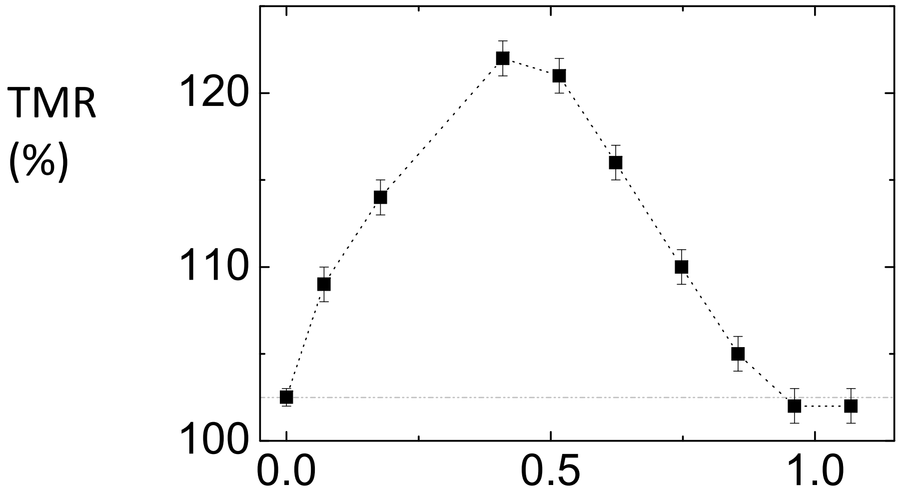

Quenching IRS, increases TMR

TUNNELING ANISOTROPIC MAGNETORESISTANCE (TAMR)

Angular dependence of the tunneling resistance

attributed to a significant anisotropy in the DOS linked to the magnetization direction along different crystal axes –**SOC related**

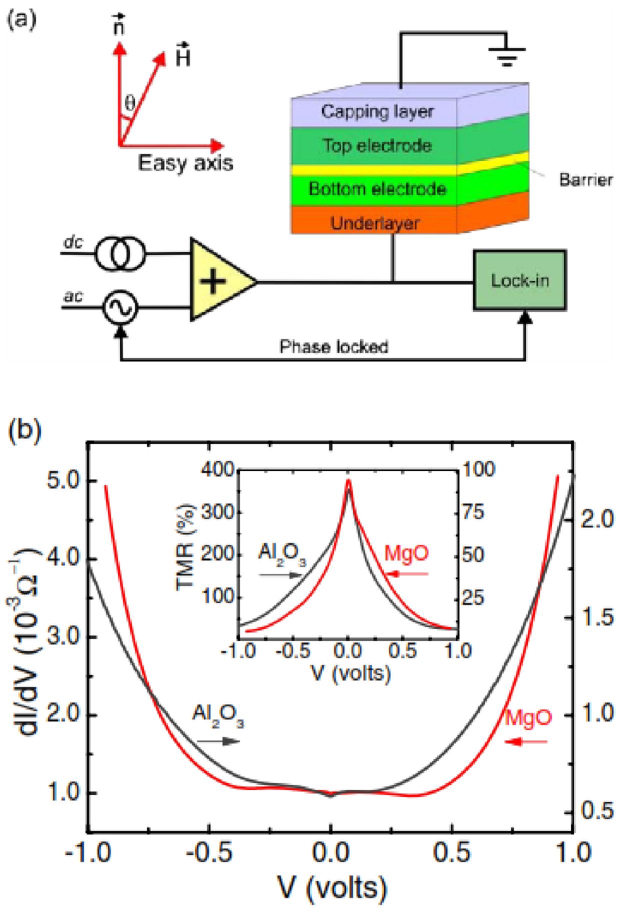

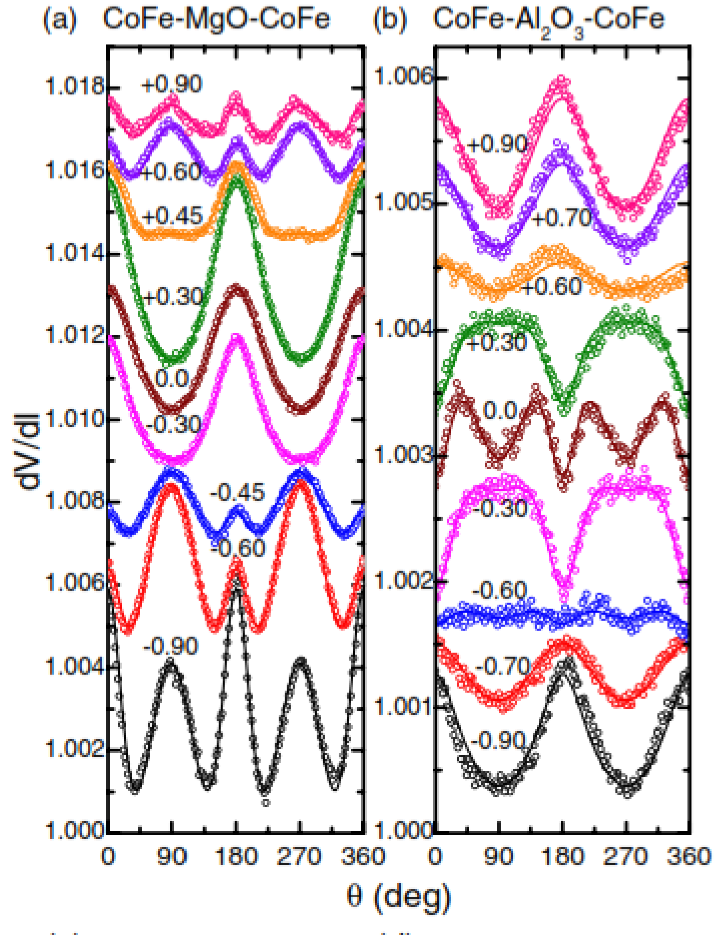

L. Gao et al, PRL ***99, 226602 (2007)***

!!! 2nd FM electrode not necessary

Spin-orbit coupling effect by minority interface resonance states in single-crystal magnetic tunnel junctions

Y. Lu, C. Tiusan et al,
PHYSICAL REVIEW B **86**, 184420 (2012)

SO negligible in 3D FM metals, however large in IRS
If IRS activated = large SO efects in transport

IRS demonstrated by tunneling spectroscopy experiments (see next slide)

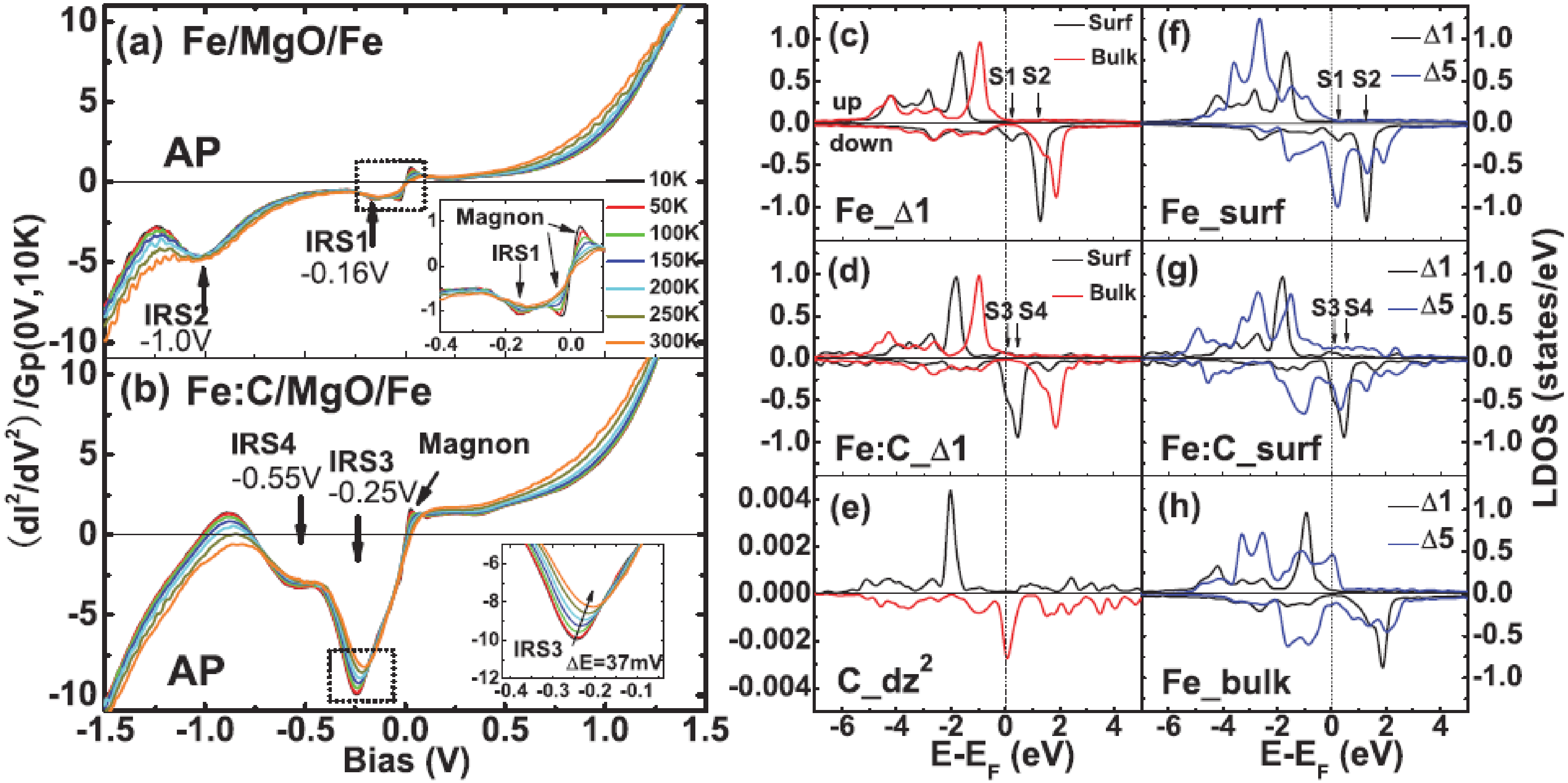

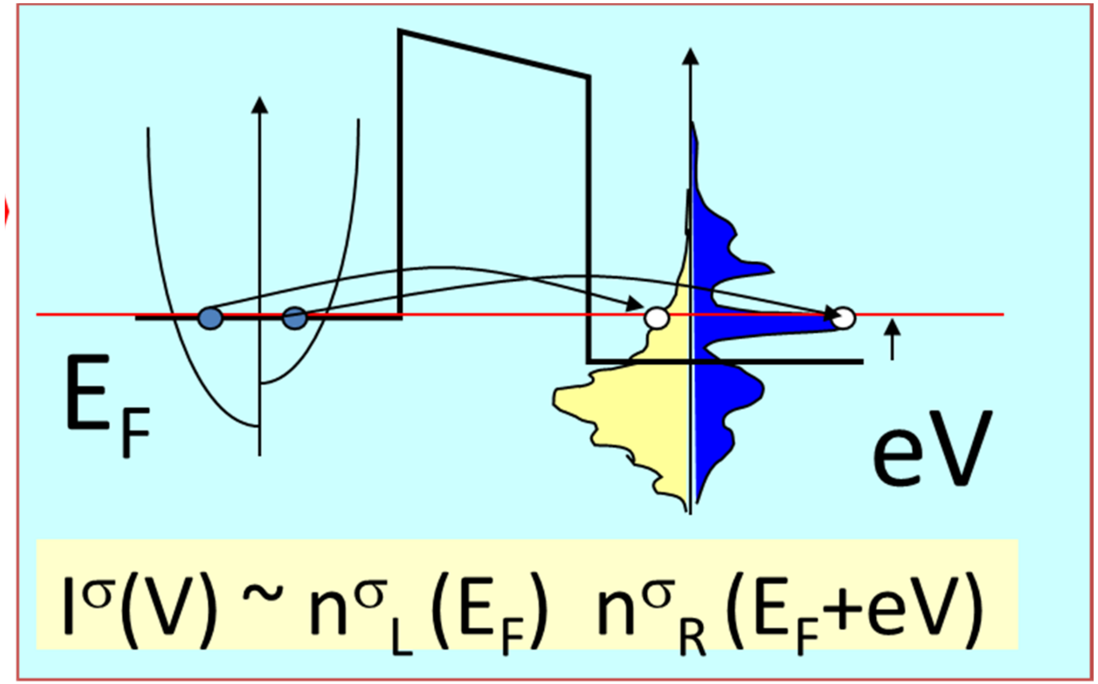

By tunneling spectroscopy on probe empty states in the Right electrode (occupied in the L but seing larger barrier)

Interfacial SO effects at Fe/MgO interface responsible on large PMA

M. Chsiev et al, PHYSICAL REVIEW B **88**, 184423 (2013)

Anatomy of perpendicular magnetic anisotropy in Fe/MgO magnetic tunnel junctions:

- ❑ the origin of the large PMA values is far beyond simply considering the hybridization between Fe-3d and O-2p orbitals
- ❑ anisotropy energy is not localized at the interface but it rather propagates into the bulk showing an attenuating oscillatory behavior depending on the orbital character of the state
- ❑ The MgO thickness has no influence on PMA, and the PMA oscillates as a function of Fe thickness with a period of 2 ML

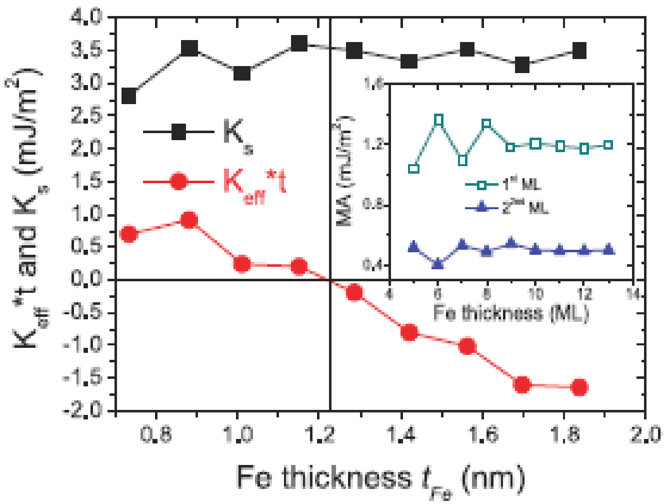

Even if SO is small in 3D metals, for some orbitals it can be significant,
Lifts degenerancies for some states and affects the occupation and energies
!important for anisotropies, transport, etc…

Engineering of the voltage response in single crystal MTJ
by interfacial chemistry/ electronic structure

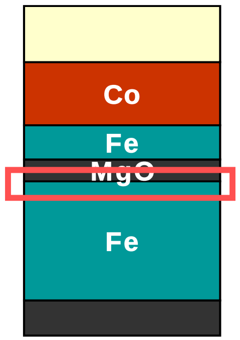

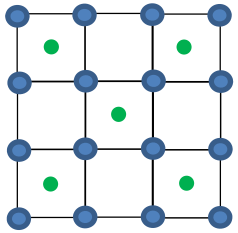

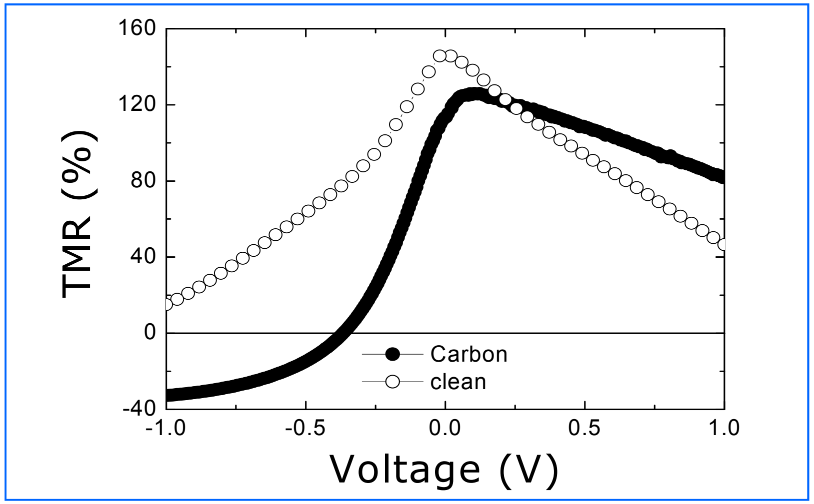

Clean Fe/MgO interface

C layer at Fe/MgO interface

Clean Fe(001)

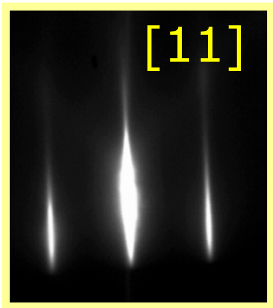

c(2x2) C on Fe(001)

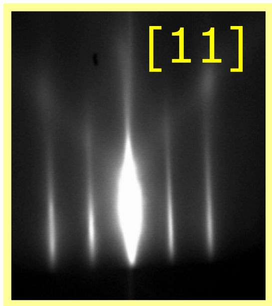

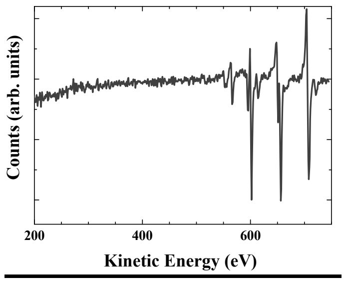

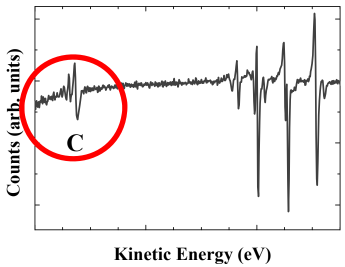

Applications: MTJ operated at finite voltage

TMR(V) extremely important

Optimization of the output signal by interfacial structure

C Tiusan et al, Appl. Phy. Lett. ***88,*** *62512, (2006).*

C. Tiusan, et al, J. Phys.: Condens. Matter ***18*** *, 941-956 (2006).*

Engineering of TMR in single crystal MTJ
by metallic adlayers

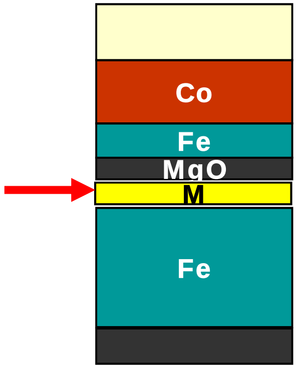

- TMR enhancing by eliminating the Δ_5 contribution

  → candidate : *bcc* Co(001)

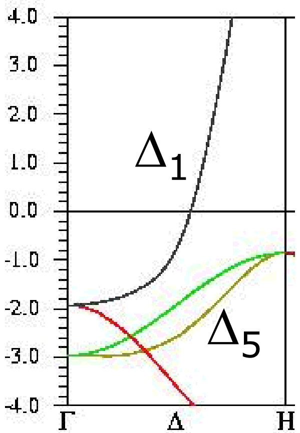

Giant tunneling magnetoresistance up to 410% at room temperature in fully epitaxial Co/MgO/Co magnetic tunnel junctions with bcc Co(001) electrodes

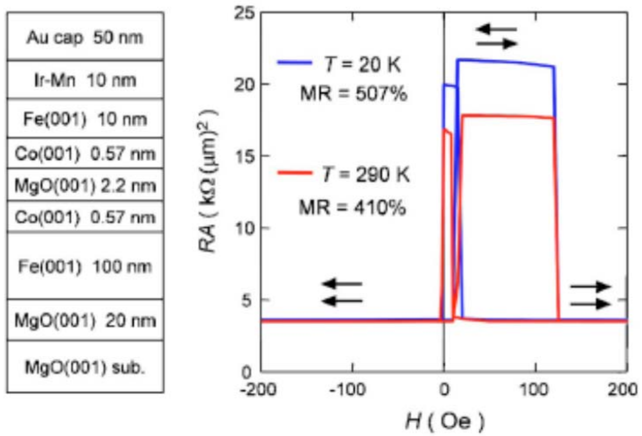

Yuasa, Ando, App. Phys. Lett., 89 042505 (2006)

- Eliminate (reduce) the Δ_1 contribution to have a complete overview of filtering effect in Fe/MgO-based MTJs

  → candidate : *bcc* Cr(001)

Symmetry dependent interfacial barriers

Fe

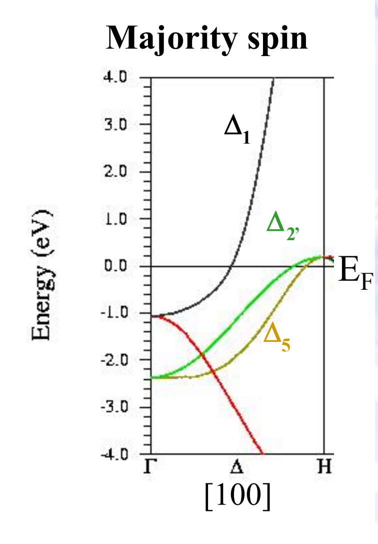

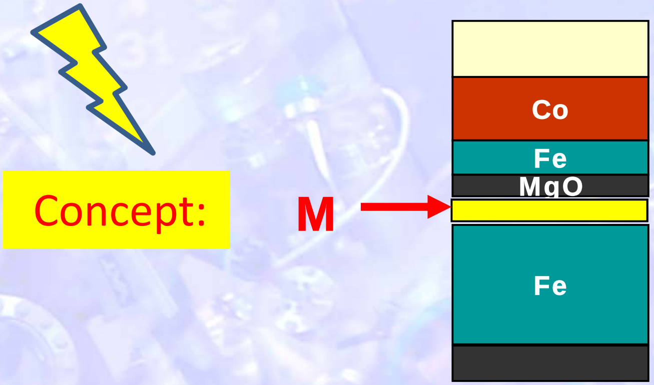

- **Barrier for Δ_1 symmetry**
  → candidate : **M**=*bcc* Cr(001)

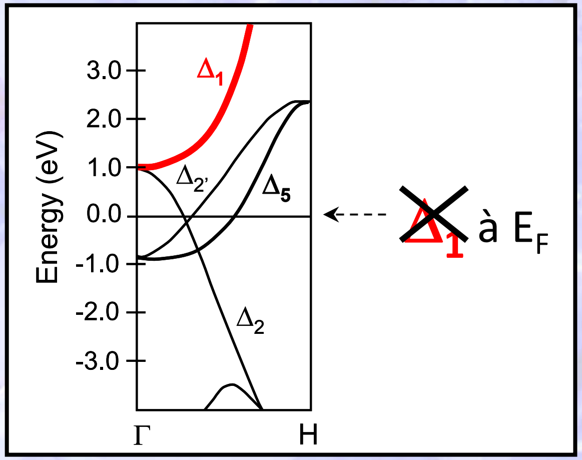

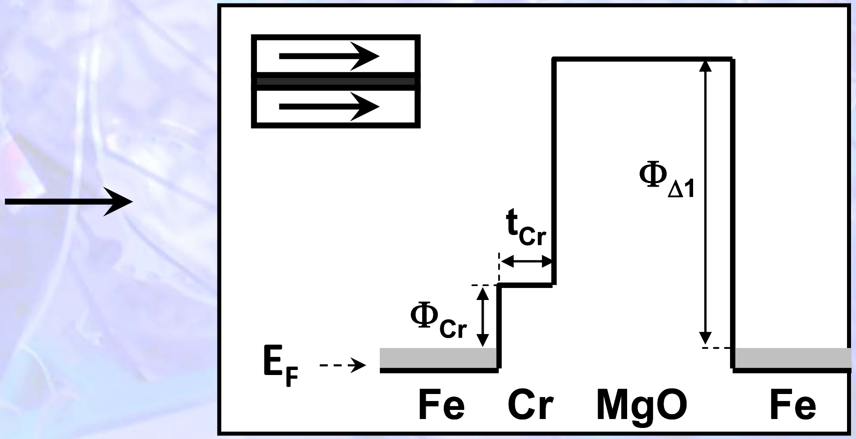

Cr (001) symmetry dependent barrier (1eV) → attenuation of Δ_1 propagation

Layer by layer growth of Cr on Fe : precise control of thickness

Lattice mismatches

Fe-**Cr** → 1.5%

Cr-MgO → 2.25%

(rotation 45°)

→ **Symmetry conservation**

2D growth **Cr** on **Fe**

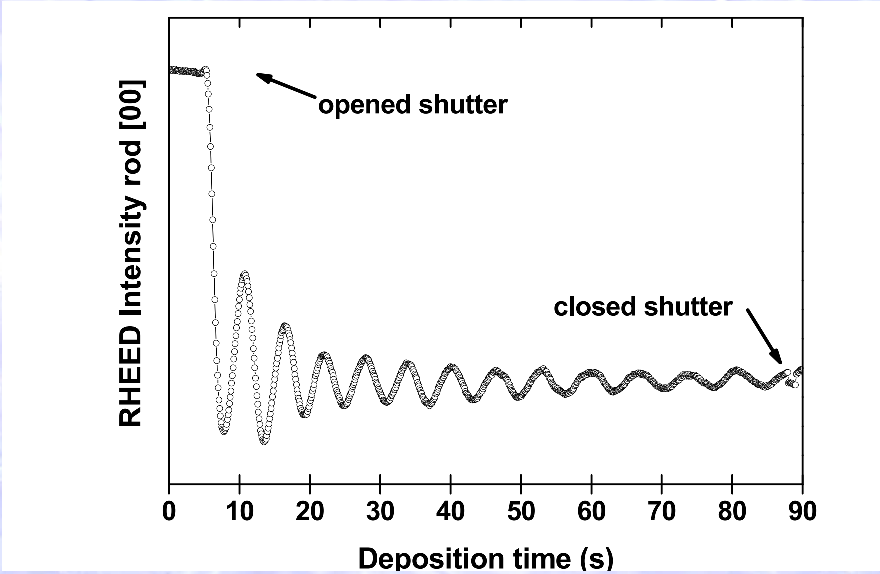

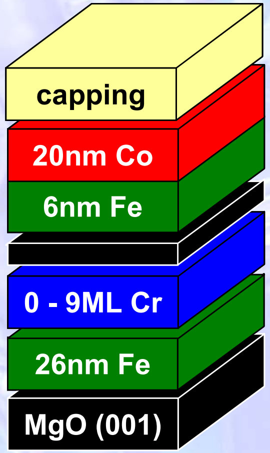

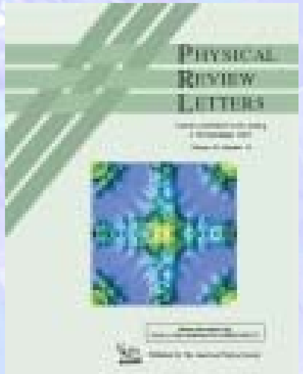

C. Tiusan et al, Phys. Rev. Lett. 99, 187202 (2007)

PRL 99, 187202 (2007) PHYSICAL REVIEW LETTERS week ending 2 NOVEMBER 2007

Evidence of a Symmetry-Dependent Metallic Barrier in Fully Epitaxial MgO Based Magnetic Tunnel Junctions

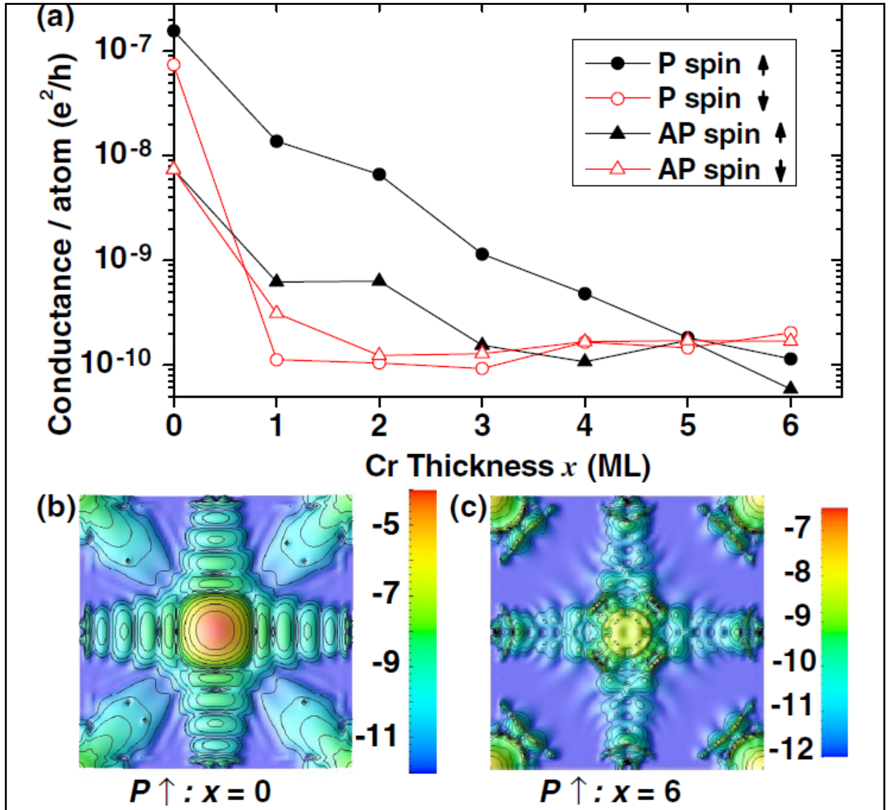

FIG. 3 (color online). Fe/Cr(x ML)/MgO(10 ML)/Fe: (a) evolution of the P↑, P↓, AP↑, and AP↓ conductance channels with increasing Cr thickness x. Transmission probability of the dominant P↑ conductance channel as a function of $k_{\|}$ for (b) $x = 0$ and (c) $x = 6$.

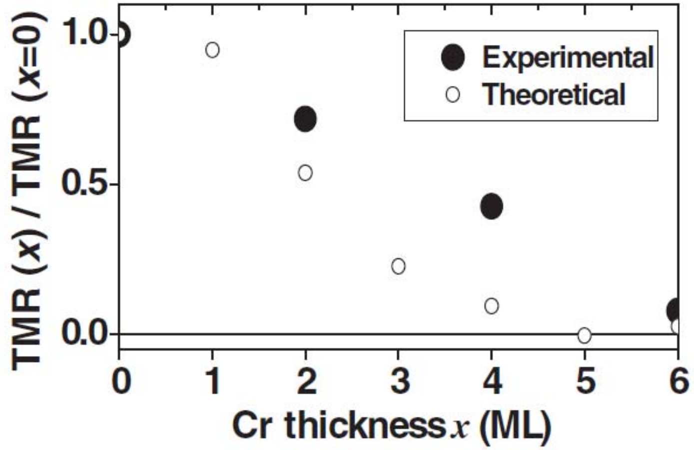

LKKR

Cr(001) behaves as a metallic tunnel barrier

C. Tiusan et al, Phys. Rev. Lett. 99, 187202 (2007)

Building quantum well structure for Δ_1

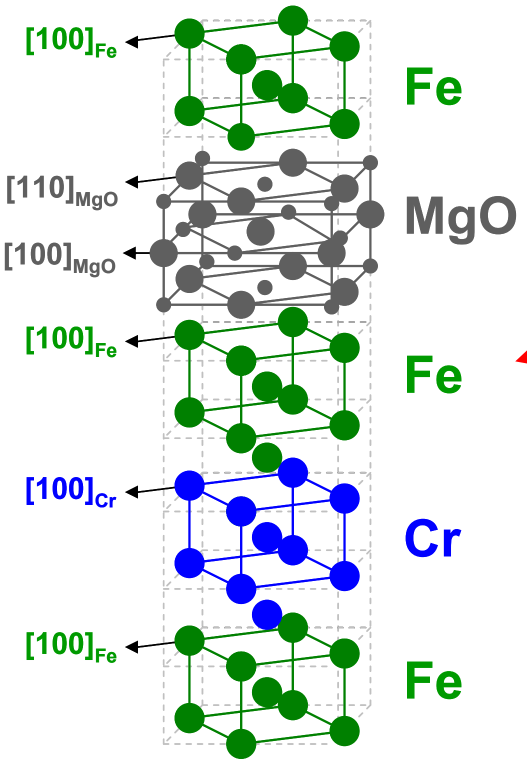

Insertion of thin Fe between Cr and MgO

Potential profiles for Δ_1 in parallel configuration (P)

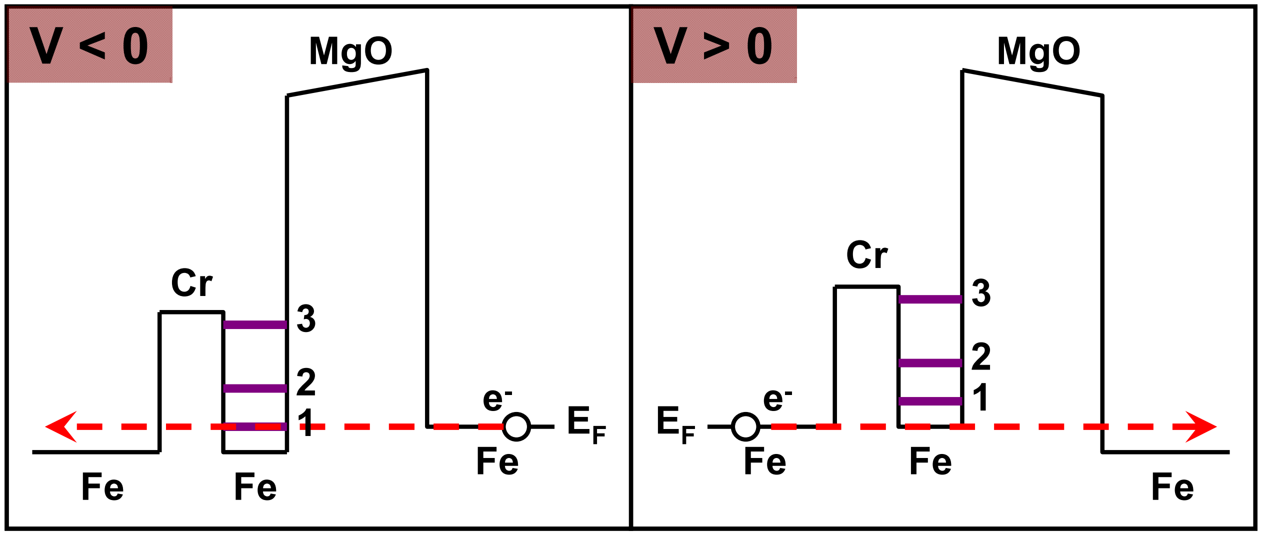

C. Tiusan et al, Phys. Rev. Lett. 99, 187202 (2007)

Symmetry dependent quantum well structure for Δ_1 electrons (RT)

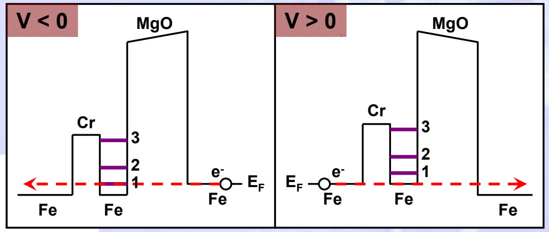

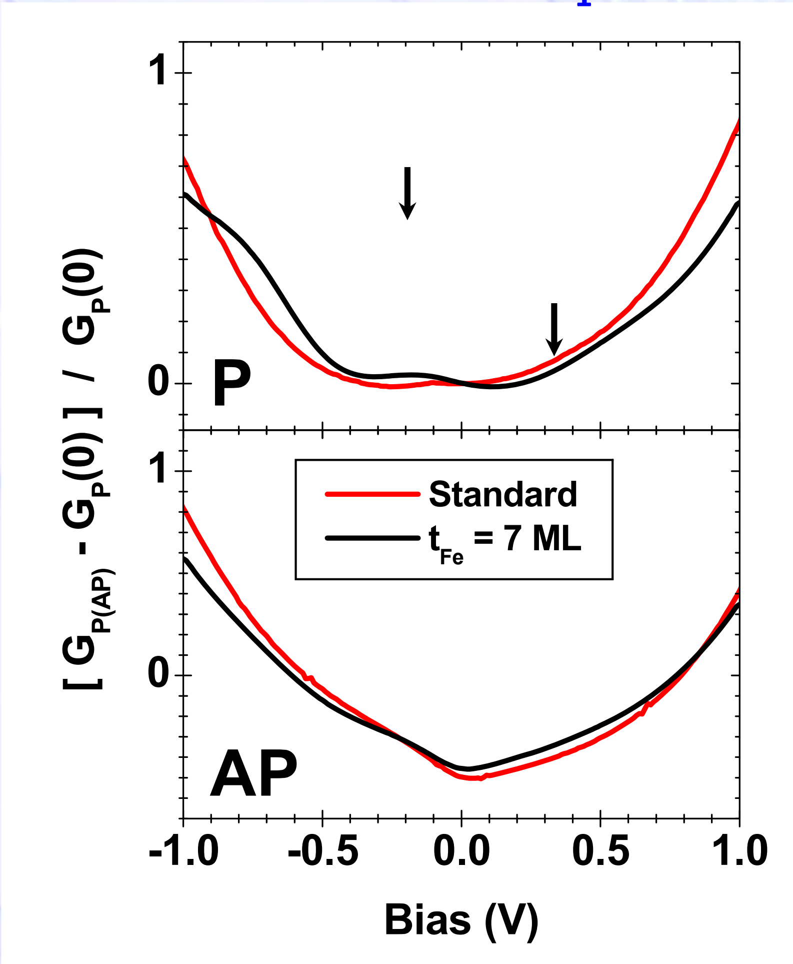

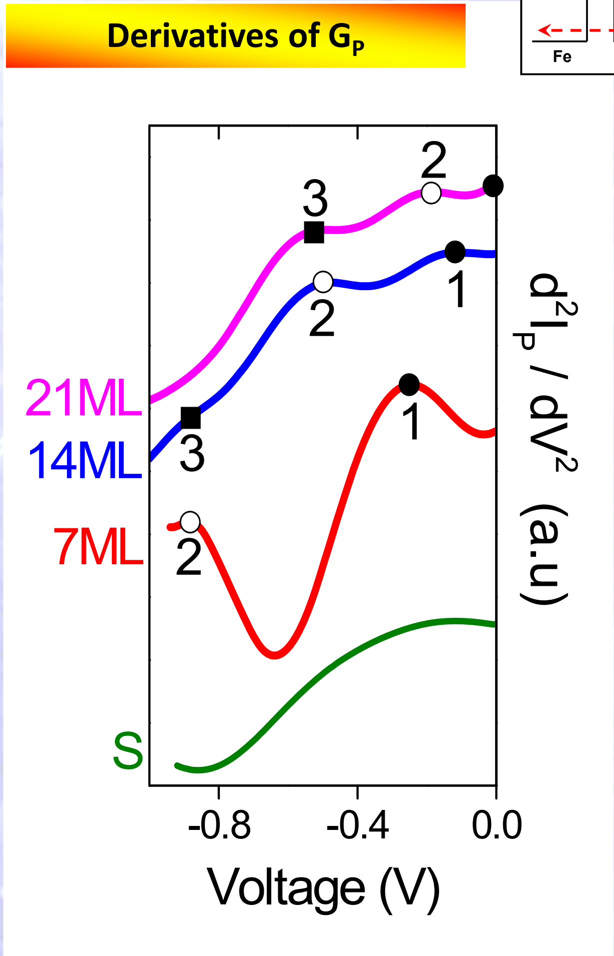

Increasing t_{Fe} :

→conductivity maxima shifted towards lower voltages

→**quantum well states for Δ_1**

C. Tiusan et al, Phys. Rev. Lett. 99, 187202 (2007)

Polarisation (TMR) amplitude tunning using FeCo alloy bcc electrodes

Preserve bcc(001) symmetry and all filtering proeprties of MgO(100) but enhance polarization of FM:

adjunction of Co in Fe shift upwards E_F, enhances spectral density of majority $\Delta 1$, shifts downwards the minority IRS

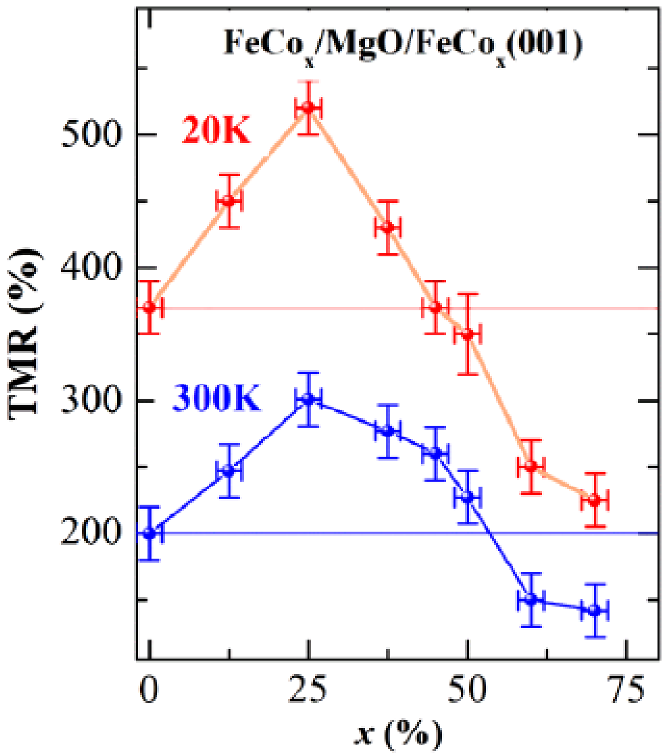

FIG. 1 (color online). TMR measured at 20 K and 300 K on a series of bcc $Fe_{1-x}Co_x/MgO/Fe_{1-x}Co_x(001)$ MTJs grown by MBE.

F. Bonnel et al, PRL 108, 176602 (2012)

Textured Fe/MgO/Fe ≈
single crystal Fe/MgO/Fe

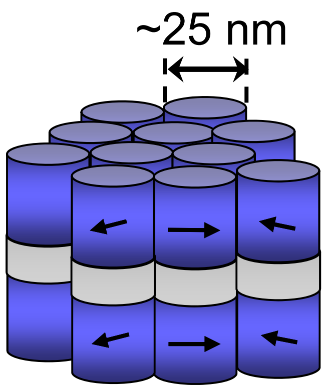

Textured MTJS grown by MBE

grain-to-grain epitaxy

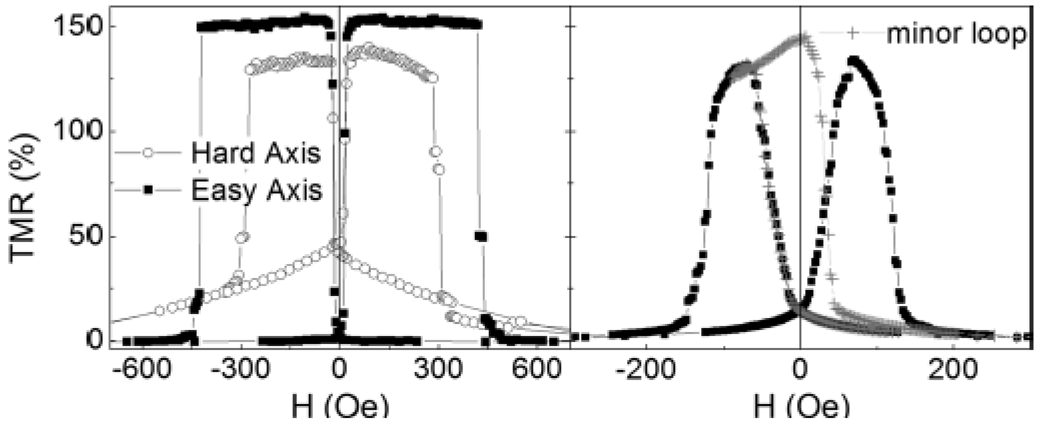

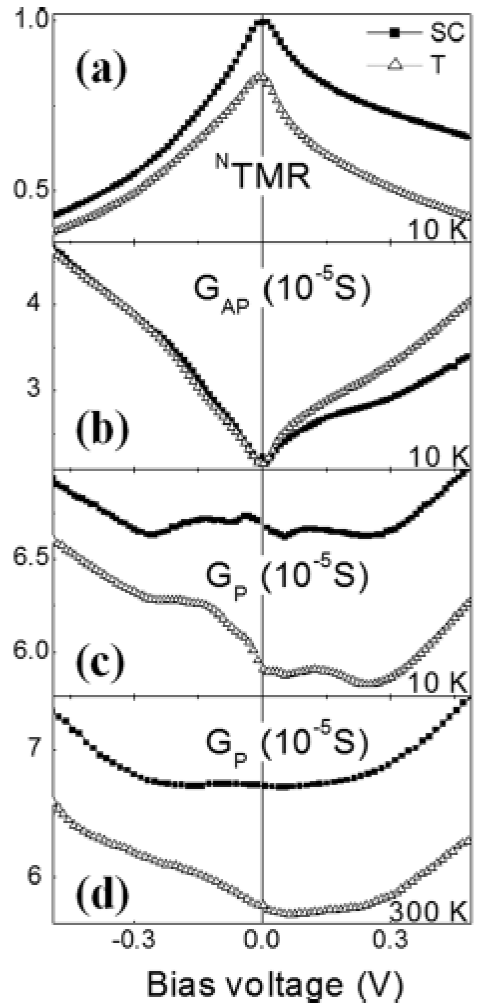

Similar TMR ratios and conductivity vs voltage curves

A. Duluard, C. Tiusan et al,
APPLIED PHYSICS LETTERS **100**, 072408 (2012)

I. **TMR**: current control via the magnetization configuration

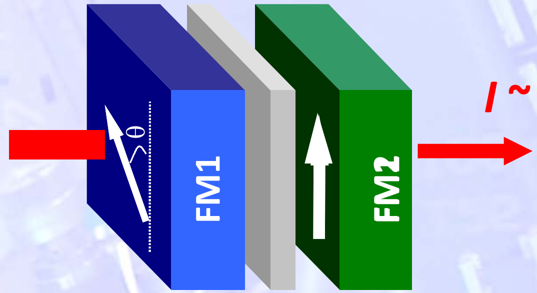

$I \sim \cos\theta$

Recall Bauer, Slonczewski torque in half-metals

II. ? Magnetization control via the current

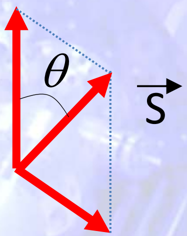

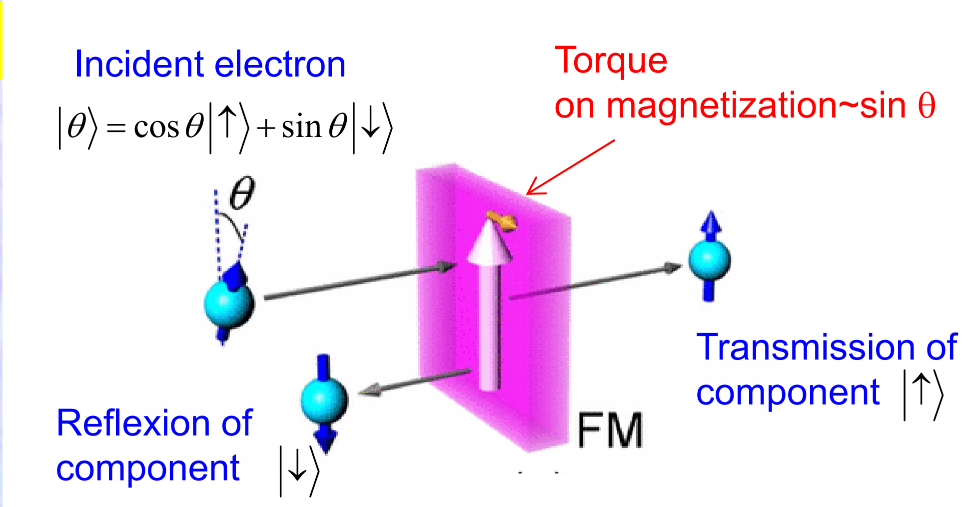

Spin filtering in an ideal FM
removes from the current the $\sin\theta|\downarrow\rangle$ component of the spin angular moment
This is adsorbed by the magnetization, => torque.

Current induced
spin transfer torque

Anathomy of spin torque (QM)

See M. Chshiev, Th 03/09

Particle transport

Particle density:

$$n(\mathbf{r}) = \sum_{i\sigma} \psi^*_{i\sigma}(\mathbf{r})\, \psi_{i\sigma}(\mathbf{r})$$

Current density:

$$\mathbf{j}(\mathbf{r}) = \mathrm{Re}\sum_{i\sigma} \psi^*_{i\sigma}(\mathbf{r})\, \hat{\mathbf{v}}\, \psi_{i\sigma}(\mathbf{r})$$

where $\hat{\mathbf{v}} = -(i\hbar/m)\nabla$

Continuity equation:

$$\nabla \cdot \mathbf{j} + \frac{\partial n}{\partial t} = 0$$

Spin transport

Spin density:

$$\mathbf{m}(\mathbf{r}) = \sum_{i\sigma\sigma'} \psi^*_{i\sigma}(\mathbf{r})\, \mathbf{s}_{\sigma,\sigma'}\, \psi_{i\sigma'}(\mathbf{r})$$

Spin current density:

$$\mathbf{Q}(\mathbf{r}) = \sum_{i\sigma\sigma'} \mathrm{Re}[\psi^*_{i\sigma}(\mathbf{r})\, \mathbf{s}_{\sigma,\sigma'} \otimes \hat{\mathbf{v}}\, \psi_{i\sigma'}(\mathbf{r})]$$

where $\mathbf{s} = (\hbar/2)\boldsymbol{\sigma}$ Vector of Pauli matrices

Continuity equation:

$$\nabla \cdot \mathbf{Q} + \frac{\partial \mathbf{m}}{\partial t} = -\frac{\delta \mathbf{m}}{\tau_{\uparrow\downarrow}} + \mathbf{n}_{\mathrm{ext}}$$

External torques

Spin accumulation

Spin density:

$$\mathbf{m}(\mathbf{r}) = \sum_{i\sigma\sigma'} \psi^*_{i\sigma}(\mathbf{r})\, \mathbf{s}_{\sigma,\sigma'}\, \psi_{i\sigma'}(\mathbf{r}) \Rightarrow \begin{cases} m_x = \frac{\hbar}{2}\sum_i \left(\psi^*_{i\uparrow}\psi_{i\downarrow} + \psi^*_{i\downarrow}\psi_{i\uparrow}\right) \\ m_y = \frac{\hbar}{2}\sum_i \left(i\psi^*_{i\downarrow}\psi_{i\uparrow} - i\psi^*_{i\uparrow}\psi_{i\downarrow}\right) \\ m_z = \frac{\hbar}{2}\sum_i \left(\psi^*_{i\uparrow}\psi_{i\uparrow} - \psi^*_{i\downarrow}\psi_{i\downarrow}\right) \end{cases}$$

Spin current density:

$$\mathbf{Q}(\mathbf{r}) = \sum_{i\sigma\sigma'} \mathrm{Re}[\psi^*_{i\sigma}(\mathbf{r})\, \mathbf{s}_{\sigma,\sigma'} \otimes \hat{\mathbf{v}}\, \psi_{i\sigma'}(\mathbf{r})] \Rightarrow \begin{cases} \mathbf{Q}_x = \mathrm{Re}\sum_i \left(\psi^*_{i\uparrow}\hat{\mathbf{v}}\psi_{i\downarrow} + \psi^*_{i\downarrow}\hat{\mathbf{v}}\psi_{i\uparrow}\right) \\ \mathbf{Q}_y = \mathrm{Re}\sum_i \left(i\psi^*_{i\downarrow}\hat{\mathbf{v}}\psi_{i\uparrow} - i\psi^*_{i\uparrow}\hat{\mathbf{v}}\psi_{i\downarrow}\right) \\ \mathbf{Q}_z = \mathrm{Re}\sum_i \left(\psi^*_{i\uparrow}\hat{\mathbf{v}}\psi_{i\uparrow} - \psi^*_{i\downarrow}\hat{\mathbf{v}}\psi_{i\downarrow}\right) \end{cases}$$

Tensor quantity with elements $Q_{ij}(\mathbf{r})$ with i=x,y,z in spin space and j=x,y,z in real space

$$\nabla \cdot \mathbf{Q} = \partial_k Q_{ik}$$

Current flows in **x** direction $\Rightarrow \begin{cases} Q_{xx} \neq 0 \\ Q_{yx} \neq 0 \\ Q_{zx} \neq 0 \end{cases}$

General continuity equation (spin+magnetization)

$$\nabla \cdot \mathbf{Q} + \frac{\partial \mathbf{m}}{\partial t} = -\frac{\delta \mathbf{m}}{\tau_{\uparrow\downarrow}} + \mathbf{n}_{\text{ext}}$$

Spin accumulation

$$\delta \mathbf{m} = (|\mathbf{m}| - m_{\text{eq}})\hat{\mathbf{m}}$$

All external torques

For example, Landau-Lifshitz-Gilbert torque density:

$$\mathbf{n}_{\text{ext}} = -(g\mu_B/\hbar)\mathbf{m}\times\mathbf{B}_{\text{eff}} + \alpha\,\hat{\mathbf{m}}\times\dot{\mathbf{m}}$$

exchange, anisotropies, external fields

damping

$$\frac{\partial \mathbf{m}}{\partial t} = \mathbf{n}_c + \mathbf{n}_{\text{ext}}$$

$$\mathbf{n}_c = -\frac{\delta \mathbf{m}}{\tau_{\uparrow\downarrow}} - \nabla \cdot \mathbf{Q}$$

⟹ **Current-induced contribution to the torque density**

(M. D. Stiles and A. Zangwill, PRB 66 (2002) 014407)

Magnetization dynamics (LLG equation + spin torque)

Spin current influences the magnetization dynamics (LLG eq.)

Zhang et al., PRL 88, 236601 (2002)

$$\frac{\partial \hat{m}}{\partial t} = \underbrace{\boxed{-\gamma \hat{m} \times \left(\vec{H}_E\right)}}_{\text{precession}} + \underbrace{\boxed{\alpha \hat{m} \times \frac{\partial \hat{m}}{\partial t}}}_{\text{damping}} \underbrace{- \gamma b_J \hat{m} \times \hat{p}}_{\text{Field like term}} \underbrace{- a_J \hat{m} \times \left(\hat{m} \times \hat{p}\right)}_{\text{Spin transfer term}}$$

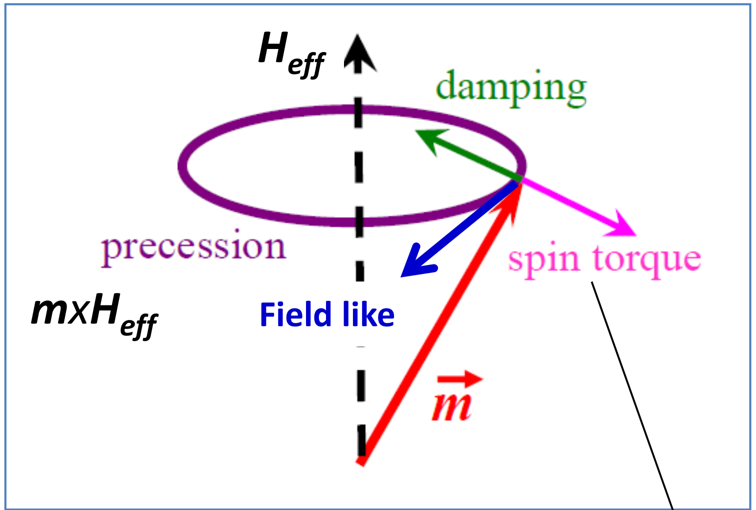

STT direction depends on sign of current I

Magnetization manipulation by spin transfer torque

- Magnetization control strategy in STT-RAM and ST-HFO

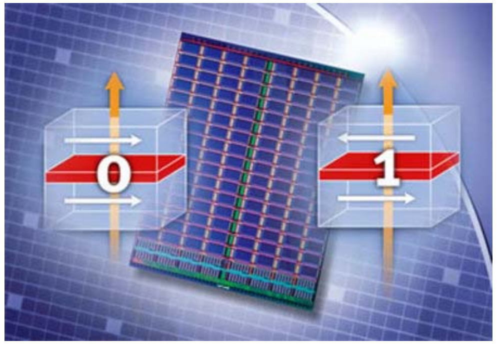

When a current is applied, **the direction of the spin transfer torque** is either **parallel** to the damping torque or **antiparallel to it**, depending on the sign of the current

Trajectories of spin-torque-driven dynamics for the magnetization vector M

- For the sign of the current that produces a spin-torque contribution in the same direction as the damping, there are no current induced instabilities in the free-layer orientation. The current increases the value of the effective damping, and M simply spirals more rapidly back to the H_{eff} direction.

- For the sign of the current that produces a spin-torque contribution opposite to the direction of the damping (STT=acts as **negative damping**) => large angle magnetization dynamics excited

=> From steady precession to switch through spin current

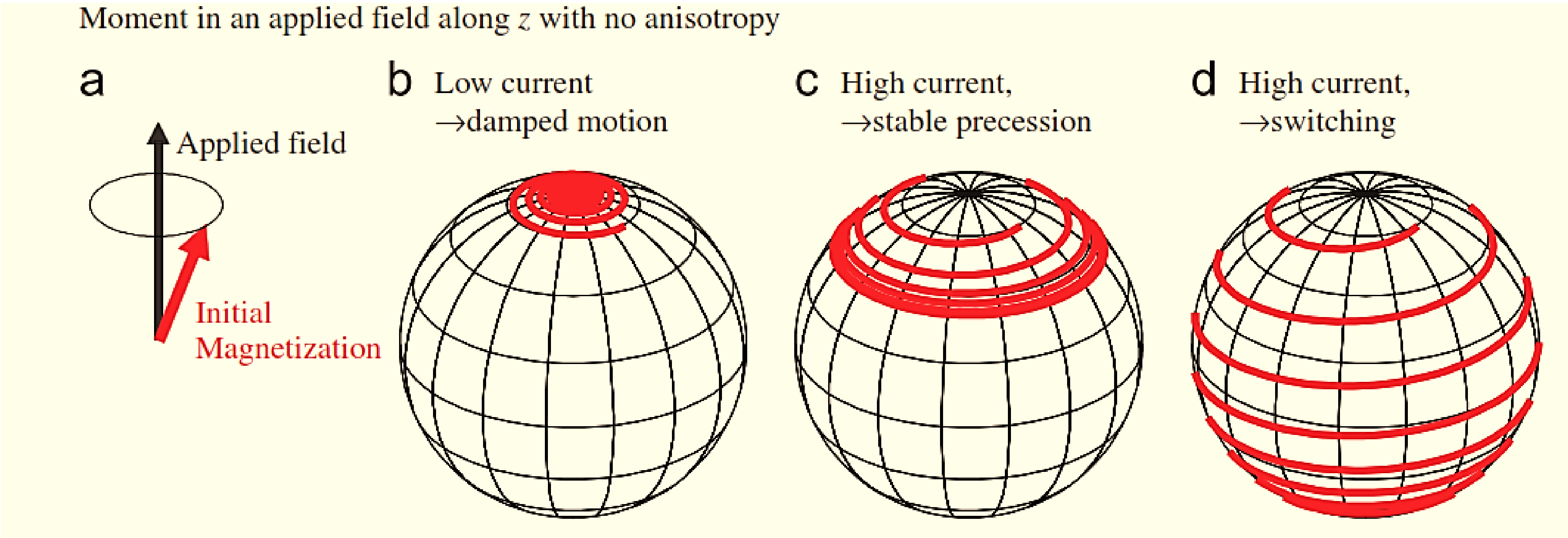

D.C. Ralph, M.D. Stiles / J. Magn. Magn. Mater. 320, 1190, (2008)

Spin torque effects in MTJs

MTJ: Experimental request for out-of-equilibrium spin torque analysis

- ❑ **torque** ~*exp(-kd)* => thin barriers required
- ❑ + high curent density density **J** for stable precession and switching (10^6 - 10^7 A/cm^2)

➡ nanometric MTJ pillars required

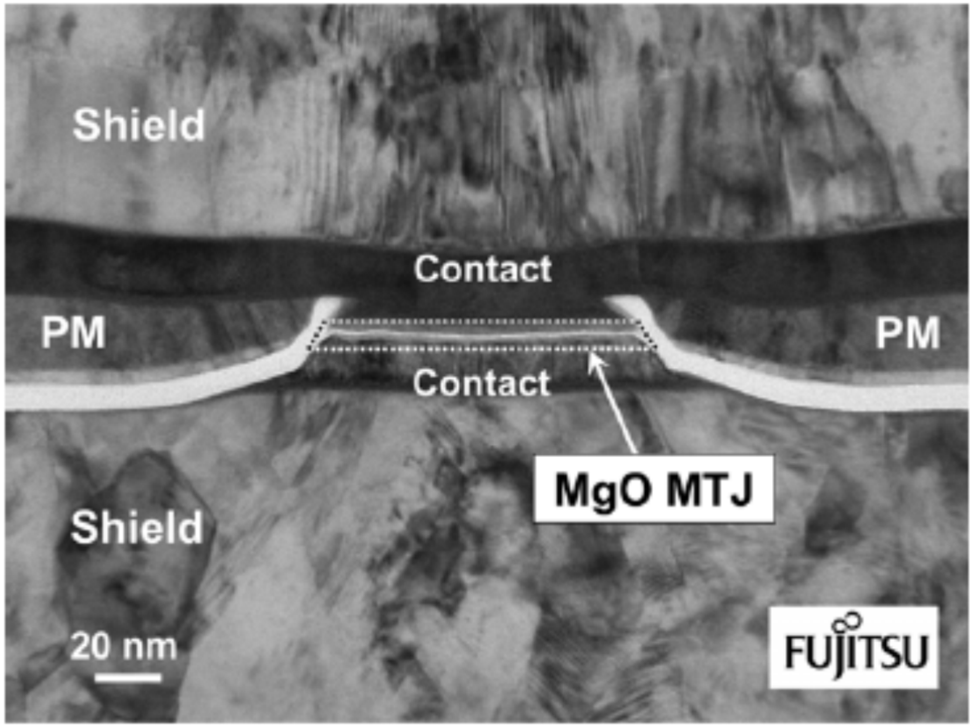

Figure 31. Cross-sectional TEM image of MgO-TMR read head for HDD with recording density of 250 Gbit/inch^2. (Courtesy of Fujitsu Corporation.)

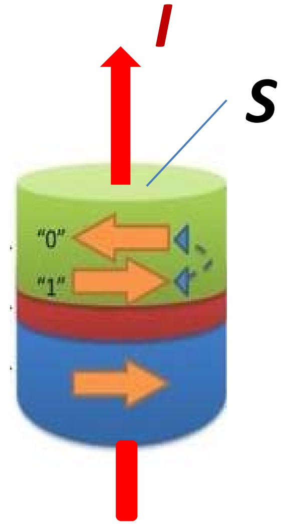

J =I/S

Complex patterning (lithographic) issues

MTJ: Out of equillibrium torque

First experiments on pillars:
Cornell (Katine et al, PRL 2000)
CNRS/Thales (Grollier et al, APL 2001)
IBM (Sun et al, APL 2002)

Current driven magnetization switching

Tohuku team

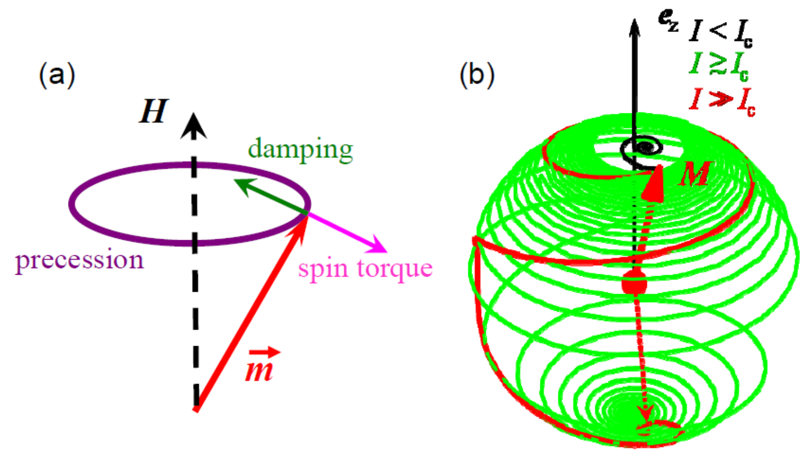

Fig. 2.4 (a) Geometric illustration of Landau-Lifshitz-Gilbert (LLG) equation with a spin transfer torque term; (b) Dynamics of the magnetic moments in the free layer (FL) when the damping term is larger, comparable, or smaller than the spin-torque term with various magnitudes of spin polarized current.

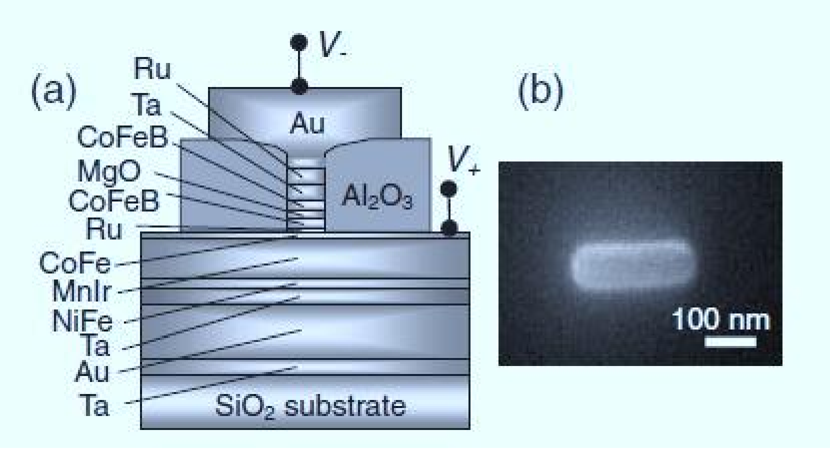

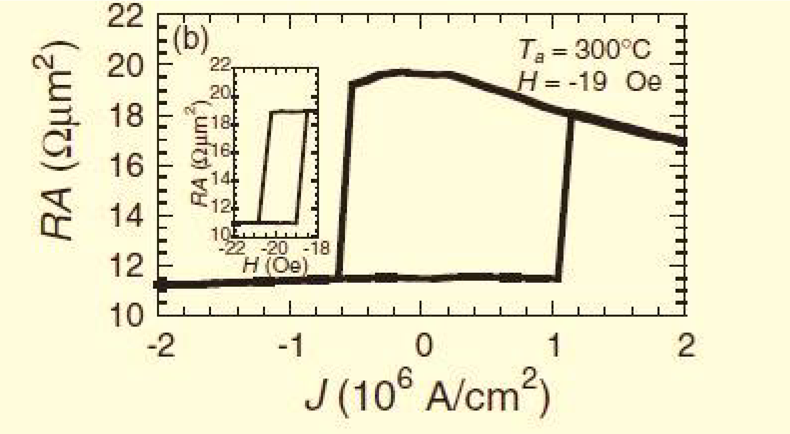

Average Jc ≈ 8x10^5 A/cm^2

typical switching current MTJ ≈ 10^{6}A/cm^2): target 5*10^{5}A/cm^2 tailoring materials with low damping and large polarization (e.g. Heusler)

switching time can be as short as 0.1 ns *(Chappert et al)*

Applications: STT-MRAM

Switching of reprogrammable devices (example: MRAM)

1) By external magnetic field

(present generation of MRAM, nonlocal, risk of « cross-talk » limits integration)

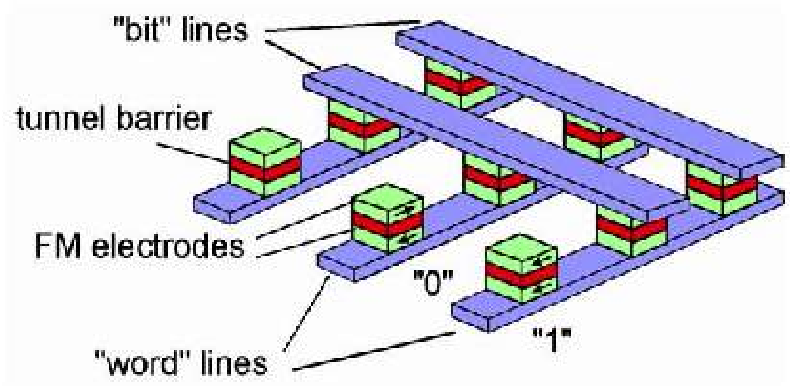

2) «Electronic» reversal by spin transfer from current

(ST-MRAM: next generation of MRAM, with demonstrations by EVERSPIN, Sony, Hitachi, NEC, etc)

Current pulse

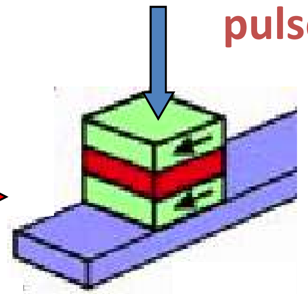

Spin torque nano-oscillator:
Spin torque compensates damping

(a) in-plane magnetized fixed (polarizer) layer and an out-of-plane magnetized free layer. (b) Microwave spectra as a function of d.c. current bias I at zero applied magnetic field

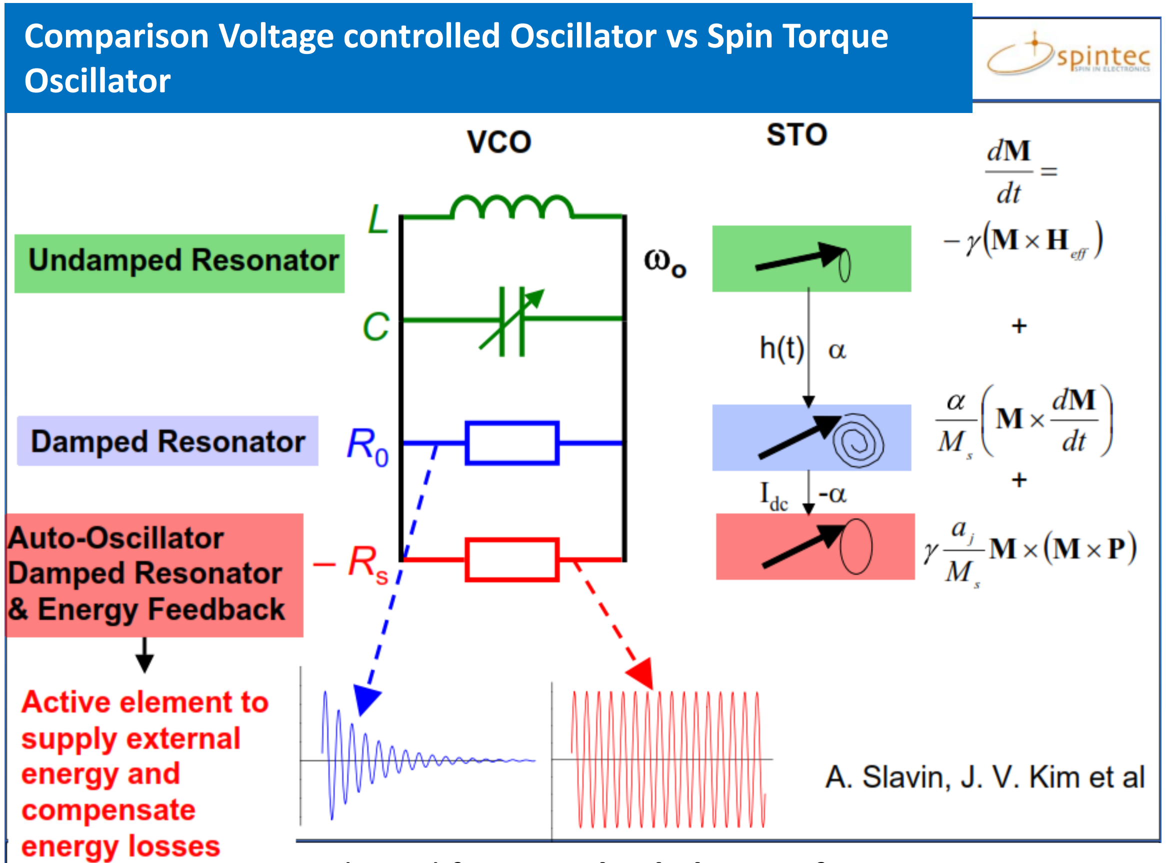

Adapted from **ursula.ebels@cea.fr**

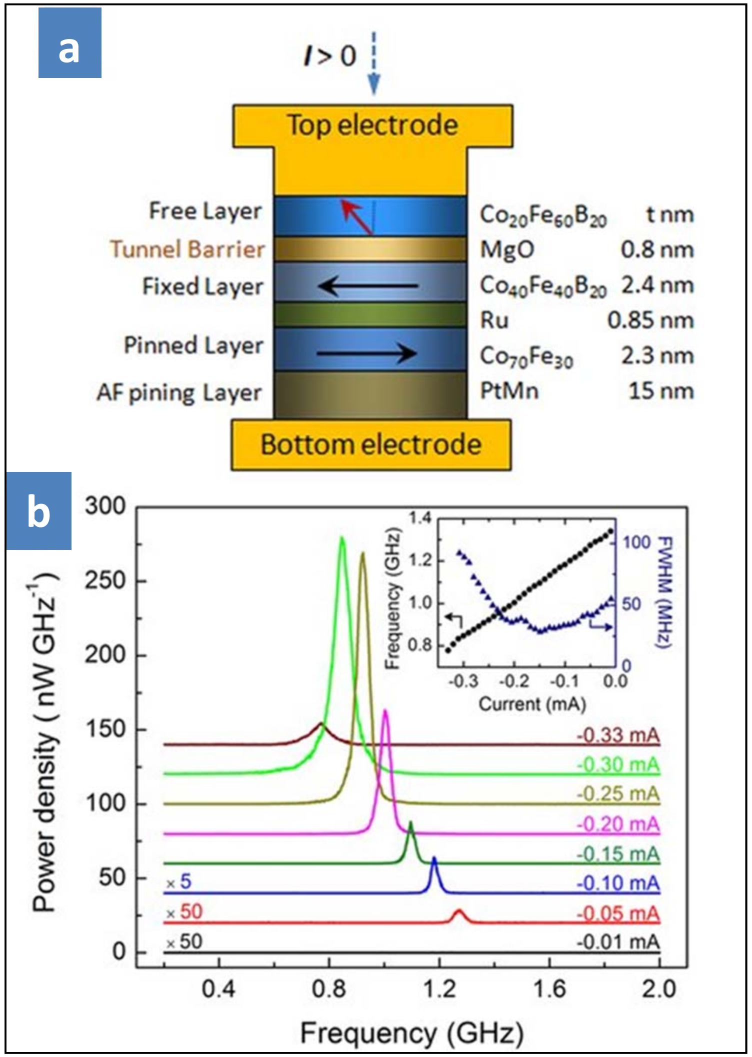

Z. Zeng et al, Scientific Reports 3, 1426 (2013)

Future telecommunications: multi standard / multi band applications require to cover a large range of frequencies using a single device

VCO's

- Limited frequency tuning range (few hundred MHz)
- Large space due to inductances (mm²)
- Long tuning time (µs to ms)

STO Advantages:

- ❑ Enhance tunning range GHz; direct oscillation in the microwave range (5-40 GHz)
- ❑ agility: control of frequency by dc current amplitude, (frequency modulation , fast switching)
- ❑ Fast tuning (ns)
- ❑ high quality factor
- ❑ small size (≈ 0.1µm) (on-chip integration)
- ❑ oscillations without applied field
- ❑ **Remaining chalanges:**
  - ❑ **Large Output Power and Small Linewidth**
    - ❑ increase of power by synchronization of a large of number N of STO (x N^2)

f/f∆f ≅ 18000 in point contacts

W. H. Rippard, et al, PRB, 2004, 70, 100406(R).

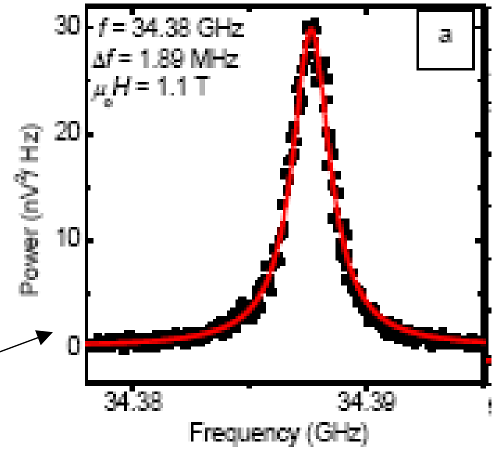

MgO MTJs with large TMR good candidates

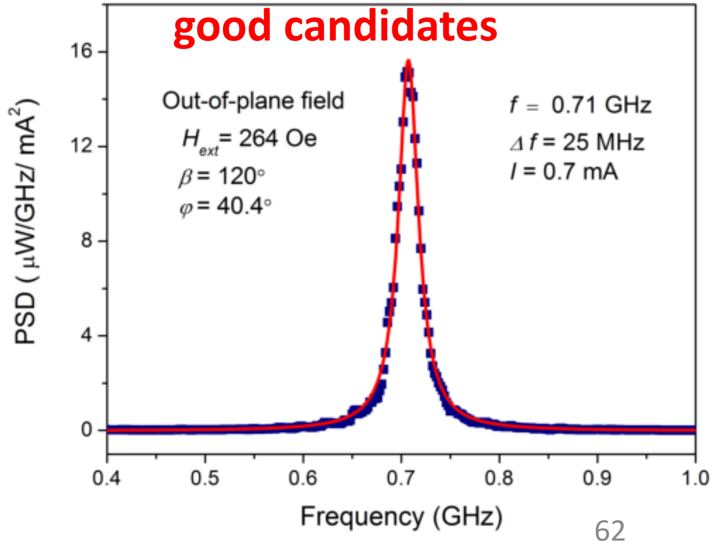

? STT experiments without patterned nanopillars

YES: zero bias (equillibrium) torque in continuous MTJ structures with extremelly thin barriers

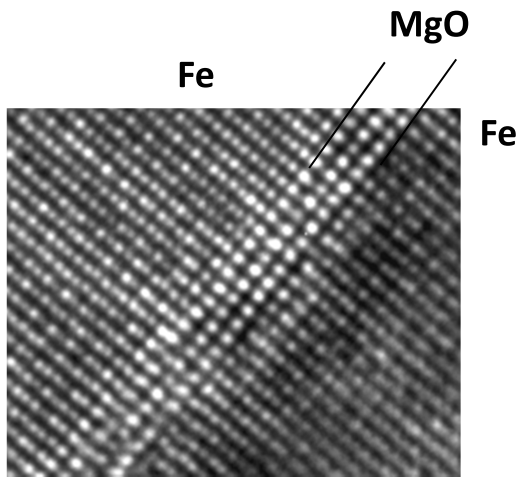

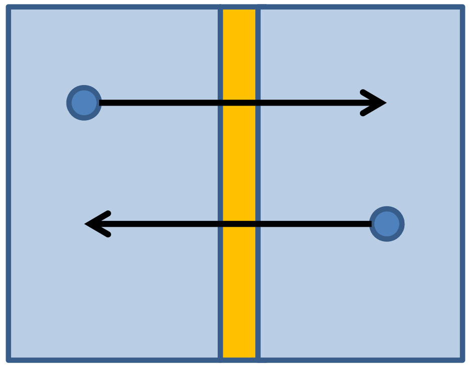

Net charge current I=0
Spin current ≠ 0

The equilibrium torque determines an
effective interfacial exchange coupling (Heinsenberg) ***– J cosθ***

J.C. Slonczewski, PRB 39, 6995, (1989).

MTJ: equilibrium (zero bias) torque

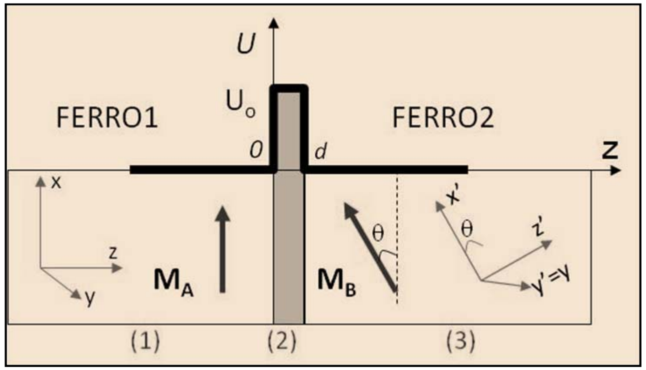

Net charge current I=0
Spin current ≠ 0

$$Q_{\alpha\beta}(\mathbf{x},t)=\frac{\hbar}{2im}\left[\Psi^*(\mathbf{x},t)\sigma_\beta\frac{\partial\Psi(\mathbf{x},t)}{\partial x_\alpha}-\frac{\partial\Psi^*(\mathbf{x},t)}{\partial x_\alpha}\sigma_\alpha\Psi(\mathbf{x},t)\right]$$

$\alpha = x,y,z$ in spin space and $\beta = x,y,z$ in real space

$$\begin{cases} Q_{xz}=0 \\ Q_{zz}=0;\ \boxed{Q_{yz}\neq 0} \end{cases} \Rightarrow \text{torque}$$

Vector in the spin space
Direction of $\mathbf{M_A X M_B}$

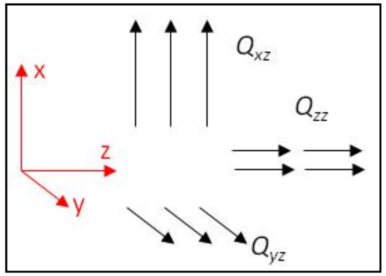

$$\frac{\partial\langle S(t)\rangle}{\partial t}=-\nabla\cdot Q=\frac{\partial Ec}{\partial\theta}=\left(J+J_{BQ}\cos\theta\right)\sin\theta$$

E_c= energy of exchange coupling

⇒ **The equilibrium torque determines an**
effective interfacial exchange coupling (Heinsenberg) **– $J\cos\theta$**

J.C. Slonczewski, PRB 39, 6995, (1989).

⇒ Free electrons – *asymptotic expression*

$$J=\frac{\boxed{(U-E_F)}}{8\pi^2\boxed{d^2}}\frac{8k^3\boxed{(k^2-k_\uparrow k_\downarrow)}(k_\uparrow-k_\downarrow)^2(k_\uparrow+k_\downarrow)}{(k^2+k_\uparrow{}^2)(k^2+k_\downarrow{}^2)}\boxed{e^{-2kd}}$$

Sign of coupling
AF: $k^2<k_\uparrow k_\downarrow$
F: $\mathbf{k^2>k_\uparrow k_\downarrow}$

MTJ: equilibrium (zero bias) torque in Fe/MgO/Fe MTJs

Continuous MML films

Spin current decays exp with t_{MgO}
=> **extremelly thin MgO required**

NANCY: First experimental proof of:

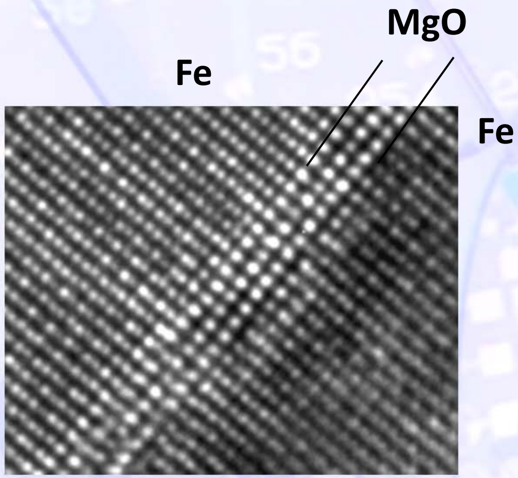

Courtesy E. Snoek CEMES, Toulouse

AF Magnetic interactions

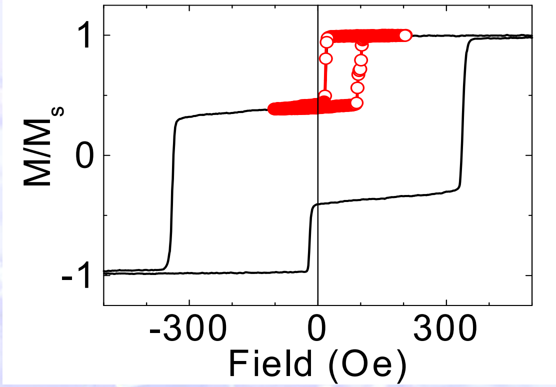

Heinseberg interfacial coupling

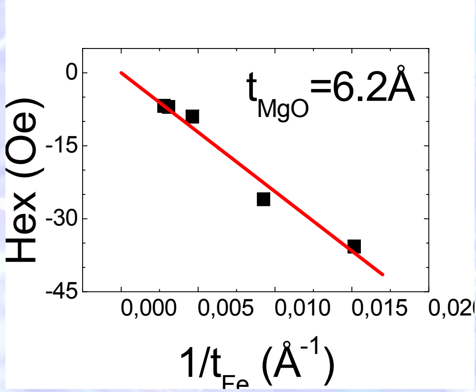

by spin polarized tunneling

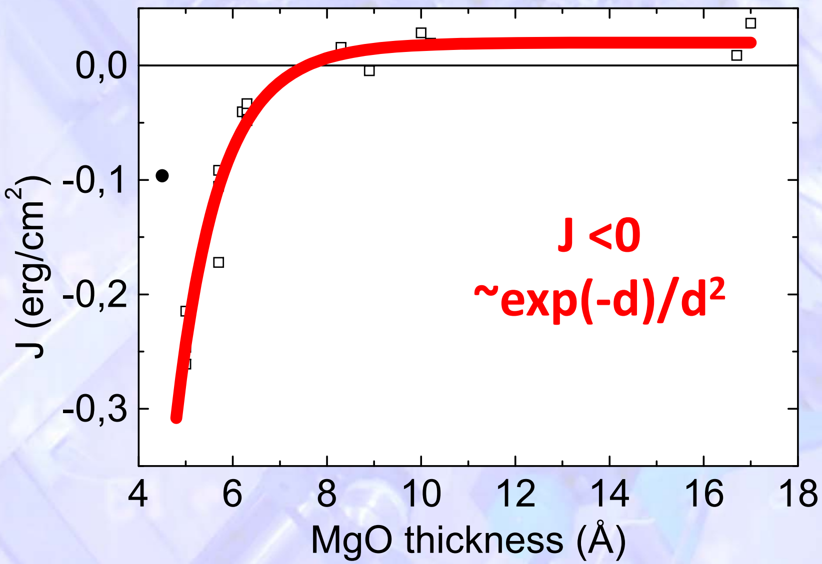

Equilibrium coupling

Signature of torque
(nonzero spin current)
for zero charge current

C. Tiusan et al, Phys. Rev. Lett. 89, 107206 (2002).

Engineering of coupling by interfacial electronic structure (Fe/MgO)

A. Duluard et al, Oral: EG02
56th Annual MMM, Scottsdale, Arizona
30 Oct-3 Nov 2011

- UHV MBE growth:

Annealed bottom Fe layer

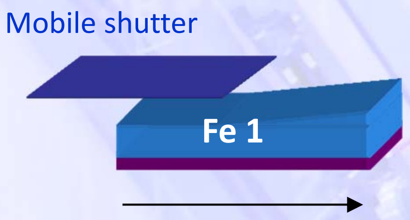

Desposition of Fe islands
-variable size **(RHEED)**

0 to 2 – 3 Fe monolayer

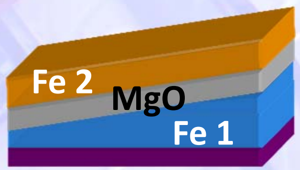

Complete stack

Deposition techniques:
- Fe → Knudsen cell
- MgO → electron gun

- H applied along easy axis, measured by Kerr and/or VSM

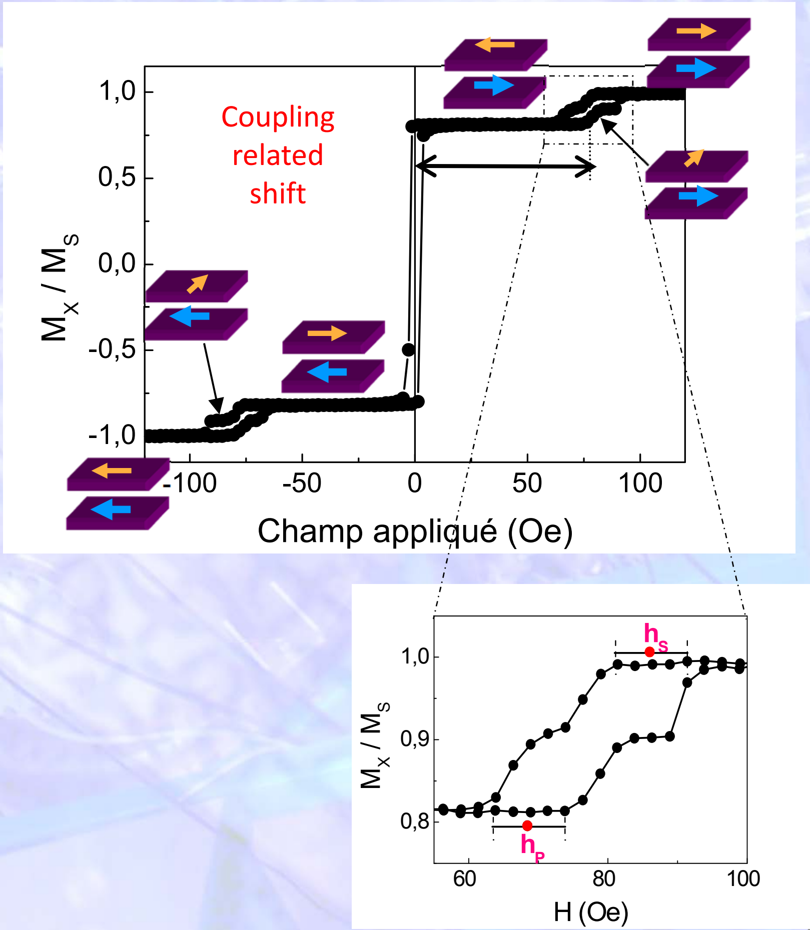

Engineering of coupling by interfacial electronic structure (Fe/MgO)

From SW – modelling => J

A. Duluard et al, Oral: EG02
56th Annual MMM, Scottsdale, Arizona
30 Oct-3 Nov 2011

- With insulator thickness and coverage

Normalized coupling

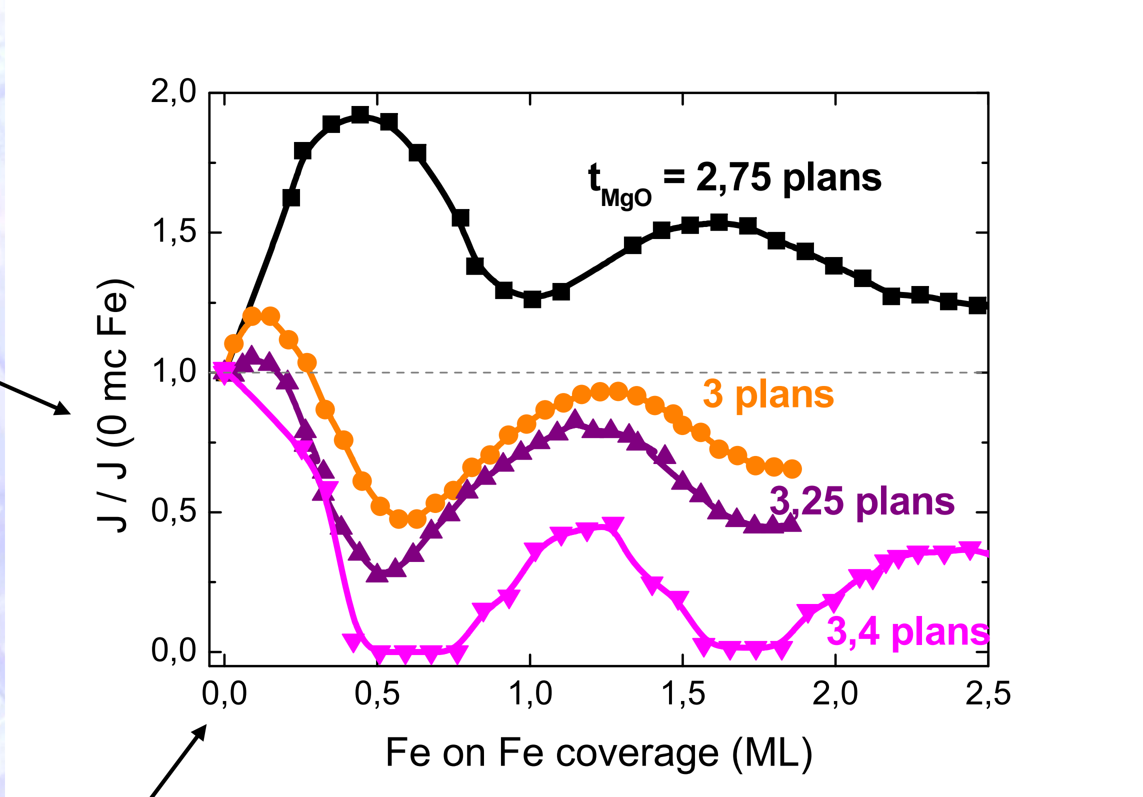

Smooth bottom Fe interface (annealed)

Bottom Fe interface with Fe islands ≠ sizes

Main applications of MTJs

SENSORS

- **Magnetic field, position, Read heads**, etc. similar to GMR but…
  Tunnel junctions would then offer a superior signal to noise ratio than metal based CIP or CPP sensors.

DATA STORAGE

- **Unit in magnetic random access memories (MRAM)**
  Tehrani et al, IEEE.Trans.Magn., 35, 2814, (1999).
- **Basic element of reprogrammable logic gates**
  Johnson IEEE Spectrum 33, (2000).
- **Magnetoresistive sensor for CPP read-heads**
  Nakashio J.Appl.Phys.89, 7356 (2001).

MICROWAVE APPLICATIONS

- **Microwave detection** by *Spin-torque diode effect*
  (DC voltage induced by AC flowing current)
  Tulapurkar A A et al Nature ***438,*** *339, (2005).*
- **Microwave emission**
  negative damping STT in pillars produces M steady precession
  Kiselev S I et al Nature ***425 380*** *(2003).*

The requirements of the properties, especially the product of resistance and area (R.A) are different for these various applications.

Schematics of four generations of magnetic sensing technology

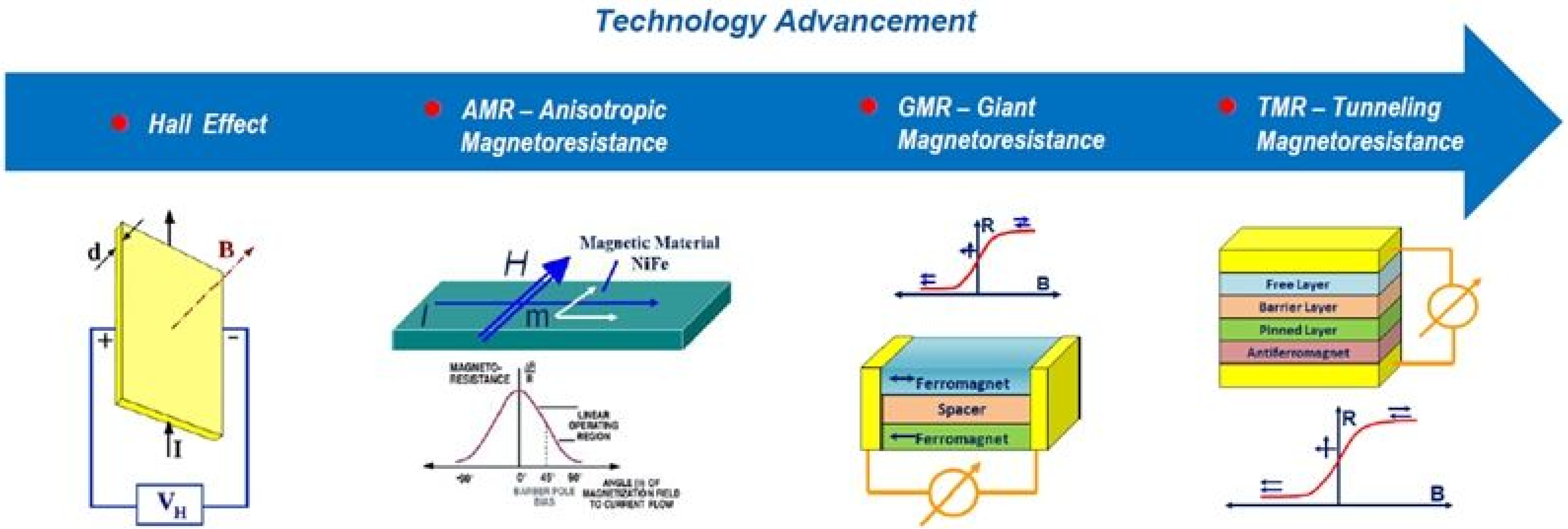

Technology	Hall Effect	AMR	GMR	TMR
Power Consumption (mA)	5 ~ 20	1 ~ 10	1 ~ 10	0.001 ~ 0.01
Die Size (mm^2)	1 × 1	1 × 1	1 × 2	0.5 × 0.5
Field Sensitivity (mV/V/Oe)	~ 0.05	~ 1	~ 3	~ 100
Dynamic Range (Oe)	~ 10000	~ 10	~ 100	~ 1000
Resolution ($nT/Hz^{1/2}$)	>100	0.1 ~ 10	1 ~ 10	0.1 ~ 10
Temperature Performance (℃)	< 150	< 150	< 150	< 200

Comparison of Magnetic Sensing Technology Parameters

2. MAGNETIC TUNNEL JUNCTION – Read Head in HDD

>250 Gb/inch^2

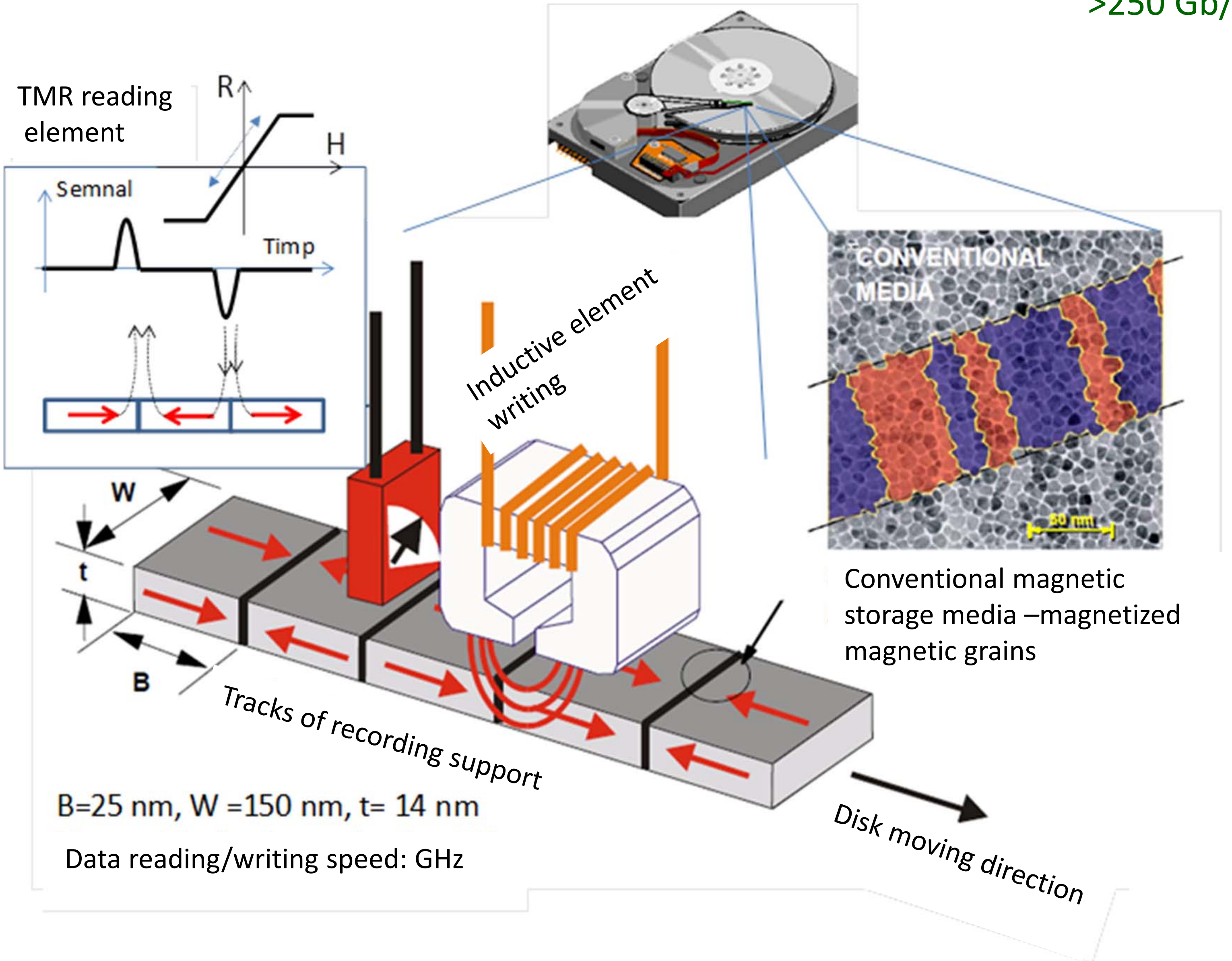

B=25 nm, W =150 nm, t= 14 nm

Data reading/writing speed: GHz

Future of HDD read heads?

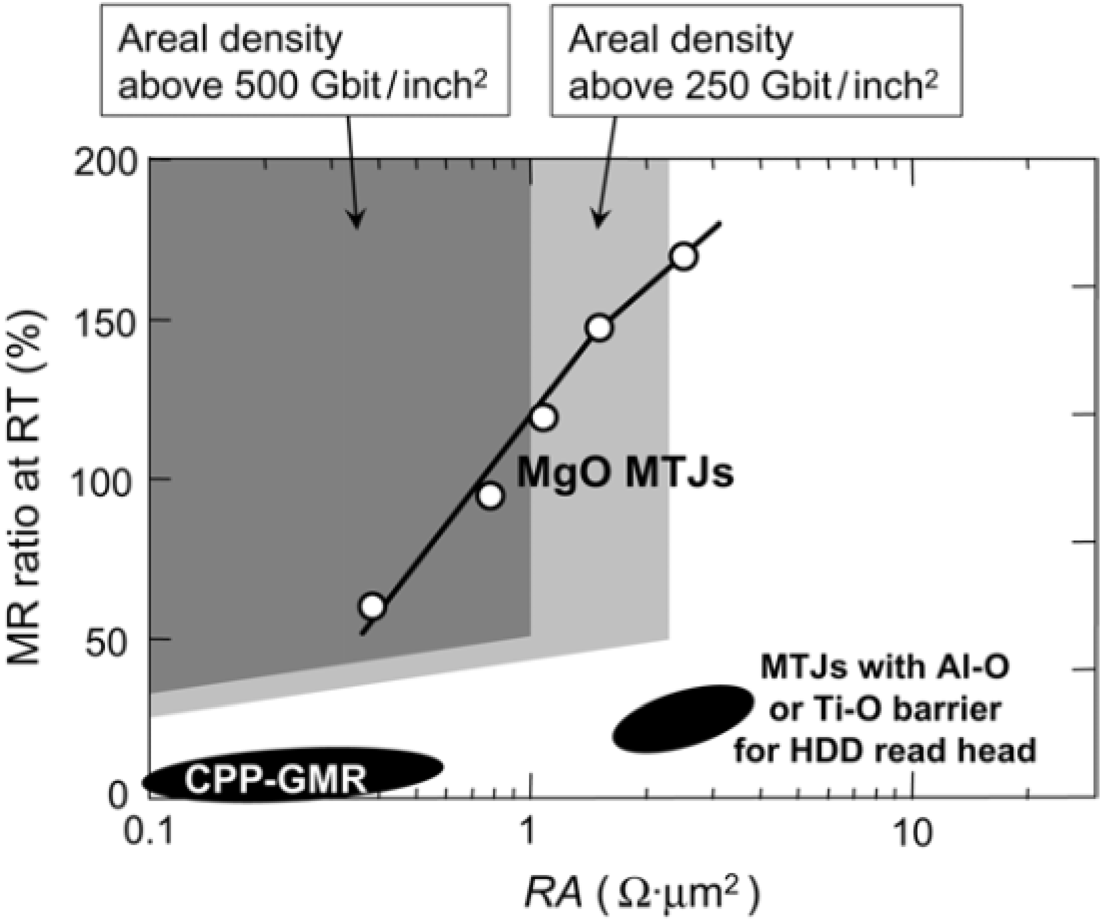

MgO-TMR head for ultrahigh-density HDD

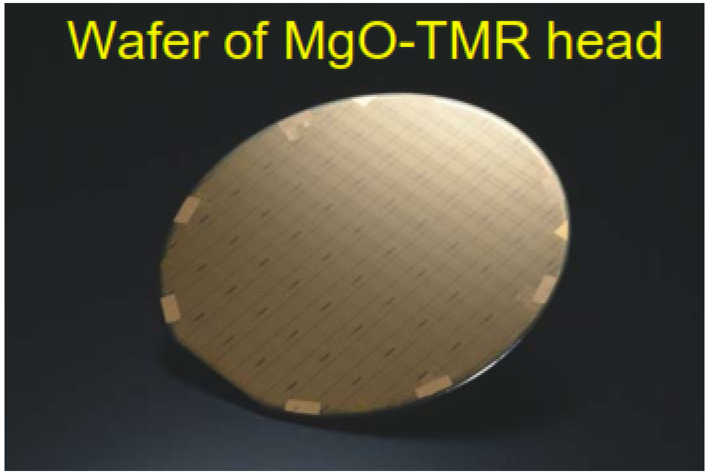

Cut

Inte-
gration

Inte-
gration

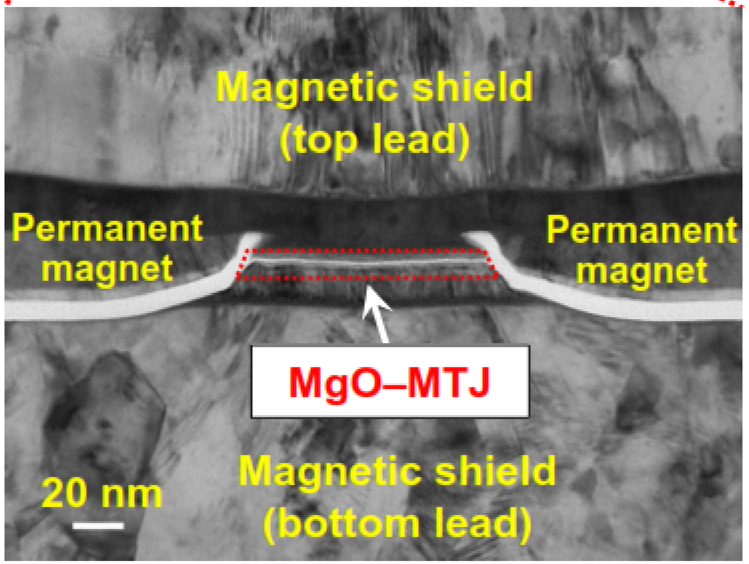

TEM image

- **Commercialized in 2007**.
- Density **> 250 Gbit / inch²** achieved.
- Applicable up to **1 Tbit / inch²**.

3. MAGNETIC TUNNEL JUNCTION – elementary cell of magnetic random access memories (MRAM)

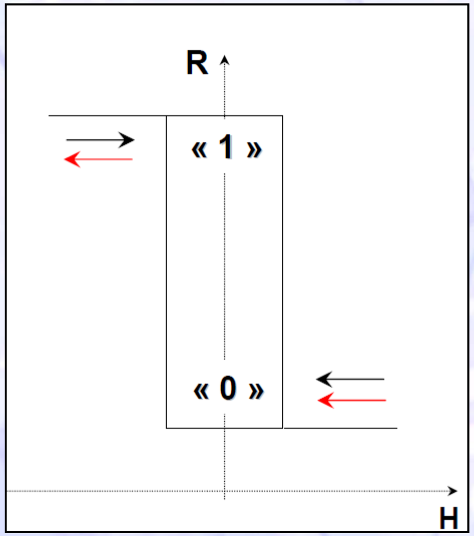

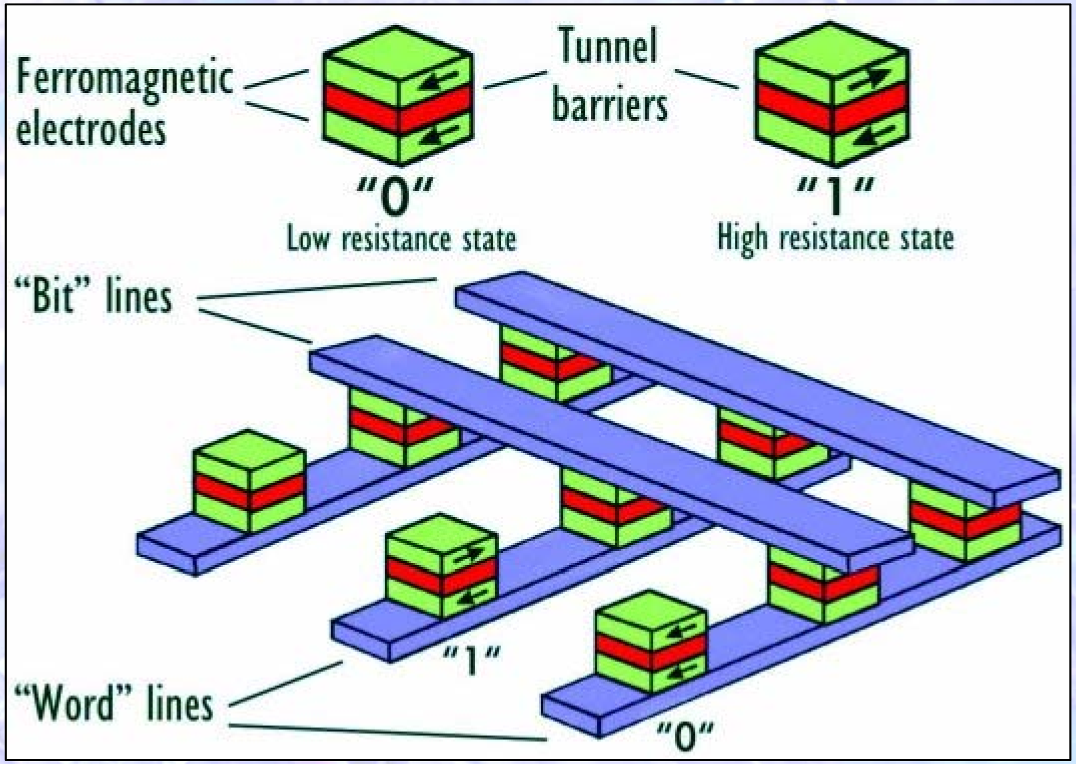

Everspin (Freescale 2006)

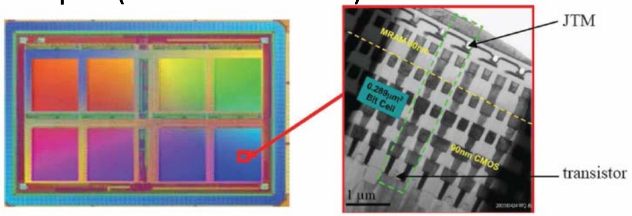

2011

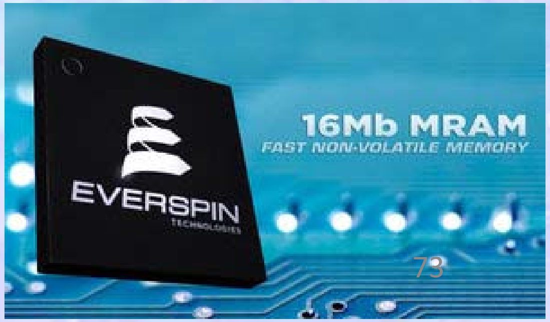

Magnetic random access memories (MRAM)

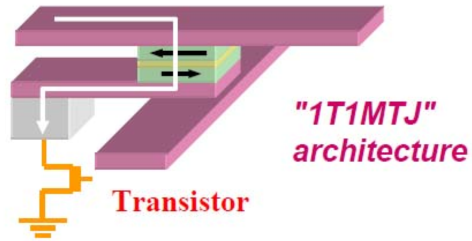

Electric characteristics

- ❑ **High resistance** ⇒ low power consumption
- ❑ **Large ΔR** ⇒ high signal/noise
- ❑ Perpendicular transport, low mean free path
  ⇒ high integration potential
- ❑ Exponential variation of current with voltage, barrier thickness

Magnetic characteristics

- ❑ non volatile

Other characteristics

- ❑ no mechanic pieces
- ❑ stable against radiations

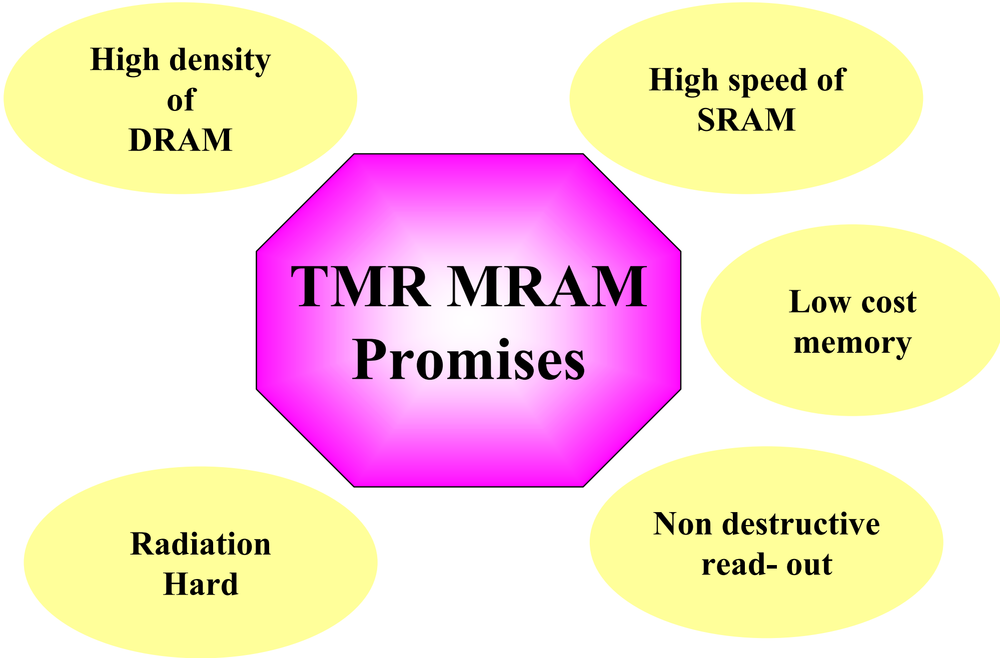

Perpendicular MTJs, basis for STT-MRAM

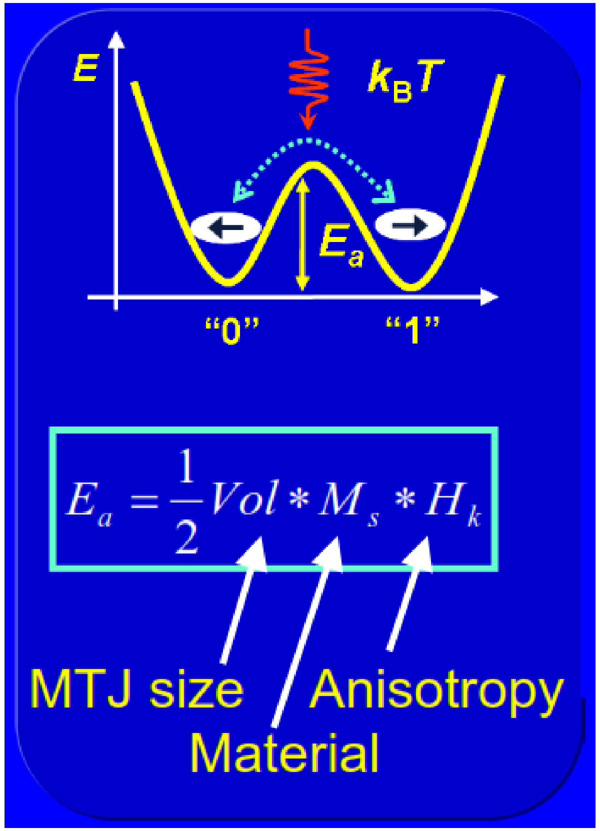

Thermal stability factor
E_a/k_BT >40 for non volatility

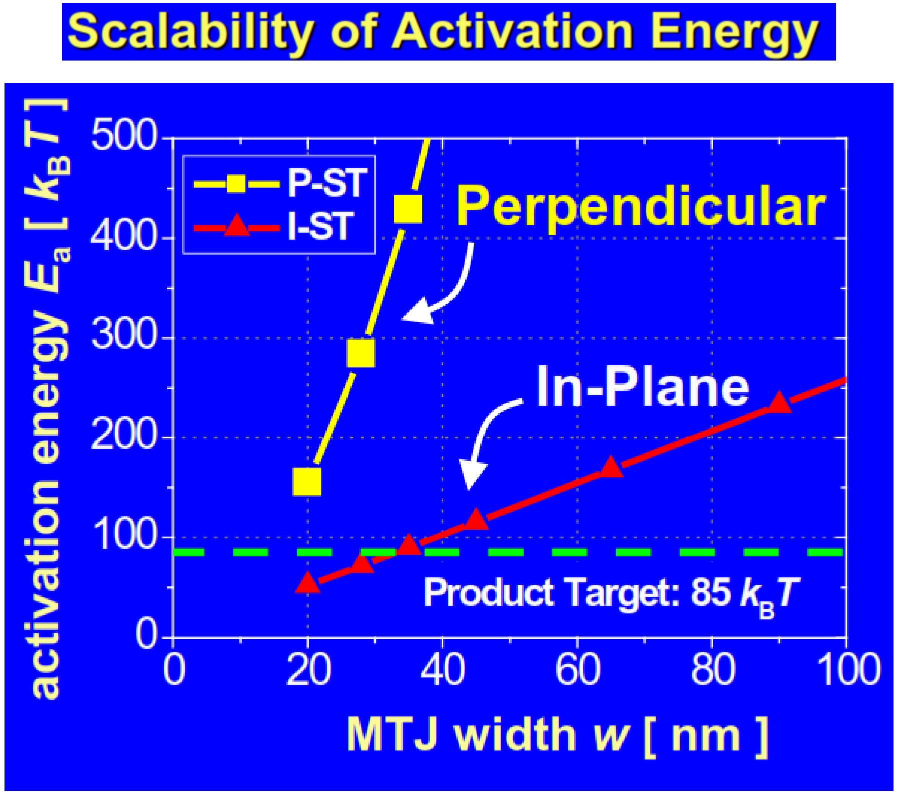

$$I_{C0} = \alpha \frac{\gamma e}{\mu_B g} M_s H_K V = 2\alpha \frac{\gamma e}{\mu_{Bg}} E$$

PMA provides

- ❑ Large H_k which **ensures thermal stability for scaling below 20nm**
- ❑ Micromagnetic switching features non dependent on pilar shape/aspect ratio => reproducibility
- ❑ Smaler intrinsic threshold current $\mathbf{I_{C0}}$ for current-induced swithing
  proportional to E:
  smaller in PMA-MTJ (**E=Ea)** than in IPA-MTJ (***$E=E_a+E_{demag}=Ea+4\pi M_s^2$*** = large)

MTJs with FM having PMA

next-generation of high-density non-volatile memory and logic chips with high thermal stability and low critical current for current-induced magnetization switching

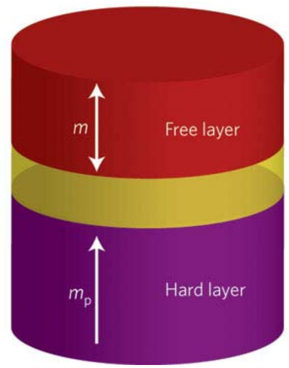

Requests for MTJ integration with CMOS in MRAM

- ❑ high tunnel magnetoresistance (TMR) ratio over 100%,
- ❑ switching current lower than the corresponding transistor drive current
- ❑ high thermal stability for sufficient retention time,
- ❑ annealing treatment stability at 350–400°C for back end process.

➡ Ta/CoFeB/MgO/CoFeB/Ta p-MTJs with the smallest feature size of 17 nm

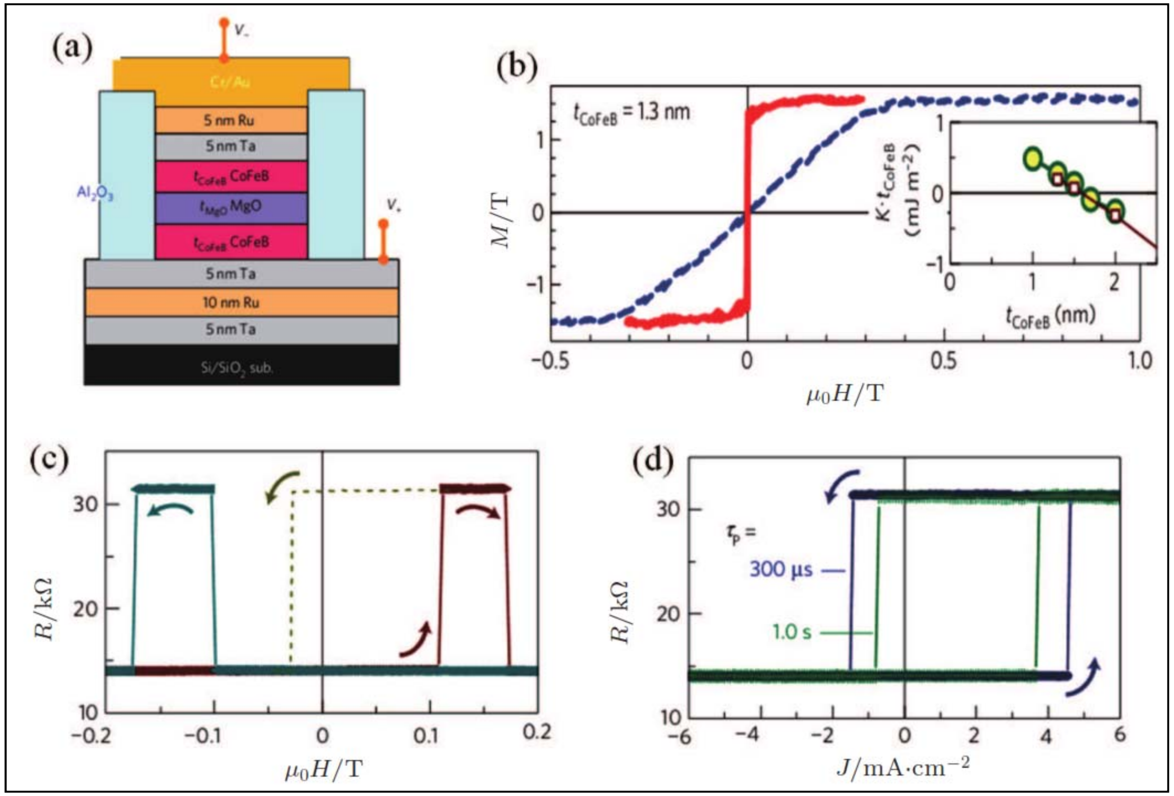

Ikeda S et al, Nature Materials 9, 721–724 (2010)

Feature size 40nm

TMR=120% RT

Other modern issues

- ➢ Electric field effect on anisotropy
  E assisted switching

Domain wall devices

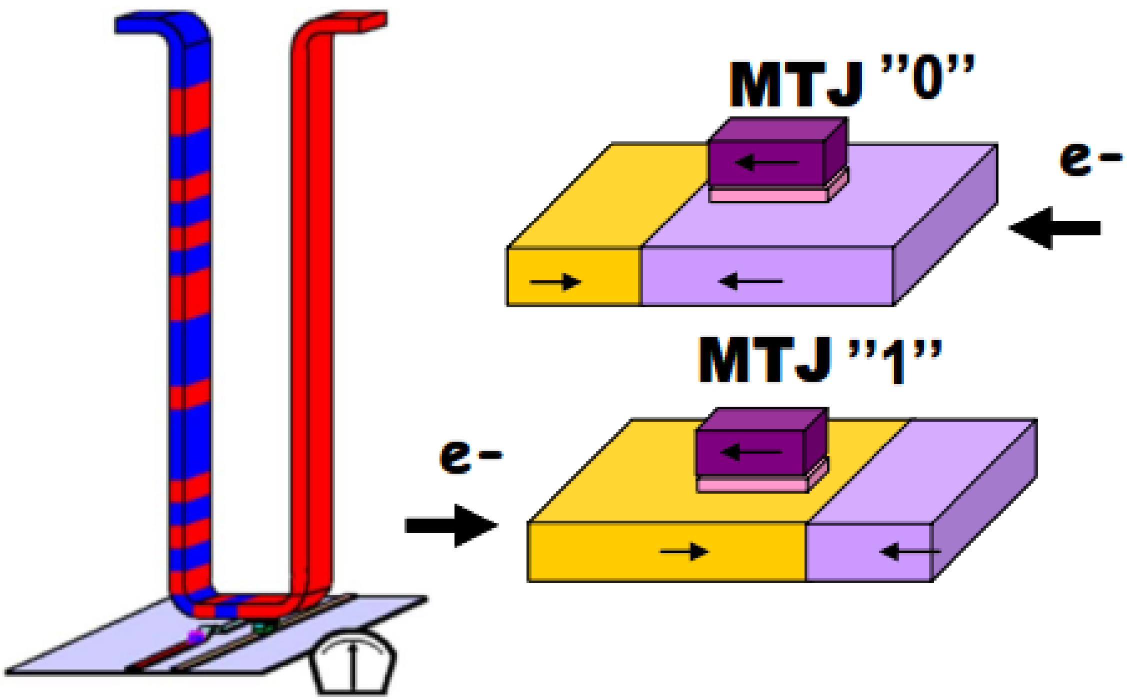

Parkin et al., Science **320**, 190 (2008).

- No mechanical moving parts
- Domain walls moved by STT effects
- MTJ reads (0) and (1) by TMR effect

Magnetic Race Track Memory
[Parkin, US patents 6,834,005 (2004) & 6,898,132 (2005), Science (2008)]

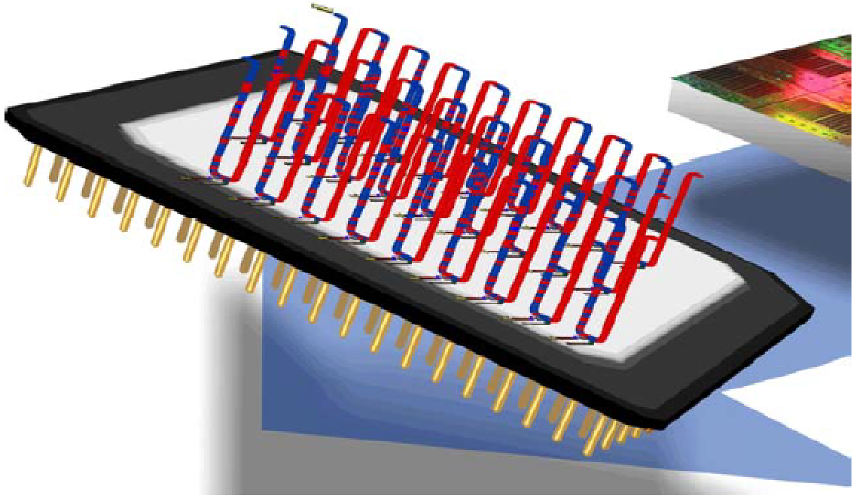

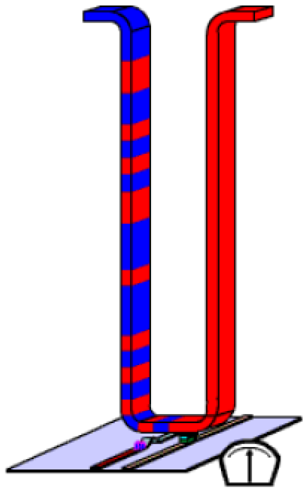

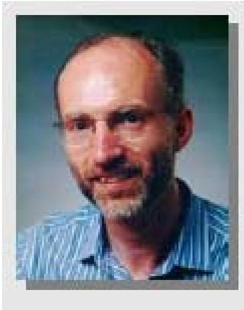

From 2D to 3D memories

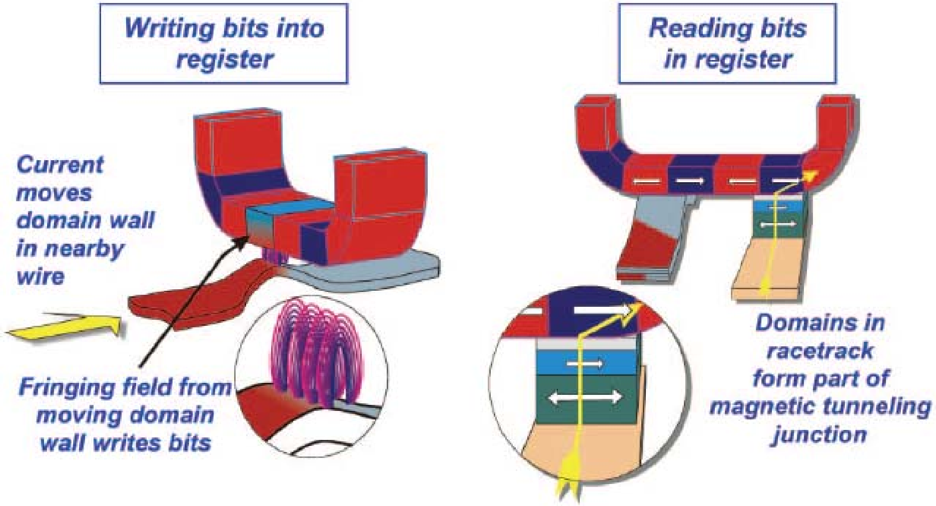

Racetrack Memory!

Very compact, low power and low cost

Horizontal racetrack → density of Flash memory but much faster and no wear-out

Vertical racetrack → density of magnetic hard disk drive but much faster

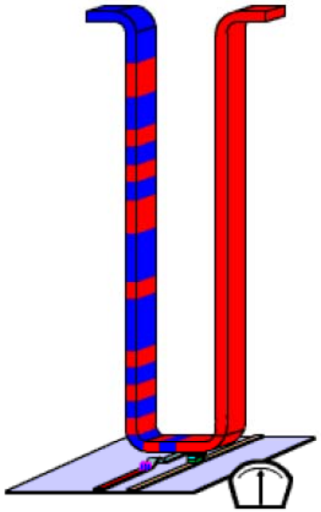

Magnetic RaceTrack: *A hard disk drive on a chip!*

→ The future of digital data storage!

→ An innately three-dimensional technology!

SST based applications => MTJs with Heusler electrodes

Heusler alloys

- ❑ half-metals: large spin polarization (100%)
- ❑ low Gilbert damping, important for STT based applications (**switching, HFO**)

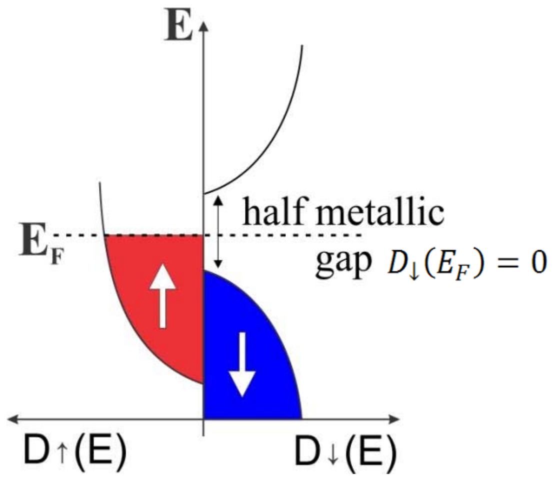

$$P = \frac{D_\uparrow(E_F) - D_\downarrow(E_F)}{D_\uparrow(E_F) + D_\downarrow(E_F)} = 100\%$$

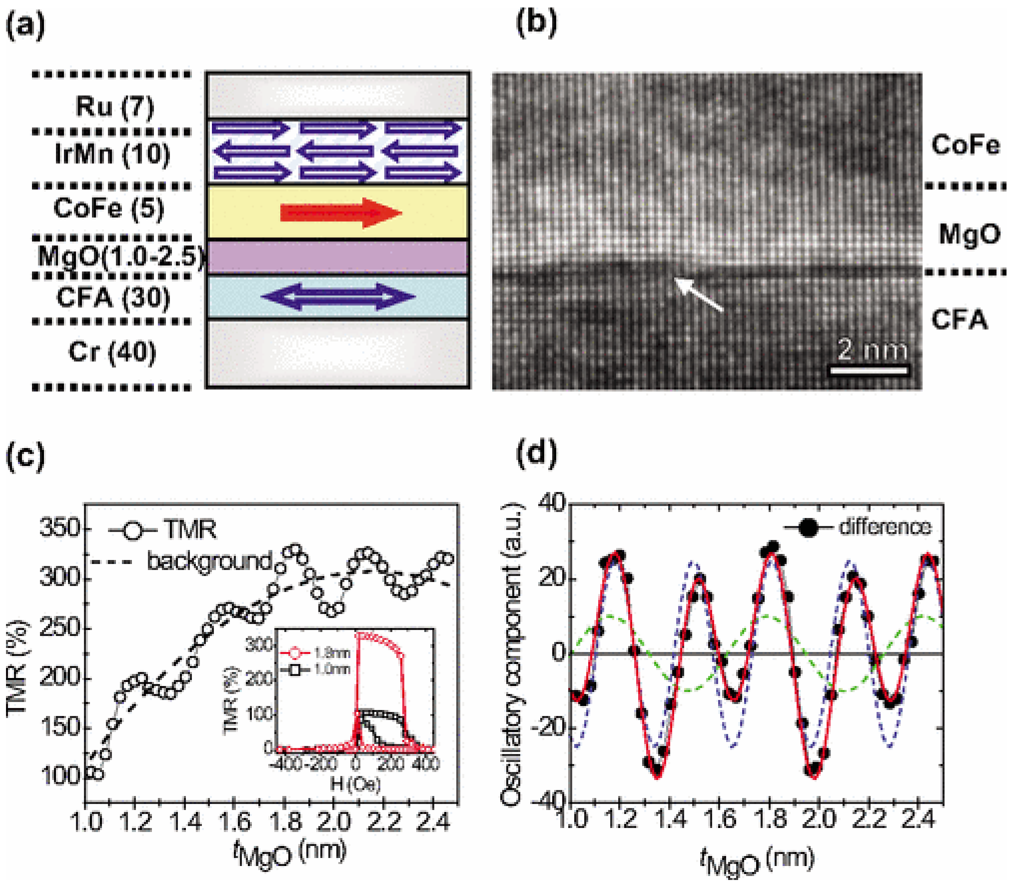

*W. Wang et al, Phys. Rev. B **81**, 140402(R) (2010)*

TMR in Heusler based MTJs, both AlOx and MgO barriers

Development of the TMR ratio for MTJs with Heusler electrodes

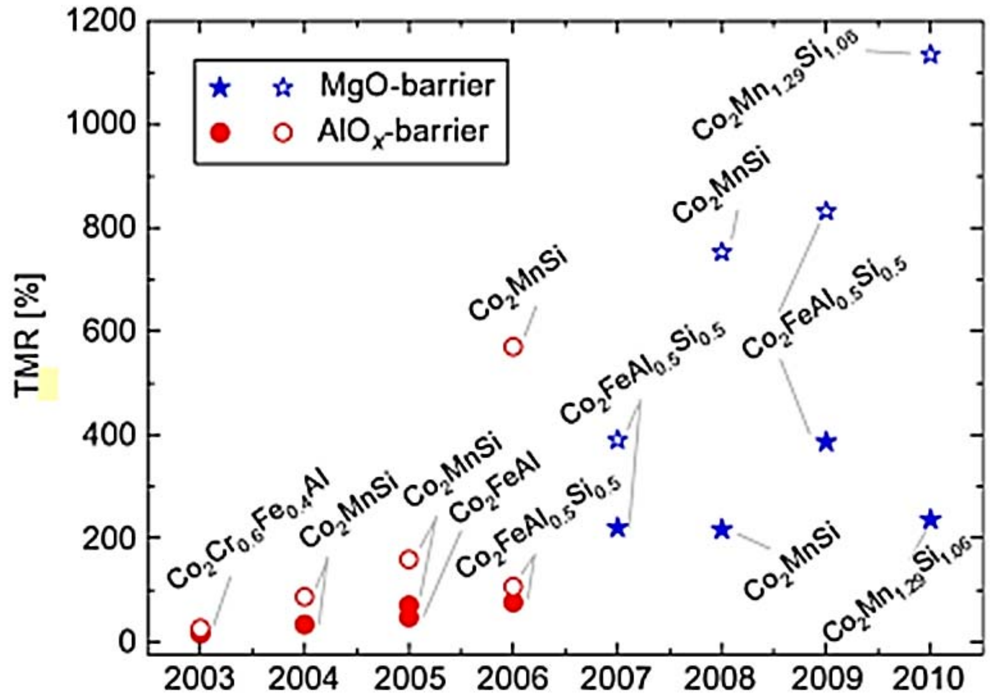

Handbook of Magnetic Materials, Vol. 21 (Ed. K.H.J. Buschow) (2010)
*ZHAOQIANG BAI et al, SPIN **02**, 1230006 (2012)*

However

small damping = easy M manipulation by STT by large mag-noise
=> necessity to tune damping (i.e. by spin Hall effect)

Modulation of effective damping constant using spin Hall effect

Permalloy/Pt bilayer

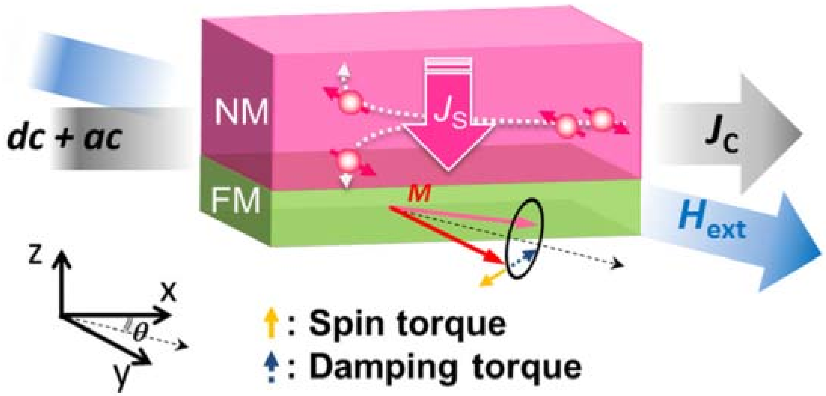

FIG. 1. Schematic illustration of SHE-induced EDM. J_s denotes spin current (density) due to dc inside Pt layer through SHE, which exerts spin transfer torque on magnetization inside FM layer and effectively reduces damping torque. The FMR spectrum can be detected as a dc voltage spectrum with applying an ac through the mixing of the ac and oscillatory change of anisotropic magnetoresistance.

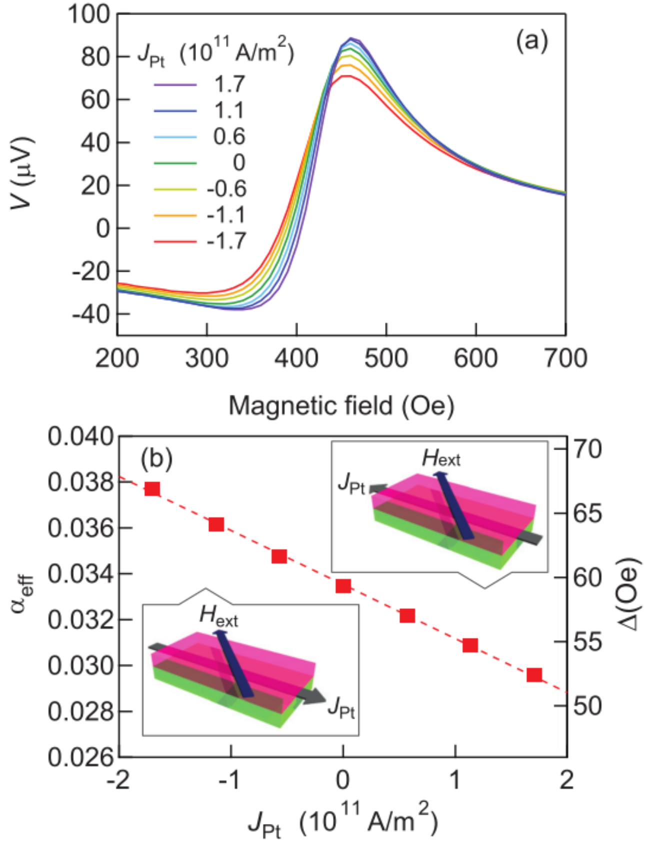

FIG. 2. (a)ST-FMR spectra for various dc's applied to Py (1.9 nm)/Pt (3.5 nm) sample with $\theta = 45°$. (b) J_{Pt} dependence of α_{eff} and Δ.

S. Kasai et al, APPLIED PHYSICS LETTERS 104, 092408 (2014)

MTJs with M manipulated by STT of spin currents generated by spin-orbitronic effects

Spin-Torque Switching with the Giant Spin Hall Effect of Tantalum

L. Liu et al, Science 336 , 555, (2012) - **Cornell**

MTJ devices

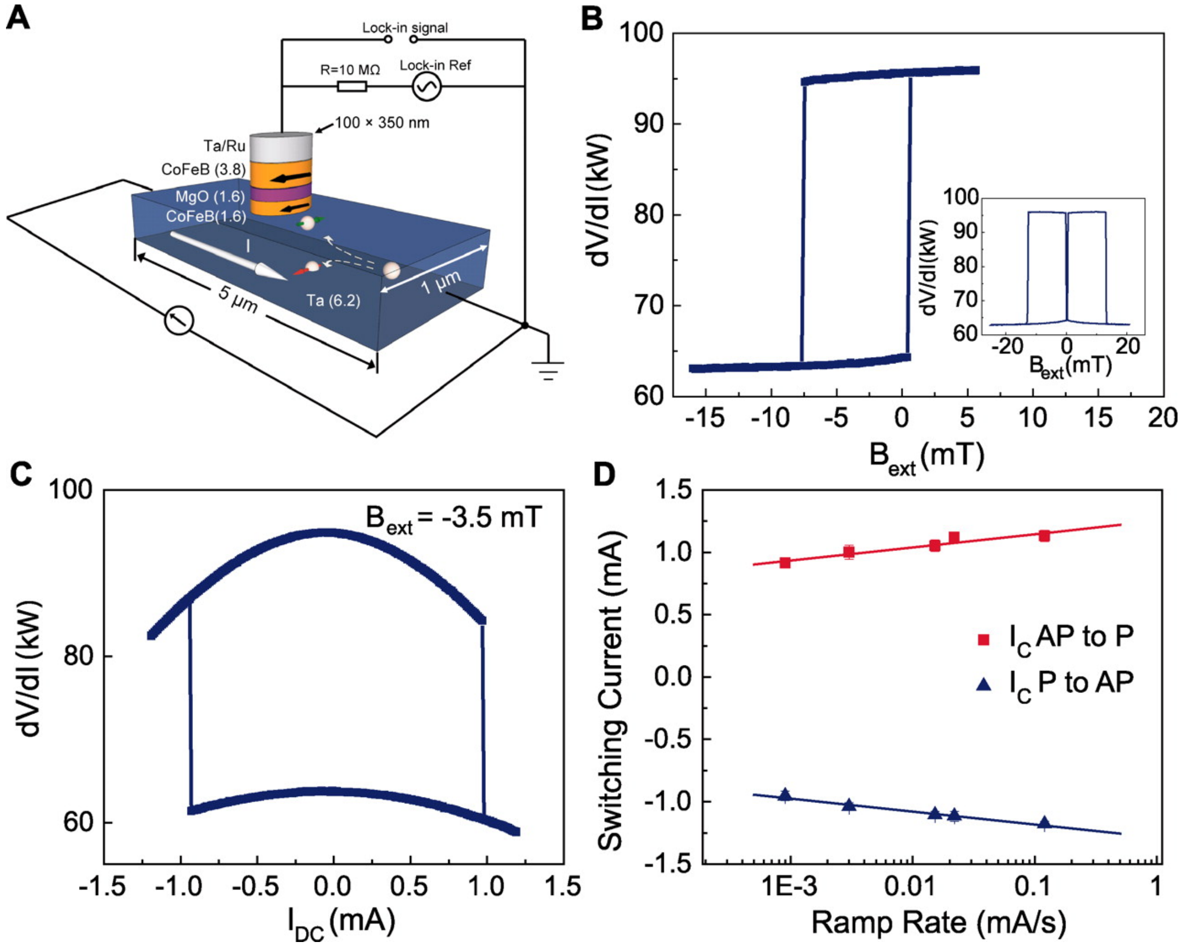

Buhrman and Ralph groups, Cornell Univ. Work performed at Cornell NanoScale Facility

Thank you !